

UCD--472-132

DE89 009007

LABORATORY FOR ENERGY-RELATED HEALTH RESEARCH

SCHOOL OF VETERINARY MEDICINE
UNIVERSITY OF CALIFORNIA, DAVIS

ANNUAL REPORT FISCAL YEAR 1986

Issued February 1989
By

THE STAFF OF THE LABORATORY FOR
ENERGY-RELATED HEALTH RESEARCH
JAMES W. OVERSTREET, DIRECTOR
OTTO G. RAABE, ASSOCIATE DIRECTOR FOR SCIENCE
DANA L. ABELL, EDITOR

DISCLAIMER

This report was prepared as an account of work sponsored by an agency of the United States Government. Neither the United States Government nor any agency thereof, nor any of their employees, makes any warranty, express or implied, or assumes any legal liability or responsibility for the accuracy, completeness, or usefulness of any information, apparatus, product, or process disclosed, or represents that its use would not infringe privately owned rights. Reference herein to any specific commercial product, process, or service by trade name, trademark, manufacturer, or otherwise does not necessarily constitute or imply its endorsement, recommendation, or favoring by the United States Government or any agency thereof. The views and opinions of authors expressed herein do not necessarily state or reflect those of the United States Government or any agency thereof.

Prepared under
Contract DE-AC03-76SF00472
for the
Department of Energy

DOE

DISTRIBUTION OF THIS DOCUMENT IS UNLIMITED

DISCLAIMER

This report was prepared as an account of work sponsored by an agency of the United States Government. Neither the United States Government nor any agency thereof, nor any of their employees, makes any warranty, express or implied, or assumes any legal liability or responsibility for the accuracy, completeness, or usefulness of any information, apparatus, product, or process disclosed, or represents that its use would not infringe privately owned rights. Reference herein to any specific commercial product, process, or service by trade name, trademark, manufacturer, or otherwise does not necessarily constitute or imply its endorsement, recommendation, or favoring by the United States Government or any agency thereof. The views and opinions of authors expressed herein do not necessarily state or reflect those of the United States Government or any agency thereof.

DISCLAIMER

Portions of this document may be illegible in electronic image products. Images are produced from the best available original document.

FOREWORD

This report to the U.S. Department of Energy summarizes research activities for the period from 1 October 1985 to 30 September 1986 at the Laboratory for Energy-related Health Research (LEHR) which is operated by the University of California, Davis, for the Office of Health and Environmental Research of the Office of Energy Research of the U. S. Department of Energy via Contract No. DE-AC03-76SF00472 administered by the San Francisco Operations Office. Both Department of Energy programmatic research and selected related work for other agencies and organizations as approved by the Department of Energy are reported.

This is the twenty-first annual report of the Laboratory for Energy-related Health Research (LEHR) (formerly called the Radiobiology Laboratory). LEHR is an Organized Research Unit of the University of California, Davis, and is associated with the School of Veterinary Medicine. The Director reports to the Dean of Veterinary Medicine, Dr. Edward A. Rhode, concerning University administrative matters and to the Dean of Graduate Studies and Research, Dr. Allen G. Marr, concerning Laboratory research activities including University collaborations and graduate student training at LEHR. The personnel at LEHR are listed on page 85.

The laboratory's research objective is to provide new knowledge for an improved understanding of the potential bioenvironmental and occupational health problems associated with energy utilization to contribute to the safe and healthful development of energy resources for the benefit of mankind. This research encompasses several areas of basic investigation that relate to toxicological and biomedical problems associated with potentially toxic chemical and radioactive substances and ionizing radiation, with particular emphasis on carcinogenicity. Studies of systemic injury and nuclear medical diagnostic and therapeutic methods are also involved. This is an interdisciplinary program spanning physics, chemistry, environmental engineering, biophysics and biochemistry, cellular and molecular biology, physiology, immunology, toxicology, both human and veterinary medicine, nuclear medicine, pathology, hematology, radiation biology, reproductive biology, oncology, biomathematics, and computer science. The principal themes of the research at LEHR center around the biology, radiobiology, and health status of the skeleton and its blood-forming constituents; the toxicology and properties of airborne materials; the beagle as an experimental animal model; carcinogenesis; and the scaling of the results from laboratory animal studies to man for appropriate assessment of risk.

LEHR began as a small research project on the Davis campus of the University of California in 1951 in which studies were done of the biological effects of X-rays on laboratory animals under the support of the U.S. Atomic Energy Commission. In 1957 a major project was initiated by the Atomic Energy Commission to study the biological effects associated with low-level chronic exposure of the skeleton to beta particle irradiation from skeletal deposits of the bone seeking radionuclide, ^{90}Sr , a fission product found in fallout from atmospheric tests of nuclear weapons and a constituent of nuclear wastes from nuclear power plants. The beagle was chosen as the experimental subject that could be studied in sufficient detail to scale the results to human populations that might be exposed. To assist in this scaling from results in beagles to expected risks in people, parallel studies were planned utilizing the bone-seeking radionuclide ^{226}Ra , to which some people had been exposed in watch-dial painting and in medicine earlier in this century. This main study was the basis for the formation of the Radiobiology Laboratory in 1965 under the direction of Leo K. Bustad as an Organized Research Unit of the University of California, Davis, and the building and administration of the Radiobiology Laboratory by the Atomic Energy Commission. The main study is now nearing completion after some twenty-four years since the first beagles were exposed to ^{90}Sr in the planned long-term experiments. The last beagle (D05Y16) out of the 1063 which were involved in all the various phases of this research over the years died on February 27, 1986, at the age of 18.5 years; he had been exposed to radiostrontium at the lowest level of the study. The first section of this report documents the current status of this important lifetime study of internally deposited radionuclides in beagles.

The Radiobiology Laboratory grew as the main project expanded, and the research interests of the laboratory broadened to consider all aspects of the radiobiological effects of the irradiation of the skeleton. Special interest in cellular biology focused on the blood-forming and immunological functions of bone marrow cells and their alterations by ionizing radiation. In the early 1970's we designed and constructed an outdoor ^{60}Co irradiation field (nominal source strength 170 Curies) for chronic exposure of beagles to up to about 10 rem/day. This facility has been beneficially utilized for research on the cellular and systemic effects of penetrating gamma ray irradiation on the bone marrow in beagles and has been especially valuable for studies of the radiation induction of leukemia. Some of our current research based on these external radiation effects studies is reported herein as part of the cellular and molecular studies aimed at improving our understanding of the genetic and cellular nature of leukemia.

In 1975 the Laboratory was asked to tackle new non-nuclear research activities by the new Energy Research and Development Administration (ERDA), with interagency support from the U. S. Environmental Protection Agency. Research activities in this area focused on the potential health effects of release to the atmosphere of combustion products from fossil fuel power plants, with emphasis on coal fly ash. A new program was initiated in basic aerosol science to link the evaluation of airborne materials and the laboratory study of these materials utilizing cellular and animal models. This led to the first report in the literature of the presence of mutagenic chemicals on the surface of coal fly ash particles, and yielded detailed studies of the chemical and physical properties of coal fly ash including chronic inhalation toxicity studies with experimental animals. In the succeeding years, the scope of the research expanded more broadly into environmental and occupational toxicology, and in 1980 the Laboratory's name was changed to the Laboratory for Energy-related Health Research to more properly reflect the expanded mission and research orientation. Programmatic needs in recent years led to a reduction in Department of Energy projects in the non-nuclear area, but the laboratory has continued to conduct toxicological research under the sponsorship of other agencies. These projects are documented in reports to those agencies. One major area of work has related to occupational health issues associated with nerve agents, conducted for the U.S. Army.

In 1983 we finished construction of the new Toxic Pollutant Health Research Laboratory, a specialized facility for the total containment and safe study of highly toxic and/or carcinogenic agents, including both radioactive and chemical materials. This facility was designed for studies utilizing laboratory animals and exposures to toxic materials by dermal, intravenous, oral-gastrointestinal, intratracheal and inhalation routes. Current work in TPHRL includes studies of ^{241}Pu behavior in beagles and monkeys.

This report has been divided into several topical sections outlining the scope of research at LEHR including "Radionuclide Toxicity Studies," "Skeletal Biology Studies," "Cellular and Molecular Studies," and "Nuclear Medical Studies." Emphasis at LEHR is placed on open literature publications. A list of publications and presentations is appended.

We hope that this progress report will provide needed information concerning the status of the various funded projects at LEHR and reflect the intellectual and scientific pride and enthusiasm of the research faculty and staff concerning the important advances in knowledge that are resulting from this program. As always, we appreciate comments and suggestions concerning the content of this report and the direction of future research.

Respectively submitted,



Otto G. Raabe
Associate Director for Science

ACKNOWLEDGMENTS

We thank Pamela Carroll and Charles Baty for organizing and typing this report. We wish to extend special thanks to all of our associates in animal care for their efforts in this most important area.

The active interest and advice of Dean Edward A. Rhode of the School of Veterinary Medicine, Dean Allen G. Marr of Graduate Studies and Research, our Advisory Committee and our consultants and collaborators are sincerely appreciated.

The research described in this report involved animals maintained in facilities approved by the American Association for the Accreditation of Laboratory Animal Care (AAALAC).

TABLE OF CONTENTS

RADIONUCLIDE TOXICITY STUDIES	1
Rosenblatt, Culbertson, Parks, Spangler	Strontium-90 and radium-226 toxicity in beagle dogs: Current status
White, Rosenblatt	A problem-oriented medical record system
Miyabayashi, Morgan, Atilola, Muhamuza	Emptying time for the small intestine in normal beagle dogs.
SKELETAL BIOLOGY STUDIES	
Parks, Jee, Dell, Miller	Assessment of cortical and trabecular bone distribution in the a beagle skeleton by neutron activation analysis.
CELLULAR AND MOLECULAR STUDIES	
Kawakami, Cain	Allotransplantation of canine myeloid leukemia
NUCLEAR MEDICAL STUDIES	
Parks, Harris, Keen, Cooper, Zidenberg-Cherr, Musker, Bharadwaj, Schneider	Coordination chemistry of the ^{212}Pb - ^{212}Bi nuclear transformation: Alpha- emitting radiopharmaceuticals.
Lagunas-Solar, Carvacho, Nagahara, Mishra, Parks	Cyclotron production of no-carrier-added ^{206}Bi (6.24 d) and ^{205}Bi (15.31 d) as tracers for biological studies and for development of alpha-emitting pharmaceuticals.
Bharadwaj, Musker	A 1,1-dithiocarboxylate ligand with an easily derivatizable group: Synthesis and structure of tris[2-(ethylamino)- cyclopent-1-ene-1-dithiocarboxylato]- bismuth(III)
RADIONUCLIDE METABOLISM STUDIES	
Raabe, Al-Bayati, Gielow	Metabolic evaluation in nonhuman primates of bone and liver risks from internally deposited actinides.
PUBLICATIONS AND PRESENTATIONS	
LABORATORY FOR ENERGY-RELATED HEALTH RESEARCH PERSONNEL	
ADVISORY COMMITTEE AND COLLABORATORS	
AUTHOR INDEX	

RADIONUCLIDE TOXICITY STUDIES

STRONTIUM-90 AND RADIUM-226 TOXICITY IN BEAGLE DOGS: CURRENT STATUS

L. S. Rosenblatt
M. R. Culbertson
N. J. Parks
W. L. Spangler

We are investigating biologic effects of ^{90}Sr and ^{226}Ra in the beagle in order to predict the possible long-term hazards to people from chronic exposure to low levels of irradiation. Animals received either radionuclide by several means of administration: (a) continual ingestion of ^{90}Sr , (b) a single intravenous injection of ^{90}Sr , or (c) a series of eight intravenous injections of ^{226}Ra . Although administration of ^{90}Sr and ^{226}Ra ended at 540 days of age, the animals continued to receive chronic, low-level radiation doses from these bone-seeking radionuclides throughout life. The last of the dogs died in this year at age 18.5, but we are continuing to investigate the significance of these long-term exposures given at low dose rates with regard to cancer production, physiologic well-being, and shortening of life through the detailed records that were kept and by study of preserved materials.

The major goal of this study on the toxicity of ^{90}Sr and ^{226}Ra is to provide information on long-term consequences expected to occur in people from chronic exposure to α - and β -emitting bone-seeking radionuclides. To meet this goal, we are evaluating the biologic effects of the two radionuclides in the beagle. Similarities between dogs and people provide a valuable base for the scaling of potential hazards from radionuclide contamination from canine to human populations.

Experimental Design

Radium-226 was injected intravenously into dogs beginning at 435 days and every two weeks thereafter until 540 days of age. Activities over an approximately 500-fold range were administered to these animals in 6 treatment levels plus controls; together they comprise the R-dogs (Table 1).

Table 1. EXPERIMENTAL DESIGN AND STATUS OF RADIUM-226 TOXICITY STUDY

226Ra Injection Series (8 Biweekly Injections Starting at 435 Days of Age)					
Treatment Code	Multiple of 10 level	$\mu\text{Ci/kg/inj}$	Total ($\mu\text{Ci/kg}$)	Number of Dogs	Median Survival (Years)
R00	0	0	0	85	14.6
R05	0.3	0.003	0.024	46	14.5
R10	1	0.008	0.064	40	13.8
R20	6	0.047	0.376	42	10.9
R30	18	0.14	1.12	40	7.4
R40	54	0.42	3.36	41	5.1
R50	162	1.25	10.0	41	4.3
				335	

The activity per injection ranged from 0.003 to 1.25 $\mu\text{Ci}/\text{kg}$. The nominal quantity injected for a 10-kg dog ranged from 0.24 to 100 μCi of ^{226}Ra .

The activity at R10 was computed to represent the canine equivalent of 10 times the maximum permissible skeletal burden for man (0.1 μCi ^{226}Ra), based on the assumption of a 25% skeletal retention of the injected quantity. The time of injection, from 14 to 18 months of age, was chosen to approximate the temporal pattern of ^{226}Ra assimilation by the radium dial painters, a human population to which the experimental canine population would be compared. Strontium-90 was administered in the food, with the dietary concentration of ^{90}Sr maintained at a constant level with respect to dietary calcium levels. Activities were administered to 7 treatment groups (plus controls) over a 1500-fold range; these are the D-dogs (Table 2).

Table 2. EXPERIMENTAL DESIGN AND STATUS OF STRONTIUM-90 TOXICITY STUDY

90Sr Ingestion Series (in utero to 540 days of Age) Data include 15 dogs fed throughout life in D30, D40 and D50.						
Treatment Code	Multiple of 10 Level	μCi 90Sr per g dietary Ca	Ingested $\mu\text{Ci}/\text{d}$	Total Ingested (μCi)	Number of Dogs	Median Survival (Years)
D00	0	0	0	0	80	14.5
D05	0.3	0.007	0.02	10	77	14.2
D10	1	0.021	0.07	40	42	13.5
D20	6	0.123	0.44	240	66	14.4
D30	18	0.37	1.3	700	64	14.1
D40	54	1.11	4	2200	71	12.0
D50	162	3.33	12	6500	65	5.2
D60*	486	10.0	36	19400	19	2.2
					484	

*D60 dogs were not in the original experimental design but were added in 1967.

90Sr Injection Series
(Single IV Injection at 540 Days of Age)

Treatment Code	Multiple of 10 Level	$\mu\text{Ci}/\text{kg}/\text{inj}$	Total $\mu\text{Ci}/\text{kg}$	Number of Dogs	Median Survival (Years)
S20	6	3.7	3.7	20	13.5
S40	54	33	33	26	13.3
Total				46	
				865	

Administration of ^{90}Sr began in utero at the beginning of the second trimester of gestation when the dams began to receive radioactive feed. Pups were nursed while their mothers continued on the dietary regimen, and they were weaned onto the same ^{90}Sr -containing diet. Feeding continued until 540 days of age, at which time the animals began to receive the standard (nonradioactive) laboratory ration. The nominal quantity ingested was 10 to 19,400 μCi ^{90}Sr . The time of administration, from prior to birth until 18 months of age, includes the period of skeletal maturation, and was chosen to represent human exposures by ingestion of ^{90}Sr -contaminated foods during early life.

Two additional small groups of dogs (S-) were given their ^{90}Sr as a single injection at 540 days of age, to serve in the comparison of the two modes of administration (injection vs. ingestion). These groups were included to also act as a common link between the project at Davis and a related DOE-funded study at the University of Utah.

Survival

The last surviving dog, D05Y16, died on 02/27/86 at 18.5 years

The cumulative survival rates of R05- and R10-level dogs appear indistinguishable from control animals through 17 years (Figure 1). Cumulative survival rates of other treatment groups are significantly different from controls ($p < 0.05$) after 7.5 years of age for R20 dogs, 6 years for R30s, 5 years for R40s, and 3 years for R50s.

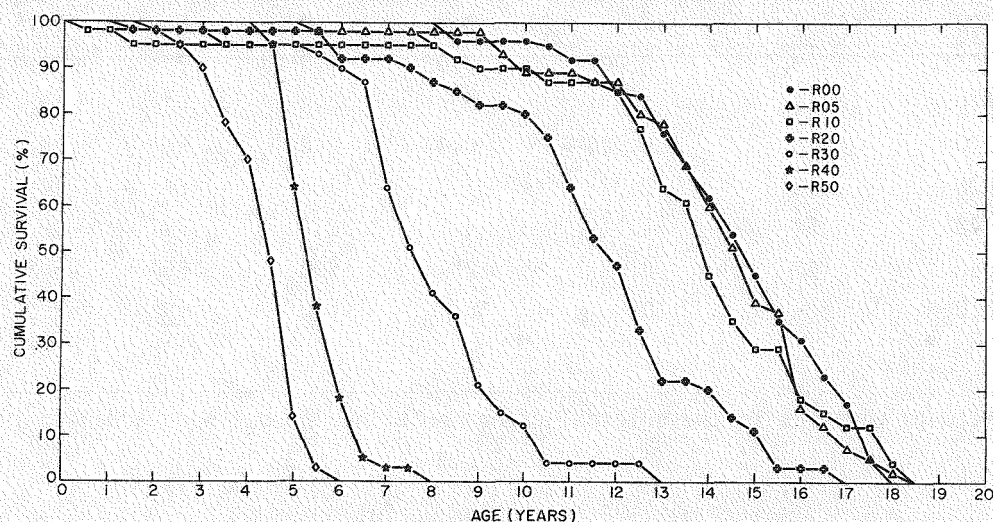


Fig. 1. Cumulative survival curves of beagle dogs given eight fortnightly intravenous injections of ^{226}Ra , the last of which occurred at 540 days of age.

Strontium-90 fed dogs at D05, D20, and D30 levels were not different from controls through 17 years of age (Figure 2), whereas D40s were significantly different from controls from 3 to 6 years and after 10 years of age; D50s after 3 years of age; and D60s after 2 years of age. Cumulative survival rates of S20 dogs were not different from controls (Figure 3).

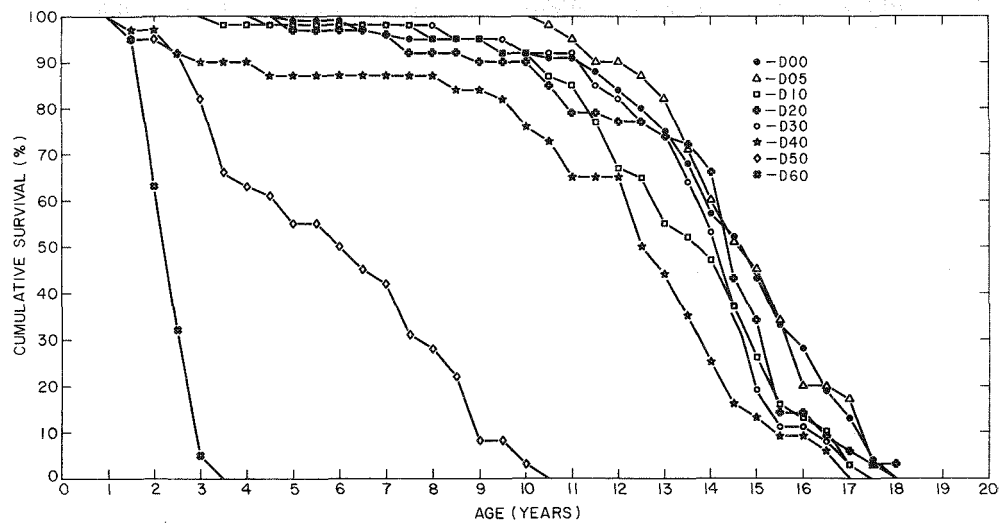


Fig. 2. Cumulative survival of beagles fed ^{90}Sr until 540 days of age.

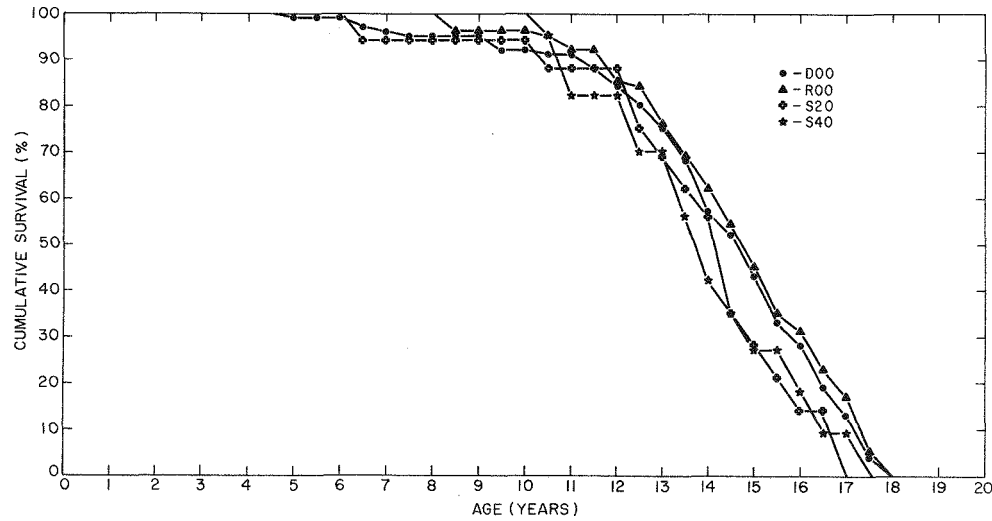


Fig. 3. Cumulative survival of beagles given a single intravenous injection of ^{90}Sr at 540 days of age.

The median survival time for unirradiated control beagles is 14.5 yr for D00s and 14.6 yr for R00s. Median survivals for each of the dose groups are given in Tables 1-3, above.

Radiation Doses

From the wide range of administered activities presented in Tables 1 and 2, variable body burdens of ^{226}Ra and ^{90}Sr were obtained. Soon after cessation of treatment, most of the radionuclides distributed in soft tissue were eliminated. The body burden, therefore, is essentially equivalent to the skeletal burden. Longer-term retention and, therefore, radiologic dose also varied among and within treatment levels.

Cumulative average skeletal doses (means for each group) are included in Table 3. Primarily because of differences in longevity, the 500-fold range of injected dosages for the radium dogs (Table 1) is reduced to a 180-fold range of average skeletal doses. Further, the 1500-fold range of ingested activities of ^{90}Sr is reduced to a 430-fold range.

Table 3. CUMULATIVE AVERAGE SKELETAL DOSES (MEAN VALUES FOR EACH GROUP).

Level	Mean (\pm SEM) Dose (rads)	Level	Mean (\pm SEM) Dose (rads)
R00	--	D00	--
R05	90 \pm 3	D05	30 \pm 2
R10	290 \pm 20	D10	130 \pm 5
R20	1400 \pm 50	D20	800 \pm 30
R30	3100 \pm 110	D30	2600 \pm 90
R40	7800 \pm 330	D40	6100 \pm 270
R50	16000 \pm 700	D50	9700 \pm 540
		D60	13000 \pm 870
		S20	750 \pm 70
		S40	6200 \pm 420

Causes of Death of Control, ^{90}Sr -, and ^{226}Ra -Treated Beagles

The causes of death are presented in Table 4 (pages 10-26) of this report. The following description applies to the individual tabulated data:

The study evolved in three production runs. The "Pilot Series" was initiated in 1961-63 with ^{90}Sr feeding of D05-, D20-, D30-, D40-, and D50-level dogs prior to completion of construction of all facilities. In the "First Run," 1963-64, half of the controls, the ^{90}Sr -fed or -injected dogs, and the ^{226}Ra -injected dogs were treated, with maximum facility utilization. At this time, 15 dogs (7 D30s, 4 D40s, and 4 D50s) were fed ^{90}Sr , but instead of ^{90}Sr administration ending at 540 days of age, it continued for their lifetimes. These dogs are designated "continuous feeding" dogs and have been discussed recently (Book et al., 1982). The "Second Run," 1965-67, completed the required number of experimental animals. In 1967 a group of beagles was introduced at the D60 level to provide toxicity data for a higher exposure level. At about the same time, a small group of dogs (designated R5X) received their R50-level injections beginning at either 60 or 120 days of age, rather than at 435 days, for the study of ^{226}Ra effects in early life.

Dogs dying or otherwise removed from the study prior to weaning (at 42 days of age) are not included. No difference in mortality of young beagles before weaning was found between control and irradiated groups (Rosenblatt et al., 1972). Previous reference to

"scheduled sacrifice" dogs has been deleted because there were no "scheduled sacrifices." Special sacrifices are listed in the comments column of Table 4. Some unexposed R dogs and young D dogs previously listed have also been deleted.

In the individual data, both birthdate and age are given and litters are grouped. Dogs with the same 3 digits in the "Litter Number" column are littermates. "Age at Termination" refers to the age at which some treatment or procedure was initiated which may affect interpretation of the results--BCG therapy for mammary cancer, for example.

For each dog that received radioactivity, the peak body burden in μ Ci and in μ Ci/kg body weight is presented. Values are the highest actual counts determined by periodic whole body counting. For S-dogs, counts were made 3-4 weeks after the single injection of ^{90}Sr ; hence, the "peak" in this instance is less than the quantity injected (Table 2).

"Exposure Days" refers to the time of exposure to radioactivity, equal to age for D-dogs, but equal to age minus 540 for S-dogs and age minus 435 for all R-dogs other than R5X. For the R5X dogs, exposure days is age minus 119 for F01, age minus 124 for M02 and M03, and age minus 63 for M04, M05, and M06. For dogs with termination dates, exposure ends at termination rather than at death.

"Total Dose" is the cumulative skeletal rads received by each animal and is the lifetime integration of the skeletal rads/day curve determined by periodic counting of whole body radioactivity. For these calculations, we assumed the skeletal burden to be 100% of the body burden for ^{226}Ra , 98% of the body burden for ^{90}Sr after cessation of ^{90}Sr feeding, and 88% of the body burden for ^{90}Sr during ^{90}Sr feeding. Other aspects of dose calculations have been discussed previously (Raabe et al., 1981).

"Comments" summarize our assessment of the primary factor contributing to each animal's death. The diagnoses are not necessarily final and should be considered preliminary. As additional information is gained, the comments may require change. Hence, the reader should use caution when drawing conclusions from these data. In addition, these comments do not include secondary and complicating factors, some of which may have a radiation-related etiology. For instance, an animal that had died of a myeloproliferative disorder may also have had a microscopic bone tumor. Although induced by irradiation and so noted in the dog's records, this latter occurrence would not appear in this summary. The "Comments" in this report differ from previous reports in that they represent a reappraisal of the clinical and histopathologic records. Particular attention was paid to those deaths previously listed as accidental.

The following symbols are used:

MPS - myeloproliferative syndrome

C - continuous (lifetime) feeding of ^{90}Sr

BCG - treatment of mammary tumor with intralesional injection of BCG (Bacillus of Calmette Guerin)

A - indicates an amputation of a limb. A list of those dogs and reasons for amputation was given in the 1984 Annual Report (UCD 472-130, pp. 6-8).

REFERENCES

Book, S. A., W. L. Spangler and L. A. Swartz. Effects of lifetime ingestion of ^{90}Sr in beagle dogs. 1982. *Rad. Res.* 90:244.

Rosenblatt, L. S., S. W. Bielfelt and D. J. Della Rosa. 1972. In M. Goldman and L. K. Bustad (eds.), Biomedical Implications of Radiostrontium Exposures. AEC Symposium No. 25, p. 334.

Raabe, O. G., S. A. Book, N. J. Parks, C. E. Chriss and M. Goldman. 1981. Lifetime studies of ^{226}Ra and ^{90}Sr toxicity in beagles - a status report. *Rad. Res.* 86:515-538.

Table 4. DATA FOR CONTROL BEAGLES AND BEAGLES EXPOSED TO ^{90}Sr AND ^{226}Ra .

(Table 4 follows on pages 10 ~ 26)

BEAGLE NUMBER	LITTER NUMBER	BIRTH DATE	AGE AT TERM.	AGE AT DEATH	PEAK BODY (UCI)	BURDEN (UCI/KG)	EXPOSURE DAYS	TOTAL DOSE (RADs)	COMMENTS
FIRST RUN									
D00F01	307A	12/14/63		17.3					METASTATIC MAMMARY CARCINOMA
D00F02	307B	12/14/63		15.3					LEIOMYOSARCOMA-URETHRA
D00F03	307C	12/14/63		12.5					METASTATIC THYROID CARCINOMA
D00M04	307D	12/14/63		14.0					PERITONITIS SECONDARY TO DUODENAL ULCERS
D00F05	329A	3/11/64		15.5					METASTATIC MAMMARY CARCINOMA
D00M06	329B	3/11/64		17.0					METASTATIC SEMINOMA
D00F08	346B	4/23/64		14.4					METASTATIC HEMANGIOSARCOMA
D00M09	346C	4/23/64		15.6					LYMPHOSARCOMA
D00M10	346D	4/23/64		12.0					LYMPHOSARCOMA
D00F11	347A	4/23/64		13.7					METASTATIC MAMMARY CARCINOMA
D00F12	347B	4/23/64		11.2					MALIGNANT LYMPHOMA
D00M14	347D	4/23/64		6.9					CHRONIC PULMONARY DISEASE WITH COR PULMONALE
D00F16	353A	5/12/64		15.6					ACUTE NECROTIZING PNEUMONIA-ASPIRATION, AND LYMPHOSARCOMA
D00F19	353D	5/12/64		14.0					PITUITARY TUMOR
D00M20	353E	5/12/64		12.8					MALIGNANT LYMPHOMA
D00M21	353F	5/12/64		3.5					CONVULSIONS, IDEOPATHIC EPILEPSY, ASPIRATION PNEUMONIA
D00F24	364C	6/ 3/64		15.0					METASTATIC COMPLEX TUBULAR ADENOCARCINOMA-MAMMARY GLAND
D00M26	364E	6/ 3/64		14.9					METASTATIC PERIANAL ADENOCARCINOMA
D00M27	364F	6/ 3/64		14.4					DISSEMINATED BRONCHOCENIC CARCINOMA
D00M28	364G	6/ 3/64		15.0					ADRENAL CORTICAL ATROPHY
D00F29	373A	6/16/64		12.3					CHRONIC VALVULAR ENDOCARDITIS WITH CONGESTIVE HEART FAILURE
D00M31	373C	6/16/64		9.2					HYDROCEPHALUS, SECONDARY TO PITUITARY TUMOR
D00F32	375A	6/17/64		16.6					METASTATIC MAMMARY ADENOCARCINOMA(SQUAMOUS CELL CARCINOMA) TO THE LUNG
D00F34	375C	6/17/64		11.4					METASTATIC MAMMARY CARCINOMA
D00F35	375D	6/17/64		12.3					METASTATIC SPLENIC HEMANGIOSARCOMA
D00M36	375E	6/17/64		11.5					CONGESTIVE HEART FAILURE SECONDARY TO ENDOCARDIOSIS
D00M37	375F	6/17/64		16.0					SENILE CEREBRAL ATROPHY
D00F39	376B	6/18/64		16.0					ADRENAL MEDULLARY NEOPLASM
D00M40	A 376C	6/18/64		14.7					SARCOMA NEAR VERTEBRA, ORIGIN UNKNOWN
D00M41	376D	6/18/64		12.7					
D00M43	376F	6/18/64		17.7					TRANSITIONAL CELL CARCINOMA OF THE PROSTATIC URETHRA
D00M47	380D	6/20/64		16.8					PULMONARY THROMBOSIS
D00M48	380E	6/20/64		6.0					UNDETERMINED CNS DISEASE
D00F49	404A	8/ 1/64		15.1					COLONIC INFARCTION AND SHOCK
D00F50	404B	8/ 1/64	4.3						DISSEMINATED MAMMARY CARCINOMA
D00M51	404C	8/ 1/64		17.2					CULLED (EPILEPSY) (GIVEN TO DR. HOLLIDAY)
D00M53	404E	8/ 1/64		13.4					INTERSTITIAL PNEUMONIA AND BRONCHIECTASIS
D00F54	428A	10/ 8/64		13.0					SALIVARY GLAND ADENOCARCINOMA OR ORAL MELANOMA
D00M57	428D	10/ 8/64		13.3					METASTATIC MAMMARY CARCINOMA
D00M58	428E	10/ 8/64		16.1					METASTATIC TRANSITIONAL CELL CARCINOMA OF THE URINARY BLADDER
									CHRONIC RENAL FAILURE / CNS DEFICIENCY
SECOND RUN									
D00F62	490C	9/10/65		17.3					ACUTE ENDOCARDITIS AND MYOCARDITIS
D00M64	490E	9/10/65		17.5					INTERVERTEBRAL DISC DEGENERATION AND HERNIATION
D00F66	507A	11/ 5/65		14.1					VACUULAR HEPATOPATHY-HEPATIC INSUFFICIENCY
D00F67	507B	11/ 5/65		17.0					DISSEMINATED MAMMARY ADENOCARCINOMA
D00F69	507D	11/ 5/65		16.4					SQUAMOUS CELL CARCINOMA, RIGHT TONSIL
D00M70	507E	11/ 5/65		14.7					SQUAMOUS CELL CARCINOMA--TONSIL
D00M71	507F	11/ 5/65		15.6					NECROTIZING MYOCARDITIS, ETIOLOGY UNKNOWN
D00F73	514B	12/22/65		17.7					CHRONIC RENAL DISEASE
D00F74	514C	12/22/65		13.6					CHRONIC SUPPURATIVE FOLLICULODERMATITIS (DEMODEX)
D00F75	514D	12/22/65		15.4					MPS
D00F78	549A	6/10/66		12.4					ACUTE ASPIRATION BRONCHOPNEUMONIA (ASPIRATED VOMITUS)
D00F80	A 549C	6/10/66		17.6					ORAL MALIGNANT MELANOMA WITH METASTASIS
D00M82	549E	6/10/66		13.2					METASTATIC HEART BASE TUMOR
D00M83	549F	6/10/66		16.0					CHRONIC SUPPURATIVE PNEUMONIA
D00F85	554A	6/25/66		13.6					ACUTE NECROTIZING PNEUMONIA-BACTERIAL
D00F86	554B	6/25/66		7.3					CHRONIC MEMBRANOPROLIFERATIVE LOMERULONEPHRITIS WITH SEVERE SECONDARY SYSTEMIC UREMIA

BEAGLE NUMBER	LITTER NUMBER	BIRTH DATE	AGE AT TERM.	AGE AT DEATH	PEAK BODY BURDEN (UCI)	EXPOSURE DAYS	TOTAL DOSE (RADs)	COMMENTS
D00F87	554C	6/25/66		14.6				HEPATIC FAILURE SECONDARY TO LYMPHOSARCOMA/MYOCARDIAL NECROSIS
D00M88	554D	6/25/66		11.9				CONGESTIVE HEART FAILURE
D00M89	554E	6/25/66		16.4				MPS
D00M90	554F	6/25/66		17.5				OSTEOSARCOMA WITH METASTASIS
D00F91	559A	7/ 2/66		15.2				SENILE ENCEPHALOPATHY (CNS DEFICIENCY). MAY ALSO HAVE HAD ENDOCARDITIS
D00F92	559B	7/ 2/66		9.3				METASTATIC HEMANGIOSARCOMA OF THE R ATRIUM
D00M94	559D	7/ 2/66		12.9				UNDETERMINED--POST MORTEM AUTOLYSIS
D00M96	559F	7/ 2/66		16.3				CHRONIC PYELONEPHRITIS
D00X03	565C	8/ 4/66		16.1				SEVERE PROGRESSIVE RENAL DISEASE
D00X04	565D	8/ 4/66		16.1				METASTATIC MAMMARY CARCINOMA
D00Y05	565E	8/ 4/66		10.3				TRANSITIONAL CELL CARCINOMA OF THE PROSTATIC URETHRA
D00Y06	565F	8/ 4/66		15.2				BACTERIAL ENDOCARDITIS
D00Y07	565G	8/ 4/66		17.4				SPINAL MYELOPATHY (LUMBAR). ALSO RENAL FAILURE
D00X08	577A	11/10/66		13				ACCIDENTAL DEATH (ANESTHETIC DEATH)
D00Y10	577C	11/10/66		14.0				CONGESTIVE HEART FAILURE/BRONCHOPNEUMONIA
D00X13	579C	11/17/66		14.8				METASTATIC PANCREATIC ADENOCARCINOMA
D00X15	580A	11/18/66		17.4				METASTATIC MAMMARY CARCINOMA
D00Y17	580C	11/18/66		13.7				EMBOLIC PNEUMONIA
D00Y18	580D	11/18/66		13.4				METASTATIC ISLET CELL CARCINOMA
D00Y19	580E	11/18/66		17.1				INTRACTABLE COUGH / PULMONARY INTERSTITIAL FIBROSIS
D00X20	620A	6/ 5/67		14.3				ADRENAL CORTICAL ATROPHY
D00X23	638B	9/12/67		14.0				LYMPHOSARCOMA
D00X24	638C	9/12/67		16.7				LYMPHOCYTIC ENTERITIS - MALABSORPTION
D00X25	638D	9/12/67		5.0				ENTEROPATHY
D00Y27	638F	9/12/67		14.6				NASAL CARCINOMA

PILOT SERIES

D05F02	098B	1/28/61		14.4	.32	.041	5267	20 METASTATIC CARCINOMA - HEPATOCELLULAR AND ADRENAL CORTICAL
D05F03	098C	1/28/61	7.8	.45	.043		19 TERMINATED (EPILEPSY)	
D05M04	098D	1/28/61		14.9	.41	.047	5443	22 MALIGNANT LYMPHOMA
D05M05	098E	1/28/61	7.8	.41	.038		30 TERMINATED (EPILEPSY)	
D05F08	099B	2/ 1/61		15.9	.25	.024	5819	22 CENTRAL NERVOUS SYSTEMS SIGNS (SEVERE PURKINJE CELL
								DEGENERATION)
D05M10	099D	2/ 1/61		16.7	.29	.027	6085	27 SEVERE POSTERIOR PARESIS, ACUTE SEVERE PROSTATIC INFECTION,
D05M11	099E	2/ 1/61		16.0	.34	.036	5850	34 PROGRESSIVE RENAL FAILURE
D05F12	102A	2/16/61	16.1	16.1	.25	.052	5883	34 CENTRAL NERVOUS SYSTEMS SIGNS (SEVERE PURKINJE CELL
D05F14	102C	2/16/61		16.2	.36	.049	5929	38 DEGENERATION)
D05F15	102D	2/16/61		13.3	.48	.100	4855	23 BRONCHOPNEUMONIA, ACUTE, CHRONIC
D05F17	209A	6/20/62		9.9	.21	.029	3621	38 AORTIC THROMBOSIS
D05F18	209B	6/20/62		12.8	.25	.041	4682	18 HEPATOCELLULAR ADENOMA
D05F19	209C	6/20/62		10.8	.29	.036	3957	18 TRANSITIONAL CELL CARCINOMA OF THE URINARY BLADDER
D05M20	209D	6/20/62		15.0	.35	.042	5482	31 METASTATIC THYROID CARCINOMA
D05M21	209E	6/20/62		16.5	.38	.039	6028	30 CHRONIC PYELONEPHRITIS, DRUG REACTION, AND CARDIOMEGALY
D05M22	209F	6/20/62		14.3	.36	.034	5215	36 DISSEMINATED INTRAVASCULAR COAGULATION,
D05F23	227A	9/20/62		14.4	.30	.036	5270	39 CLOSTRIDIUM SEPTICEMIA, THROMBOSIS
D05F24	227B	9/20/62		9.4	.34	.035	3450	30 METASTATIC ADRENAL CARCINOMA WITH DISSEMINATED INTRAVASCULAR
D05M26	227D	9/20/62		12.0	.30	.029	4401	COAGULOPATHY
D05M27	227E	9/20/62		6.6	.49	.037	2416	30 METASTATIC MAMMARY CARCINOMA
D05F28	233A	11/12/62	15.3	15.6	.29	.028	5714	28 NASAL CARCINOMA
D05M31	233D	11/12/62		5.1	.33	.032	1876	32 MALIGNANT LYMPHOMA
								32 GRANULOMATOUS ENCEPHALITIS
								26 TERMINATED-BCG EXPERIMENT
								END STAGE RENAL DISEASE SECONDARY TO BILATERAL RENAL
								ARTERIOSCLEROSIS
								21 CLOSTRIDIAL SEPTICEMIA

BEAGLE NUMBER	LITTER NUMBER	BIRTH DATE	AGE AT TERM.	AGE AT DEATH	PEAK BODY (UCI)	BURDEN (UCI/KG)	EXPOSURE DAYS	TOTAL DOSE (RADs)	COMMENTS
FIRST RUN									
D05F36	330A	3/12/64		13.1	14.9	.30	.039	5430	32 TERMINATED-BCG EXPERIMENT BCG SACRIFICE
D05F37	330B	3/12/64			17.5	.23	.040	6383	15 CHRONIC PROGRESSIVE ARTHRITIS
D05F38	330C	3/12/64		3.8	3.8	.24	.035	1386	14 ACCIDENTAL DEATH (TERMINATED FOR POSITIVE DIROFILARIASIS TEST)
D05F40	330E	3/12/64			14.9	.37	.039	5433	34 METASTATIC MAMMARY CARCINOMA
D05F42 A	338B	3/31/64		8.9	9.5	.26	.036	3485	20 METASTATIC UNDIFFERENTIATED MALIGNANT TUMOR OF THE L REAR 4TH DIGIT
D05M43	338C	3/31/64			13.7	.40	.046	5013	43 CHOLETHIASIS (BILE DUCT OBSTRUCTION) AND MULTIPLE HEPATOCELLULAR ADENOMAS
D05M44	338D	3/31/64			16.5	.43	.049	6036	30 PHEOCHROMOCYTOMA
D05F46	349A	4/26/64			11.0	.27	.037	4029	26 IDIOPATHIC EPILEPSY
D05F47	349B	4/26/64			15.1	.30	.039	5514	24 CONGESTIVE HEART FAILURE
D05F48	349C	4/26/64			13.4	.26	.041	4894	21 ANESTHETIC DEATH WITH CARDIOMEGLY, TOOTH ABSCESS AND CUSHING'S DISEASE
D05M49	349D	4/26/64			10.9	.22	.029	3981	22 EPENDYOMA OF THE THIRD VENTRICLE, BRAIN
D05M50	349E	4/26/64			15.1	.37	.037	5533	38 HEMANGIOSARCOMA
D05F53	367C	6/ 4/64			17.1	.45	.053	6258	84 METASTATIC MAMMARY CARCINOMA
D05F54	367D	6/ 4/64			10.1	.47	.047	3698	48 HEMANGIOSARCOMA OF THE SPLEEN
D05M59	367I	6/ 4/64			13.6	.48	.055	4956	55 CHRONIC PROSTATITIS
D05F60	383A	7/ 2/64			12.9	.31	.045	4702	32 CHRONIC PYELONEPHRITIS
D05F61	383B	7/ 2/64			15.4	.18	.030	5625	18 CNS DISEASE OF UNDETERMINED ORIGIN
D05M64	383E	7/ 2/64			17.6	.30	.040	6410	55 HEPATIC ATROPHY
D05F65	403A	7/31/64			13.4	.56	.071	4899	25 METASTATIC MAMMARY CARCINOMA
D05M66	403B	7/31/64			13.3	.29	.041	4843	31 METASTATIC PULMONARY ADENOCARCINOMA
D05M67	403C	7/31/64			13.2	.37	.046	4836	45 MALIGNANT LYMPHOMA
SECOND RUN									
D05F68	491A	9/11/65		13.3	.24	.032	4857	30 MALIGNANT MELANOMA	
D05M69	491B	9/11/65		14.5	.34	.031	5288	40 CONGESTIVE HEART FAILURE	
D05M70	491C	9/11/65		13.6	.37	.043	4966	50 ADAMANTINOMA	
D05M71	491D	9/11/65		1.8	.57	.037	649	10 ACCIDENTAL DEATH (ANESTHETIC DEATH - ANESTHETIZED FOR WHOLE BODY COUNTING)	
D05F72	500A	9/28/65		13.3	.16	.026	4868	17 TRANSITIONAL CELL CARCINOMA-URETHRA	
D05F73	500B	9/28/65		13.7	.28	.034	5011	45 METASTATIC MAMMARY CARCINOMA/CONGESTIVE HEART FAILURE	
D05F74	500C	9/28/65	11.5	12.6	.38	.037	4585	43 TERMINATED-BCG EXPERIMENT METASTATIC MAMMARY CARCINOMA	
D05F75	500D	9/28/65		11.3	.28	.032	4111	45 METASTATIC MAMMARY CARCINOMA	
D05F76	500E	9/28/65		17.3	.29	.034	6315	36 CHRONIC INTERVERTEBRAL DISC DISEASE	
D05M77	500F	9/28/65		1.2	.37	.038	433	5 PERITONITIS (FROM DOG BITE)	
D05F85	569B	9/17/66		15.7	.19	.022	5732	19 INTERVERTEBRAL DISC HERNIATION	
D05F86	569C	9/17/66		15.1	.20	.026	5499	19 METASTATIC PANCREATIC ADENOCARCINOMA	
D05M88	569E	9/17/66		11.1	.24	.030	4037	27 NEPHROSCLEROSIS	
D05M89	569F	9/17/66		17.2	.29	.030	6300	28 FOOT INFECTION WITH TOXEMIA/DIC	
D05M90	569G	9/17/66		15.9	.37	.038	5798	43 INTERVERTEBRAL DISC HERNIATION	
D05M91	569H	9/17/66		15.7	.27	.027	5719	30 CHRONIC, ACUTE PERITONITIS, SEPTICEMIA	
D05F92	592A	12/21/66		14.2	.27	.026	5199	43 ACUTE BRONCHOPNEUMONIA	
D05M93	592B	12/21/66		14.8	.34	.036	5422	50 DISSEMINATED HEMANGIOSARCOMA	
D05M94	592C	12/21/66		11.4	.34	.042	4172	40 SUPPURATIVE PROSTATITIS	
D05M95	592D	12/21/66		17.5	.32	.028	6389	50 LYMPHOSARCOMA	
D05M96	592E	12/21/66		17.1	.37	.045	6245	55 CHRONIC RENAL DISEASE	
D05X02	593B	12/23/66		11.9	.27	.039	4350	36 METASTATIC MAMMARY CARCINOMA	
D05X03	593C	12/23/66		16.9	.20	.031	6164	29 CHRONIC SEVERE PYELONEPHRITIS	
D05X04	593D	12/23/66		16.5	.26	.034	6032	39 CHRONIC RENAL DISEASE	
D05X05 A	593E	12/23/66		13.4	.18	.024	4885	19 INTERVERTEBRAL DISC DISEASE, CHRONIC ACUTE	
D05Y06	593F	12/23/66		14.8	.17	.025	5411	18 ORAL MALIGNANT MELANOMA WITH PULMONARY METASTASIS	
D05Y07	593G	12/23/66		14.8	.20	.028	5416	30 METASTATIC RENAL CARCINOMA	
D05X08	602A	3/16/67		14.4	.29	.038	5276	29 METASTATIC MAMMARY CARCINOMA	
D05X09	602B	3/16/67		12.2	.27	.033	4452	26 INVASIVE ORAL NEOPLASM	
D05Y11	602D	3/16/67		12.9	.29	.039	4712	43 CHRONIC INTERSTITIAL PNEUMONIA/ARTERIOSCLEROSIS	
D05Y13	634B	8/22/67		15.9	.46	.034	5825	55 UNDETERMINED	
D05Y14	634C	8/22/67		15.8	.49	.045	5770	50 ADRENAL CORTICAL CARCINOMA METASTATIC TO LUNGS	
D05Y15	634D	8/22/67	11.3	11.3	.37	.032	4123	35 MALIGNANT LYMPHOMA (INTESTINAL)	

BEAGLE NUMBER	LITTER NUMBER	BIRTH DATE	AGE AT TERM.	AGE AT DEATH	PEAK BODY (UCI)	BURDEN (UCI/KG)	EXPOSURE DAYS	TOTAL DOSE (RADS)	COMMENTS
D05Y16	634E	8/22/67		18.5	.40	.035	6764	42	SUPPURATIVE HEPATITIS (HEPATIC ABSCESS)
D05Y17	634F	8/22/67		15.9	.35	.036	5811	32	HEPATOCELLULAR CARCINOMA/LIVER FAILURE
FIRST RUN									
D10F02	310B	12/20/63		9.5	.83	.101	3454	97	PITUITARY TUMOR WITH CUSHING'S DISEASE
D10M04	310D	12/20/63		13.7	.84	.102	4993	134	METASTATIC RENAL CARCINOMA
D10M05	310E	12/20/63		14.4	.99	.102	5247	162	URETHRAL STRICTURE SECONDARY TO PROSTATECTOMY
D10F10	361B	5/24/64		11.9	.72	.087	4363	120	METASTATIC MAMMARY CARCINOMA
D10F11	361C	5/24/64		11.1	.79	.092	4069	118	METASTATIC PULMONARY ADENOCARCINOMA
D10M12	361D	5/24/64		14.2	1.13	.121	5169	148	PRIMARY PULMONARY NEOPLASM OF BRONCHIOLAR ORIGIN
D10F17	386A	7/ 5/64		13.8	.58	.074	5027	97	ACCIDENTAL (ASPIRATED GLYCOL WHEN TREATED FOR GLAUCOMA - LED TO ASPIRATION PNEUMONIA)
D10F18	386B	7/ 5/64		15.0	.52	.070	5490		
D10M19	386C	7/ 5/64		3.4	1.02	.123	1241	88	BRONCHOGENIC CARCINOMA
D10M20	386D	7/ 5/64		15.3	1.00	.098	5570	55	MYELOMALACIA
D10F22	409A	8/11/64		12.5	.75	.093	4559	163	PITUITARY CARCINOMA
D10F25	409D	8/11/64		12.8	.80	.091	4682	119	METASTATIC MAMMARY CARCINOMA
D10M26	409E	8/11/64		14.7	.79	.090	5355	115	METASTATIC ADRENAL CARCINOMA
D10F36	423A	9/25/64		16.9	.92	.117	6173	128	CNS DISEASE OF UNDETERMINED ORIGIN
D10M39	423D	9/25/64		13.0	.90	.096	4732	153	INTERVERTEBRAL DISC DISEASE(DEGENERATIVE MYELOPATHY)
D10M40	423E	9/25/64		14.7	.98	.111	5358	127	TRANSITIONAL CELL CARCINOMA OF THE PROSTATIC URETHRA
D10F41	445A	12/ 7/64		10.7	.76	.076	3913	157	FIBROSARCOMA-NEURAL
D10F42	445B	12/ 7/64		11.2	1.06	.104	4095	96	MYOCARDIAL DEGENERATION, CARDIAC HYPERTROPHY
D10M45	445E	12/ 7/64		11.9	1.29	.125	4328	136	FOCAL ENCEPHALOMALACIA
D10M46	445F	12/ 7/64		14.5	1.15	.112	5281	178	CONGESTIVE HEART FAILURE (RUPTURED CHORDA TENDONAE)
								180	METASTATIC HEMANGIOSARCOMA
SECOND RUN									
D10F52	510B	12/ 9/65		7.6	.91	.099	2794		
D10F53	510C	12/ 9/65		17.3	.90	.083	6328	83	INTESTINAL LYMPHANGIECTASIA
D10F54	510D	12/ 9/65		14.1	.91	.090	5147	135	LACRIMAL GLAND CARCINOMA
D10F55	510E	12/ 9/65		13.0	.97	.102	4761	134	ACUTE NECROTIZING ENTERITIS (PARVOVIRUS)
D10M58	510H	12/ 9/65		16.9	1.06	.090	6157	136	CHRONIC PANCREATITIS
D10M60	543B	5/19/66		12.8	1.09	.113	4671	145	CHRONIC INTERVERTEBRAL DISC DISEASE
D10M61	543C	5/19/66		15.3	.86	.097	5574	168	CONGESTIVE HEART FAILURE
D10M62	543D	5/19/66		10.5	1.05	.099	3819	137	PLEURAL EFFUSION - ETIOLOGY UNKNOWN
D10F64	561B	7/ 8/66		12.0	1.02	.133	4367	127	POSTERIOR PARALYSIS (UNDETERMINED CAUSE)
D10M65	561C	7/ 8/66		12.9	1.20	.134	4723	140	METASTATIC MAMMARY CARCINOMA
D10M66	561D	7/ 8/66		12.7	.83	.085	4654	159	CARDIAC ARREST UNDER ANESTHESIA FOR HEMANGIOSARCOMA-SPLEEN
D10M69	562C	7/13/66		11.4	1.22	.134	4180	119	CHRONIC PYELONEPHRITIS
D10F71	581B	11/19/66		16.9	.54	.060	6166	142	MALIGNANT LYMPHOMA
D10M72	581C	11/19/66		10.2	.58	.077	3713	98	INTERVERTEBRAL DISC DISEASE
D10M73	581D	11/19/66		15.4	.96	.100	5638	86	MULTIPLE ENDOCRINOPATHY (HYPOPLASIA OR ATROPHY)
D10M74	581E	11/19/66		14.7	.68	.070	5360	157	PRIMARY LYMPHOSARCOMA OF BRAINSTEM
D10F75	618A	5/23/67		11.7	.48	.070	4287	120	METASTATIC HEMANGIOSARCOMA
D10F76	618B	5/23/67		15.7	.69	.087	5726	90	METASTATIC MAMMARY CARCINOMA
D10F77	618C	5/23/67		16.1	.93	.095	5895	136	CUSHING'S DISEASE
D10M82	618H	5/23/67		14.6	1.10	.095	5323	175	CUSHING'S DISEASE
								167	ACUTE EXUDATIVE INTERSTITIAL PNEUMONIA
PILOT SERIES									
D20F02	103B	2/16/61		15.6	2.33	.458	5713	646	HEPATIC ABSCESS
D20M04	103D	2/16/61		15.7	4.11	.563	5731	845	METASTATIC MALIGNANT MELANOMA OF THE BUCCAL CAVITY
D20F06	104A	2/20/61		17.3	4.39	.575	6336	776	LEUKOENCEPHALOMALASIA
D20M09	104D	2/20/61		.7					ACCIDENTAL DEATH (ANESTHETIC DEATH - ANESTHETIZED FOR DEBARKING)
D20M10	104E	2/20/61		14.1	4.59	.431	5149	692	ACUTE PULMONARY COAGULOPATHY, CHRONIC PULMONARY AND HEPATIC THROMBOSIS, PULMONARY VASCULITIS
D20M11	104F	2/20/61		2.9	5.27	.565	1066	221	EPILEPSY
D20F15	149B	9/30/61		10.2	3.11	.556	3720	615	CHRONIC PULMONARY DISEASE
D20F16	149C	9/30/61		13.7	4.79	.682	5014	939	METASTATIC AORTIC BODY TUMOR
D20F17	149D	9/30/61		11.7	5.11	.601	4259	830	PYOMETRA AND ACUTE PERITONITIS

BEAGLE NUMBER	LITTER NUMBER	BIRTH DATE	AGE AT TERM.	AGE AT DEATH	PEAK BODY (UCI)	BURDEN (UCI/KG)	EXPOSURE DAYS	TOTAL DOSE (RADs)	COMMENTS	
D20F21	167D	1/ 1/62		10.0	5.90	.596	3668	652	MALIGNANT LYMPHOMA	
D20M22	167E	1/ 1/62		16.3	5.12	.544	5937	911	SEVERE CNS DISEASE	
D20M24	167G	1/ 1/62		14.2	6.95	.532	5204	796	INTERVERTEBRAL DISC HERNIATION	
D20F25	197A	5/19/62		17.6	5.13	.520	6433	778	METASTATIC MAMMARY CARCINOMA	
D20F26	197B	5/19/62		14.2	5.28	.478	5197	784	CONGESTIVE HEART FAILURE (RUPTURED CHORDA TENDONAE)	
D20M28	197D	5/19/62		9.8	6.43	.548	3590	655	RENAL CARCINOMA	
D20M29	197E	5/19/62		13.4	7.25	.678	4900	887	METASTATIC HEPATOCELLULAR CARCINOMA	
D20M30	197F	5/19/62		15.3	6.47	.573	5570	849	METASTATIC RENAL CARCINOMA	
D20M31	197G	5/19/62		15.9	6.87	.608	5807	1001	SENILITY	
D20F32	263A	6/25/63		13.7	5.94	.733	5001	1137	HEPATOCELLULAR ADENOMA AND ASPIRATION PNEUMONIA	
D20F33	263B	6/25/63		10.6	4.76	.638	3889	765	HEPATOCELLULAR ADENOMA	
D20M34	263C	6/25/63		9.5	6.31	.568	3453	736	HEPATOCELLULAR CARCINOMA	
D20M35	263D	6/25/63		14.7	6.05	.599	5374	998	ACUTE PERITONITIS SECONDARY TO PROSTATITIS	
D20M36	263E	6/25/63		16.6	5.92	.771	6047	1360	INTERVERTEBRAL DISC DISEASE	
FIRST RUN										
D20F40	288B	11/ 3/63		14.1	3.22	.370	5163	614	UNDETERMINED	
D20F41	288C	11/ 3/63		13.8	3.56	.396	5026	598	BRONCHOPNEUMONIA	
D20M42	288D	11/ 3/63		12.8	4.39	.481	4685	739	NASAL CARCINOMA	
D20F53	354D	5/12/64		3.6	3.89	.477	1319	278	ASPIRATION PNEUMONIA-SECONDARY TO CONVULSIONS	
D20F54	354E	5/12/64	12.8	14.5	5.37	.554	5295	913	TUBERCULOSIS CAUSED BY BCG (GRANULOMATOUS PLEURITIS AND PERICARDITIS)	
D20M55	354F	5/12/64		10.6	5.79	.534	3868	712	ASPIRATION PNEUMONIA DUE TO CRANIAL ABSCESS SECONDARY TO CHRONIC OTITIS INTERNA	
D20M56	354G	5/12/64		15.2	7.61	.700	5552	1097	TRANSITIONAL CELL CARCINOMA-PROSTATIC URETHRA	
D20F57	357A	5/20/64		16.4	3.41	.522	5972	869	NEPHROSCLEROSIS, CHRONIC PYELONEPHRITIS	
D20M59	357C	5/20/64		15.3	3.70	.643	5599	993	INTERVERTEBRAL DISC DISEASE	
D20M60	357D	5/20/64		8.9	5.83	.627	3248	707	MALIGNANT LYMPHOMA	
D20F62	358A	5/22/64		10.6	4.42	.506	3854	618	PULMONARY ABSCESS	
D20M63	358B	5/22/64		10.2	5.80	.700	3736	775	MALIGNANT LYMPHOMA	
D20F66	378A	6/19/64		14.4	4.41	.456	5263	808	POST-SURGICAL SHOCK/PYOMETRA	
D20F67	378B	6/19/64		14.4	4.54	.569	5266	844	ACUTE NECROTIZING ENTERITIS (PARVOVIRUS)	
D20M69	378D	6/19/64		14.0	4.92	.601	5114	952	HEART FAILURE (CLINICAL THIRD DEGREE HEART BLOCK)	
D20M70	378E	6/19/64		15.5	4.68	.534	5661	762	MYOCARDIAL INFARCTION	
D20F71	405A	8/ 3/64	12.7	14.5	5.19	.525	5293	888	CONGESTIVE HEART FAILURE	
D20F73	405C	8/ 3/64		15.4	4.43	.459	5635	843	TERMINATED-BCG EXPERIMENT	
D20M75	405E	8/ 3/64		7.4	7.01	.821	2692	725	BCG SACRIFICE	
D20M76	405F	8/ 3/64		16.5	5.24	.533	6011	808	UNDETERMINED	
D20M76									METASTATIC SPLENIC LEIOMYOSARCOMA	
D20M76									CHOLANGIOHEPATITIS(COMMON BILE DUCT OBSTRUCTION)	
SECOND RUN										
D20F78	480A	8/29/65		14.8	6.10	.586	5415	979	PITUITARY ADENOMA	
D20F79	480B	8/29/65		15.4	3.98	.436	5632	804	MPS	
D20F80	480C	8/29/65		14.4	4.17	.477	5255	723	PANCREATIC INSUFFICIENCY/MALABSORPTION	
D20M82	480E	8/29/65		17.1	5.28	.592	6262	695	CHRONIC RENAL DISEASE	
D20F84	533B	3/26/66		6.8	2.63	.452	2475	1002	NEPHROSCLEROSIS	
D20F89	546A	5/28/66		15.3	3.32	.500	5584	330	CHRONIC HEART FAILURE	
D20F90	546B	5/28/66		14.9	2.93	.516	5425	827	ACCIDENTAL DEATH (HEAT EXHAUSTION)	
D20F91	546C	5/28/66		4.0	3.66	.518	1465	834	CHOLANGIOHEPATITIS	
D20M94	546F	5/28/66		14.2	4.20	.517	5187	302	SQUAMOUS CELL CARCINOMA-TONSIL	
D20M95	546G	5/28/66		14.1	4.51	.590	5149	884	ENTEROPATHY & BRONCHIAL PNEUMONIA	
D20X01	582A	11/23/66		14.9	4.97	.536	5430	878	ULTIMOBRANCHIAL NEOPLASM	
D20Y03	582C	11/23/66		11.8	6.80	.546	4320	853	COAGULATION	
D20Y04	582D	11/23/66		16.9	5.78	.605	6173	804	CHRONIC BRONCHIECTASIS	
D20Y05	582E	11/23/66	13.5	13.5	6.20	.569	4943	928	PITUITARY NEOPLASM	
D20X06	586A	12/ 9/66		4.7	4.01	.597	1722	869	INTERVERTEBRAL DISC DISEASE	
D20X07	586B	12/ 9/66		15.1	3.61	.396	5523	316	SQUAMOUS CELL CARCINOMA-TONSIL	
D20Y09	586D	12/ 9/66		14.3	4.04	.498	5232	711	ENTEROPATHY & BRONCHIAL PNEUMONIA	
D20X12	596B	1/ 4/67		14.1	3.97	.539	5151	821	ULTIMOBRANCHIAL NEOPLASM	
D20X12									MALIGNANT HEART BASE TUMOR (CHEMOECTOMA)	
D20X12									COMPLEX ADENOCARCINOMA	

BEAGLE NUMBER	LITTER NUMBER	BIRTH DATE	AGE AT TERM.	AGE AT DEATH	PEAK BODY BURDEN (UCI)	EXPOSURE (UCI/KG)	EXPOSURE DAYS	TOTAL DOSE (RADs)	COMMENTS
D20X13	596C	1/ 4/67		13.1	5.92	.626	4767	823	BRONCHOGENIC CARCINOMA
D20Y15	596E	1/ 4/67		15.6	7.90	.702	5697	1331	ADRENAL NECROSIS/UNDETERMINED
D20Y16	596F	1/ 4/67		10.0	7.09	.698	3662	849	HEPATOCELLULAR ADENOMA
D20Y17	596G	1/ 4/67		17.8	8.02	.714	6502	1292	1)PROGRESSIVE POSTERIOR PARALYSIS 2)CHRONIC RENAL DISEASE
PILOT SERIES									
D30F02	A 114B	4/27/61		14.4	14.69	1.888	5277	2814	LYMPHOSARCOMA, HISTIOCYTIC TYPE
D30M10	115F	5/ 1/61		15.2	14.72	1.583	5567	2766	CONGESTIVE HEART FAILURE (RUPTURED CHORDA TENDONAE)
D30F16	121D	6/11/61		16.6	17.61	2.204	6078	3558	CEREBRAL ATROPHY
D30F19	122A	6/14/61		14.4	17.46	2.126	5250	3012	METASTATIC PULMONARY CARCINOMA
D30F20	122B	6/14/61		15.2	13.76	1.759	5536	2570	MALIGNANT LYMPHOMA
D30M21	122C	6/14/61		1.5	25.18	2.238	540	469	TERMINATED (EPILEPSY)
D30M22	122D	6/14/61		12.0	21.91	2.132	4389	2933	ACCIDENTAL (ANESTHETIC DEATH)
D30F25	194C	5/10/62		13.8	12.13	1.270	5033	1779	MALIGNANT LYMPHOMA
D30F26	194D	5/10/62	14.9	16.7	13.06	1.558	6088	2283	TERMINATED-BCG EXPERIMENT BCG-SACRIFICE
D30M27	194E	5/10/62		11.4	13.87	1.416	4180	1663	MALIGNANT MELANOMA OF THE GINGIVA
D30F28	228A	9/20/62		13.8	12.84	1.443	5053	2188	METASTATIC MAMMARY CARCINOMA
D30F29	228B	9/20/62		12.2	12.83	1.386	4459	1719	METASTATIC MAMMARY CARCINOMA
D30M30	228C	9/20/62		16.9	23.17	1.955	6158	3987	INTERVERTEBRAL DISC DISEASE
D30M31	228D	9/21/62		7.8	22.17	1.615	2859	1758	MALIGNANT LYMPHOMA
D30F33	250B	2/27/63		17.1	13.21	1.882	6236	3216	SQUAMOUS CELL CARCINOMA-GINGIVA
D30F34	250C	2/27/63		11.9	14.21	1.633	4332	2091	MPS
D30F35	250D	2/27/63		15.7	15.41	1.740	5739	2922	ACUTE NECROTIZING ENTERITIS (PARVOVIRUS)
D30F36	250E	2/27/63		10.6	15.92	1.744	3870	2158	ACCIDENTAL (ANESTHETIC DEATH - WHILE TAKING DIAGNOSTIC X-RAYS FOR LIPOMA REMOVAL)
D30M40	250I	2/27/63		7.9	13.91	1.718	2872	1575	MPS
FIRST RUN									
D30F41	296A	11/30/63		16.4	9.97	1.327	5997		
D30F43	296C	11/30/63		11.2	11.30	1.572	4099	1974	CHRONIC RENAL FAILURE/NEPHROSCLEROSIS
D30M46	296F	11/30/63		8.3	17.78	1.636	3041	1841	CHRONIC ACTIVE HEPATITIS
D30F49	299C	12/10/63		14.7	14.36	1.366	5371	1781	MALIGNANT LYMPHOMA
D30F50	299D	12/10/63		13.7	14.34	1.585	5005	2066	SQUAMOUS CELL CARCINOMA-GINGIVA
D30F51	C 299E	12/10/63		14.5	13.81	1.409	5302	2301	METASTATIC MAMMARY CARCINOMA
D30F52	299F	12/10/63		13.0	14.88	1.469	4758	3531	METASTATIC MAMMARY CARCINOMA
D30M54	299H	12/10/63		14.5	20.23	1.903	5286	2185	METASTATIC MAMMARY CARCINOMA
D30M55	299I	12/10/63		14.7	16.42	1.868	5376	2315	NASAL CARCINOMA
D30M56	C 299J	12/10/63		15.8	14.68	1.424	5768	2683	INTERVERTEBRAL DISC DISEASE WITH SPINAL MYELOPATHY
D30F57	327A	3/ 6/64		11.0	15.49	2.001	4030	3746	NASAL ADENOCARCINOMA
D30M58	327B	3/ 6/64		13.6	16.45	1.977	4980	2413	NASAL CARCINOMA
D30M59	327C	3/ 6/64		14.4	17.86	2.068	5247	2774	PITUITARY TUMOR WITH CUSHING'S DISEASE
D30M60	327D	3/ 6/64		14.9	17.21	2.074	5424	3165	INTERVERTEBRAL DISC DISEASE
D30M61	C 327E	3/ 6/64		5.3	22.10	1.868	1918	3455	CHRONIC RENAL DISEASE AND MYELOPATHY
D30F62	C 369A	6/ 9/64		13.9	10.93	1.262	5091	2188	MPS
D30F63	369B	6/ 9/64	12.8	14.5	9.65	1.520	5311	2916	CEREBRAL EDEMA SECONDARY TO CHRONIC ENTERITIS
								2112	DISSEMINATED INTRAVASCULAR COAGULATION
D30F65	369D	6/ 9/64						2464	PULMONARY ADENOCARCINOMA OR SUBCUTANEOUS HEMANGIOMA TERMINATED-BCG EXPERIMENT
D30M66	C 369E	6/ 9/64		12.5	11.62	1.306	4563		MALIGNANT LYMPHOMA
D30M67	369F	6/ 9/64		14.3	15.65	1.692	5225	2901	METASTATIC MALIGNANT MELANOMA OF THE BUCCAL CAVITY
D30M68	369G	6/ 9/64		16.6	13.87	1.611	6075	2437	PROSTATITIS, RUPTURED PROSTATIC ABSCESS
D30M78	443D	12/ 6/64		14.4	18.23	2.088	5276	2719	BRONCHOGENIC CARCINOMA
D30F79	450A	1/19/65		13.6	15.41	1.686	4973	3104	RENAL AMYLOIDOSIS
D30F80	450B	1/19/65		15.2	12.81	1.856	5538	2861	MALIGNANT LYMPHOMA
D30M81	C 450C	1/19/65		9.6	18.82	2.015	3508	2905	TRANSITIONAL CELL CARCINOMA
D30M82	C 450D	1/19/65		6.1	22.82	2.514	2233	2614	CONGESTIVE HEART FAILURE
D30M83	450E	1/19/65		12.9	17.21	1.963	4720	1993	MPS
							2780		HEPATOCELLULAR ADENOMA

BEAGLE NUMBER	LITTER NUMBER	BIRTH DATE	AGE AT TERM.	AGE AT DEATH	PEAK BODY (UCI)	BURDEN (UCI/KG)	EXPOSURE DAYS	TOTAL DOSE (RADS)	COMMENTS
SECOND RUN									
D30F86	482C	8/30/65		11.4	14.32	1.726	4174	2457	TRANSITIONAL CELL CARCINOMA OF THE URINARY BLADDER
D30F87	482D	8/30/65		11.7	11.42	1.211	4257	1978	CHRONIC INTERSTITIAL PULMONARY FIBROSIS
D30M88	482E	8/30/65		9.9	18.27	2.312	3634	2629	OSTEOSARCOMA OF THE 10TH THORACIC VERTEBRA
D30M89	482F	8/30/65		6.9	16.75	1.825	2533	1780	ACCIDENTAL DEATH (NEPHROTIC SYNDROME SECONDARY TO ANESTHESIA, AFTER SURGERY FOR IV DISK PROTRUSION)
D30M90	482G	8/30/65		4.5	20.88	1.834	1628		CHRONIC DERMATITIS, DEMODEX INFECTION
D30F92	492B	9/12/65		13.3	15.34	1.956	4846	1215	NASAL CARCINOMA
D30F93	492C	9/12/65		15.0	16.54	2.099	5481	2637	DISSEMINATED INTRAVASCULAR COAGULATION
D30M94	492D	9/12/65		17.4	17.12	2.141	6340	2996	CHRONIC RENAL DISEASE (NEPHROSCLEROSIS AND MEDULLARY NECROSIS)
D30F95	506A	11/ 3/65		14.5	15.33	2.049	5306	3421	BILIARY CYSTADENOCARCINOMA
D30F96	506B	11/ 3/65		14.6	13.17	1.655	5347		MALIGNANT MAMMARY TUMOR
D30M97	506C	11/ 3/65		15.5	18.92	2.271	5655	2868	HEMANGIOSARCOMA, BONE-RIB
D30M98	506D	11/ 3/65		14.8	18.45	2.269	5405	3945	SQUAMOUS CELL CARCINOMA-GINGIVA
D30M99 A	506E	11/ 3/65		13.9	19.39	2.436	5083	3906	HEPATITIS WITH BILIARY STASIS
D30X01	600A	3/ 9/67		14.3	16.16	1.834	5224	3710	CONGESTIVE HEART FAILURE
D30X02	600B	3/ 9/67		12.3	18.19	2.035	4497	2779	SENILE CNS DISEASE
D30X03	600C	3/ 9/67		14.4	16.98	1.674	5244	2583	POST-SURGICAL BRONCHOPNEUMONIA (AFTER SURGERY TO ENUCLEATE EYE FOR SEVERE KERATITIS)
D30Y04	600D	3/ 9/67		13.3	21.97	1.742	4863	2582	CONGESTIVE HEART FAILURE
D30Y05	600E	3/ 9/67		14.8	23.67	2.084	5418	2820	SEVERE VEGETATIVE ENDOCARDITIS
D30Y06	600F	3/ 9/67		15.1	24.88	2.154	5525	3627	PANCREATIC ACTINAR ADENOCARCINOMA
D30Y07	600G	3/ 9/67		15.6	27.29	2.359	5697		LEUKOENCEPHALOPATHY, SPONGY, CAUSE UNKNOWN
D30Y08	600H	3/ 9/67		11.8	26.77	2.092	4306	4128	OSTEOSARCOMA OF THE SPINE AT L1-2
D30Y11	617C	5/21/67		12.4	14.45	1.867	4518	3699	FIBROSARCOMA-GINGIVA
D30Y12	617D	5/21/67		16.5	10.80	1.734	6030	3155	ACCIDENTAL DEATH (CHOKED)
D30Y13	628A	7/16/67		13.4	20.01	1.476	4897	2506	ACCIDENTAL DEATH (CHOKED)

16

PILOT SERIES									
D40F03 A	152C	10/28/61		12.1	36.03	4.589	4426		
D40M04	152D	10/28/61		9.7	44.40	5.804	3555		METASTATIC OSTEOSARCOMA
D40M05	152E	10/28/61		5.9	51.10	6.317	2161	6471	TONSILLAR CARCINOMA
D40M06	152F	10/28/61		10.7	50.29	6.643	3903	6285	METASTATIC TONSILLAR CARCINOMA
D40F08	153B	10/31/61		15.1	44.50	5.401	5506	5084	MAXILLARY FIBROSARCOMA
D40M09	153C	10/31/61		8.4	61.75	5.163	3081	8392	ACCIDENTAL DEATH (CHOKED)
D40M10	153D	10/31/61		13.3	63.35	4.574	4867	8813	HEPATITIS WITH BILIARY STASIS
D40F11	161A	12/17/61		14.5	33.99	3.690	5290	4851	LEUKOENCEPHALOPATHY, SPONGY, CAUSE UNKNOWN
D40F12	161B	12/17/61		10.7	33.53	4.790	3925	4842	INTERVERTEBRAL DISC HERNIATION, OSTEOSARCOMA OF THE 4TH LUMBAR VERTEBRA, RENAL DISEASE
D40F14	161D	12/17/61		8.1	37.38	3.795	2971		ACCIDENTAL DEATH (CHOKED)
D40F15	161E	12/17/61		11.0	48.32	6.702	4022	4681	HEPATITIS WITH BILIARY STASIS
D40M25	198F	5/25/62		8.2	46.30	4.033	3002	4222	ACCIDENTAL DEATH (CHOKED)
D40F32	276A	8/28/63		13.1	50.43	5.109	4801	5798	MAXILLARY FIBROSARCOMA
D40F33	276B	8/28/63		8.6	58.18	4.893	3151	3561	ACCIDENTAL DEATH (CHOKED)
D40F34 A	276C	8/28/63		14.4	43.39	4.318	5256	7011	HEPATITIS WITH BILIARY STASIS
D40F35	276D	8/28/63	15.0	15.2	52.72	4.914	5553	6021	LEUKOENCEPHALOPATHY, SPONGY, CAUSE UNKNOWN
D40M37	276F	8/28/63		11.7	11.7	7.061	4277	8289	ACCIDENTAL DEATH (CHOKED)
D40M38	276G	8/28/63		13.0	73.56	6.639	4754		HEPATITIS WITH BILIARY STASIS
FIRST RUN									
D40F42	285D	10/26/63		14.1	38.37	3.833	5155		
D40M44	285F	10/26/63		12.2	59.69	5.268	4454	5775	ACCIDENTAL DEATH (CHOKED)
D40M45	285G	10/26/63		16.1	51.49	4.622	5879	7619	HEPATITIS WITH BILIARY STASIS
D40F49	316D	1/ 4/64		2.8	35.46	4.237	1010	8185	INTERVERTEBRAL DISC HERNIATION, OSTEOSARCOMA OF THE 4TH LUMBAR VERTEBRA, RENAL DISEASE
D40F50	316E	1/ 4/64		9.2	33.04	4.135	3361	1665	MAXILLARY FIBROSARCOMA
D40M51	316F	1/ 4/64		13.5	37.22	4.572	4937	3759	ACCIDENTAL DEATH (CHOKED)
D40F52	333A	3/24/64		10.8	46.55	5.254	3942	6192	HEPATITIS WITH BILIARY STASIS
D40M53	333B	3/24/64		13.2	40.10	4.456	4804	7129	ACCIDENTAL DEATH (CHOKED)
D40M54	333C	3/24/64		13.5	54.50	5.196	4929	6840	HEPATITIS WITH BILIARY STASIS

BEAGLE NUMBER	LITTER NUMBER	BIRTH DATE	AGE AT TERM.	AGE AT DEATH	PEAK BODY BURDEN (UCI)	(UCI/KG)	EXPOSURE DAYS	TOTAL DOSE (RADs)	COMMENTS
D40M55	C 333D	3/24/64		10.1	51.68	5.209	3677	9231	MPS
D40M56	333E	3/24/64		1.2	50.59	5.789	426	888	MPS
D40F62	C 368A	6/ 7/64		9.3	27.69	3.979	3405	5661	METASTATIC TRANSITIONAL CELL CARCINOMA OF THE RENAL PELVIS
D40F63	368B	6/ 7/64		16.6	30.92	3.462	6078	6010	METASTATIC PANCREATIC ADENOCARCINOMA
D40F64	368C	6/ 7/64		16.9	32.89	4.201	6169	7384	TRANSITIONAL CELL CARCINOMA
D40F67	C 411A	8/22/64		3.6	48.62	4.901	1332	2332	EPILEPSY
D40F68	411B	8/22/64		4.4	42.10	4.552	1590	2845	ACCIDENTAL DEATH (STRANGULATION ON CHAIN)
D40M69	411C	8/22/64		12.2	47.00	5.281	4468	8367	PITUITARY TUMOR WITH CUSHING'S DISEASE
D40M70	411D	8/22/64		12.1	60.02	5.408	4422	8312	HEPATOCELLULAR ADENOMA
D40M71	C 411E	8/22/64		2.8	46.96	4.882	1014	1883	EPILEPSY
D40M72	411F	8/22/64		12.5	60.35	4.411	4573	7311	SQUAMOUS CELL CARCINOMA OF THE GINGIVA
D40F74	429B	10/11/64		12.3	28.76	4.715	4502	6257	METASTATIC CARCINOMA OF UNDETERMINED ORIGIN
D40F75	429C	10/11/64		15.5	32.31	5.514	5659	8732	SQUAMOUS CELL CARCINOMA-GINGIVA
D40M76	429D	10/11/64		2.3	45.08	6.076	840	1958	MPS

SECOND RUN

D40F79	481C	8/30/65		12.9	13.4	31.18	4.429	4880	6386	BCG SACRIFICE
D40F80	481D	8/30/65			9.7	37.61	4.254	3530	5428	METASTATIC SQUAMOUS CELL CARCINOMA OF THE GINGIVA
D40F81	481E	8/30/65			2.1	41.01	4.836	771	1446	PROGRESSIVE APLASTIC ANEMIA
D40F90	517C	1/ 3/66			13.7	33.86	4.879	5016	6267	METASTATIC MAMMARY CARCINOMA
D40M91	A 517D	1/ 3/66		10.9	12.6	62.11	5.843	4588	8498	OSTEOSARCOMA (TO FREDERICK CANCER RESEARCH CENTER)
D40M92	517E	1/ 3/66			8.4	70.76	6.999	3062	7283	METASTATIC FIBROSARCOMA OF THE HEAD (MALAR AREA)
D40M93	517F	1/ 3/66			12.7	54.62	4.947	4624	7296	AORTIC THROMBOSIS
D40X02	558B	7/ 2/66			4.4	40.61	5.108	1593	2952	BRONCHOPNEUMONIA & MPS
D40X03	558C	7/ 2/66			10.3	38.07	3.818	3775	5805	METASTATIC MAMMARY CARCINOMA
D40X04	558D	7/ 2/66		11.9	12.0	52.86	5.564	4367	6761	MALIGNANT LYMPHOMA (LEUKEMIC)
D40Y10	A 594A	1/ 1/67			14.1	48.80	4.477	5136	7185	DISSEMINATED HEMANGIOSARCOMA
D40Y11	594B	1/ 1/67			9.8	46.89	4.428	3566	5561	NEUROFIBROSARCOMA OF THE GINGIVA
D40Y12	594C	1/ 1/67			12.3	52.51	4.446	4505	6704	RUPTURED PROSTATIC CYST
D40X14	598B	3/ 3/67			13.5	33.87	4.161	4940	6668	BACTERIAL ENDOCARDITIS
D40Y15	598C	3/ 3/67			10.6	59.86	5.652	3870	7252	SQUAMOUS CELL CARCINOMA OF THE GINGIVA
D40Y16	598D	3/ 3/67			13.1	58.58	5.649	4773	8859	SQUAMOUS CELL CARCINOMA-TONSIL
D40X18	637B	9/10/67			5.7	40.48	5.485	2097	4124	MALIGNANT LYMPHOMA
D40X19	637C	9/10/67			10.8	34.70	4.337	3945	6227	HEMANGIOSARCOMA
D40X20	637D	9/10/67			14.7	44.13	5.254	5373	7613	MESENCHYMO SPINAL CANAL
D40X21	637E	9/10/67			9.5	39.47	5.320	3461	5668	METASTATIC MAMMARY CARCINOMA
D40Y22	637F	9/10/67			2.7	60.45	4.636	976	1997	MPS
D40Y23	637G	9/10/67			14.2	56.73	5.444	5204	9028	SQUAMOUS CELL CARCINOMA OF THE GINGIVA

PILOT SERIES

D50F01	134A	7/23/61		7.5	91.83	11.000	2742	9970	SQUAMOUS CELL CARCINOMA OF THE GINGIVA
D50F04	138A	7/26/61		1.6	117.50	12.302	576	2492	ACUTE NECROTIZING ENTERITIS
D50F06	138C	7/26/61		3.0	122.83	12.930	1092	5577	ACCIDENTAL DEATH (ANESTHETIC DEATH - ANESTHETIZED FOR RADIOGRAPHIC SURVEY)
D50M08	138E	7/26/61		5.3	200.40	15.240	1929	11781	ENTERITIS
D50F14	164E	12/25/61		1.5	77.55	10.230	549	2054	MPS
D50M21	189B	4/13/62		4.7	135.24	16.062	1703	10330	CEREBRAL HEMORRHAGE
D50M26	191E	4/24/62		6.6	105.23	13.072	2417	10280	OSTEOSARCOMA OF THE R MANDIBLE
D50F29	193C	4/26/62		3.2	109.50	12.970	1174	5928	MPS
D50F30	193D	4/26/62		3.6	115.30	13.453	1331	6094	MPS
D50M31	193E	4/26/62		8.8	131.73	14.400	3197	13890	METASTATIC OSTEOSARCOMA
D50M32	193F	4/26/62		2.3	115.30	13.330	827	4171	MPS
D50M33	193G	4/26/62		1.6	155.30	16.413	571	3292	MPS
D50F34	254A	4/21/63		6.0	72.82	9.136	2180	6498	SQUAMOUS CELL CARCINOMA OF THE GINGIVA
D50F36	254C	4/21/63		10.1	102.60	10.653	3672	12142	SQUAMOUS CELL CARCINOMA OF THE GINGIVA
D50F37	254D	4/21/63		8.9	121.40	12.400	3256	13000	OSTEOSARCOMA OF THE L ISCHIUM
D50M39	254F	4/21/63		2.7	155.30	15.510	971	5553	MPS

BEAGLE NUMBER	LITTER NUMBER	BIRTH DATE	AGE AT TERM.	AGE AT DEATH	PEAK BODY (UCI)	BURDEN (UCI/KG)	EXPOSURE DAYS	TOTAL DOSE (RADs)	COMMENTS
FIRST RUN									
D50F40	305A	12/12/63		1.4	140.20	15.024	505	2882	MPS
D50M41	305B	12/12/63		3.5	133.40	16.404	1276	7737	MPS
D50M42	305C	12/12/63		6.6	135.70	16.100	2412	13572	SQUAMOUS CELL CARCINOMA OF THE GINGIVA
D50M43	305D	12/12/63		6.4	141.44	16.314	2337	13960	SQUAMOUS CELL CARCINOMA OF THE R MANDIBLE
D50F45	314B	12/25/63		7.1	117.54	15.230	2604	13073	OSTEOSARCOMA OF THE R MANDIBLE
D50F46 A	314C	12/25/63		8.6	96.92	12.190	3144	12310	SQUAMOUS CELL CARCINOMA OF L MANDIBLE
								13480	OSTEOSARCOMA OF THE 1ST CERVICAL VERTEBRA
D50F51	332C	3/23/64		7.6	107.21	14.410	2787	13790	MPS
D50F52 C	332D	3/23/64		6.0	129.42	11.820	2187	9891	OSTEOSARCOMA OF THE L MANDIBLE
D50F53	332E	3/23/64		4.9	133.60	18.172	1799	19050	METASTATIC HEMANGIOSARCOMA (PRIMARY SITE NOT IN BONE)
D50M55	332G	3/23/64		9.0	156.64	20.640	3287	10640	OSTEOSARCOMA OF THE L FEMUR & L MANDIBLE
D50F56 A	336A	3/28/64		8.4	99.96	10.120	3076	11634	OSTEOSARCOMA OF THE R PETROUS TEMPORAL BONE
D50M57	336B	3/28/64		9.6	100.72	11.580	3511	9316	GRANULOMATOUS MENINGOENCEPHALITIS
D50M58	336C	3/28/64		5.0	114.60	13.974	1825	13470	METASTATIC OSTEOSARCOMA
D50F60 A	362A	5/25/64		9.9	94.99	12.600	3608	12253	OSTEO OF L TEMPORAL BONE
D50F61	362B	5/25/64		8.6	103.50	12.114	3138	16942	SQUAMOUS CELL CARCINOMA OF THE GINGIVA
D50F62	362C	5/25/64		8.9	141.02	20.440	3242	14600	SQUAMOUS CELL CARCINOMA OF THE GINGIVA
D50M63	362D	5/25/64		10.0	105.50	12.240	3658	8353	MPS
D50M64	362E	5/25/64		3.5	170.02	16.690	1278	14684	OSTEOSARCOMA OF THE R ULNA
D50F65 C	394A	7/14/64		6.5	135.84	14.830	2361	13000	OSTEOSARCOMA OF THE PELVIS
D50F66	394B	7/14/64		7.1	123.20	14.441	2586	6363	EPILEPSY
D50M67 C	394C	7/14/64		2.9	118.91	16.160	1042	16862	OSTEOSARCOMA OF THE L MANDIBLE
D50M68	394D	7/14/64		7.4	163.53	17.760	2715	9915	MPS
D50M69 C	394E	7/14/64		4.2	130.90	14.840	1533	6853	EPILEPSY
D50M70	394F	7/14/64		3.0	180.00	15.360	1095		

SECOND RUN

D50M73	479C	8/29/65		3.3	174.21	17.150	1215	5222	SQUAMOUS CELL CARCINOMA OF THE MAXILLA
D50M74	479D	8/29/65		6.0	176.00	17.490	2181	2293	PATHOLOGIC FRACTURES R TIBIA AND R MANDIBLE
D50F75	495A	9/21/65		8.6	85.75	12.080	3130	6113	MPS
D50F76	495B	9/21/65		3.5	107.42	12.550	1275	9446	MPS
D50M77	495C	9/21/65		4.4	140.04	15.091	1599	7578	MPS
D50F79	516B	1/ 2/66		3.0	169.10	19.940	1083	2571	MPS
D50F80	516C	1/ 2/66		1.3	147.70	16.900	467	7754	MPS
D50M81	516D	1/ 2/66		3.3	187.90	16.850	1193	6847	MPS
D50M82	516E	1/ 2/66		2.5	193.60	19.130	926	2513	MPS (APLASTIC ANEMIA)
D50F83	528A	2/25/66		7.1	109.00	11.820	2611	11952	SQUAMOUS CELL CARCINOMA OF THE GINGIVA
D50F84	528B	2/25/66		5.6	123.42	15.313	2049	14852	ACCIDENTAL DEATH (HYPERTHERMIA AFTER ANESTHESIA FOR BIOPSY, EPULIS)
D50M86	528D	2/25/66		6.4	131.90	17.020	2331	7621	MPS
D50M87	528E	2/25/66		3.0	177.42	20.441	1088	15620	RADIATION OSTEODYSTROPHY R FEMUR AND OSTEOSARCOMA R ISCHIUM
D50F89	560B	7/ 6/66		8.4	100.70	13.244	3058	6730	MPS
D50F92	622A	6/13/67		3.1	123.90	13.530	1123	11212	LYMPHOID HYPOPLASIA
D50M94	622C	6/13/67		6.1	133.80	14.640	2219	5020	MPS
D50M95	622D	6/13/67		2.3	138.80	13.820	836	7871	MPS
D50M96	622E	6/13/67		3.6	137.50	17.450	1325	6193	MPS
D50X01	644A	10/ 9/67		4.2	75.98	12.180	1549	13140	ULCERATIVE GASTRITIS
D50X02 A	644B	10/ 9/67		9.7	92.47	11.443	3526	12740	CARCINOMA OF R FRONTAL SINUS
D50X03	644C	10/ 9/67		9.2	86.52	11.723	3369	3389	MPS
D50Y05	644E	10/ 9/67		1.8	127.82	12.964	667	5082	MPS
D50Y09	645C	10/15/67		2.5	119.31	13.714	898		

FIRST RUN

D60F01	520A	1/ 9/66		.4					SCHEDULED SACRIFICE (SPECIAL STUDY)
D60M03	520C	1/ 9/66		.4					SCHEDULED SACRIFICE (SPECIAL STUDY)
D60M04	520D	1/ 9/66		.1					UNDETERMINED
D60M05	520E	1/ 9/66		.4					SCHEDULED SACRIFICE (SPECIAL STUDY)
D60M06	520F	1/ 9/66		.4					SCHEDULED SACRIFICE (SPECIAL STUDY)
D60F07	521A	1/11/66		.4					SCHEDULED SACRIFICE (SPECIAL STUDY)
D60F08	521B	1/11/66		.4					SCHEDULED SACRIFICE (SPECIAL STUDY)

BEAGLE NUMBER	LITTER NUMBER	BIRTH DATE	AGE AT TERM.	AGE AT DEATH	PEAK BODY (UCI)	BURDEN (UCI/KG)	EXPOSURE DAYS	TOTAL DOSE (RADs)	COMMENTS
D60F09	521C	1/11/66		.4					SCHEDULED SACRIFICE (SPECIAL STUDY)
D60M10	521D	1/11/66		.4					SCHEDULED SACRIFICE (SPECIAL STUDY)
D60F11	524A	2/ 2/66		.4					SCHEDULED SACRIFICE (SPECIAL STUDY)
D60F12	524B	2/ 2/66		.4					SCHEDULED SACRIFICE (SPECIAL STUDY)
D60M13	524C	2/ 2/66		.4					SCHEDULED SACRIFICE (SPECIAL STUDY)
D60M14	524D	2/ 2/66		.4					SCHEDULED SACRIFICE (SPECIAL STUDY)
D60M15	524E	2/ 2/66		.4					SCHEDULED SACRIFICE (SPECIAL STUDY)
D60F16	526A	2/10/66		.4					SCHEDULED SACRIFICE (SPECIAL STUDY)
D60F17	526B	2/10/66		.4					SCHEDULED SACRIFICE (SPECIAL STUDY)
D60M19	526D	2/10/66		.4					SCHEDULED SACRIFICE (SPECIAL STUDY)
D60M20	526E	2/10/66		.4					SCHEDULED SACRIFICE (SPECIAL STUDY)
D60M21	526F	2/10/66		.4					SCHEDULED SACRIFICE (SPECIAL STUDY)
SECOND RUN									
D60F22	610A	5/ 6/67		3.0	367.80	43.120	1080	18910	OSTEOSARCOMA OF THE L HUMERUS & L ULNA
D60F23	610B	5/ 6/67		1.6	379.70	40.051	586	8462	MPS
D60M24	610C	5/ 6/67		2.0	716.60	56.430	731	15700	MPS
D60M25	610D	5/ 6/67		1.4	447.70	45.410	496	7605	PANCYTOPENIA
D60M26	610E	5/ 6/67		3.0	395.61	42.360	1111	19363	CHONDROSARCOMA OF THE 1ST CERVICAL VERTEBRA
D60M30	612D	5/12/67		2.5	456.70	52.794	926	14480	HEMANGIOSARCOMA OF THE L HUMERUS
D60M31	612E	5/12/67		1.6	417.80	46.012	579	9160	POSTERIOR PARALYSIS (UNKNOWN ETIOLOGY)
D60F32	627A	7/12/67		2.5	304.10	36.724	902	12882	SQAMOUS CELL CARCINOMA OF THE GINGIVA
D60F33	627B	7/12/67		2.8	338.20	42.270	1009	17564	OSTEOSARCOMA OF THE PELVIS
D60F35	627D	7/12/67		2.4	331.20	34.864	868	12551	OSTEOSARCOMA OF THE PELVIS
D60M36	627E	7/12/67		1.6	388.63	47.340	602	10190	APLASTIC ANEMIA
D60M37	A 627F	7/12/67		2.8	305.51	34.560	1009	14840	OSTEOSARCOMA OF THE SKULL
D60M38	627G	7/12/67		2.2	466.30	41.262	799	14430	OSTEOSARCOMA OF THE L TIBIA
D60M39	627H	7/12/67		1.6	447.00	45.430	576	10263	OSTEOSARCOMA OF THE R HUMERUS
D60M40	627I	7/12/67		2.1	547.30	53.033	763	16130	OSTEOSARCOMA OF THE L HUMERUS
D60F41	636A	9/ 2/67		1.6	197.60	33.373	594	6823	PANCYTOPENIA
D60F42	636B	9/ 2/67		2.3	198.80	25.131	844	8323	MPS
D60M43	636C	9/ 2/67		1.9	473.60	66.700	681	11820	MPS
D60M44	636D	9/ 2/67		2.6	301.71	31.693	958	12760	OSTEOSARCOMA OF THE L FEMUR & L TIBIA
FIRST RUN									
ROOF03	282C	10/20/63		14.3					METASTATIC MAMMARY CARCINOMA
ROOF04	282D	10/20/63		14.9					TRANSITIONAL CELL CARCINOMA METASTATIC TO LUNGS
ROOM05	282E	10/20/63		16.1					CHRONIC PROSTATITIS
ROOF11	322A	2/22/64		12.7					METASTATIC MAMMARY CARCINOMA
ROOM12	322B	2/22/64		14.7					MALIGNANT LYMPHOMA
ROOM13	322C	2/22/64		13.2					MALIGNANT LYMPHOMA
ROOM14	322D	2/22/64		17.2					BRONCHOGENIC CARCINOMA
ROOF15	323A	2/27/64		14.4					DIABETES MELLITIS
ROOF16	323B	2/27/64		11.9					METASTATIC MAMMARY CARCINOMA
ROOM17	323C	2/27/64		17.4					CHRONIC PNEUMONIA
ROOM18	323D	2/27/64		16.5					MENINGIOMA
ROOF20	326A	3/ 3/64		13.4					DISSEMINATED MAMMARY CARCINOMA
									NORMAL SACRIFICE
ROOF21	326B	3/ 3/64		5.0					NEPHROSCLEROSIS
ROOM22	326C	3/ 3/64		14.8					CEREBRAL HEMORRHAGE
ROOM23	326D	3/ 3/64		11.9					RUPTURED PROSTATIC ABSCESS
ROOM24	326E	3/ 3/64		15.2					MALIGNANT LYMPHOMA, AND FIBRINOLYTIC SYNDROME SECONDARY
ROOF28	340C	4/ 2/64		13.3	13.6				TO DRUG TREATMENT FOR LYMPHOMA
									CHRONIC BRONCHOPNEUMONIA
ROOM30	340E	4/ 2/64		16.8					CHRONIC RENAL DISEASE/NEPHROSCLEROSIS
ROOM33	350C	5/ 2/64		16.4					ACCIDENTAL DEATH (ANESTHETIC DEATH - ANESTHETIZED FOR WHOLE BODY COUNTING)
ROOM34	350D	5/ 2/64		1.6					METASTATIC BILE DUCT CARCINOMA
ROOM35	350E	5/ 2/64		15.0					METASTATIC MAMMARY CARCINOMA
ROOF38	370C	6/11/64		13.8					CHRONIC ACTIVE PNEUMONIA AND RENAL AMYLOIDOSIS
ROOF42	393A	7/14/64		10.6					

BEAGLE NUMBER	LITTER NUMBER	BIRTH DATE	AGE AT TERM.	AGE AT DEATH	PEAK BODY BURDEN (UCI)	(UCI/KG)	EXPOSURE DAYS	TOTAL DOSE (RADs)	COMMENTS
ROOF43	393B	7/14/64		17.0					SENILE CNS DISEASE
ROOF44	393C	7/14/64		15.2					DEGENERATIVE ENCEPHALOPATHY
ROOF45	393D	7/14/64		13.1					METASTATIC MAMMARY TUMORS
				12.7					UNDETERMINED CNS DISEASE-SENILE ENCEPHALOPATHY
ROOM46	393E	7/14/64		17.4					MYELOPATHY, TERMINAL
ROOF48	401A	7/26/64		17.1					RENAL CARCINOMA
ROOM50	401C	7/26/64		17.4					ACCIDENTAL DEATH (UTERINE PERFORATION DURING ANTIBIOTIC INFUSION)
ROOF52	418A	9/14/64		5.8					MALIGNANT LYMPHOMA
ROOM54	418C	9/14/64		14.9					PERFORATING ESOPHAGEAL ULCER
ROOM55	418D	9/14/64		16.3					BCG SACRIFICE
ROOF57	419B	9/17/64		14.3					METASTATIC MAMMARY CARCINOMA
ROOF58	419C	9/17/64		16.4					METASTATIC MAMMARY CARCINOMA
ROOF59	419D	9/17/64		11.6					FIBROSARCOMA OF THE GINGIVA
ROOM60	419E	9/17/64		13.7					METASTATIC UNDIFFERENTIATED SPLENIC TUMOR
ROOM61	419F	9/17/64		13.5					METASTATIC TRANSITIONAL CELL CARCINOMA (RENAL PELVIS)
ROOF63	441B	12/ 3/64		8.3					METASTATIC MAMMARY CARCINOMA
ROOF64	441C	12/ 3/64		14.4					CHRONIC NEPHROSCLEROSIS/RENAL ARTERIOSCLEROSIS
ROOM67	441F	12/ 3/64		17.6					
SECOND RUN									
ROOF70	472C	8/ 3/65		15.7					FIBROSARCOMA-ORAL CAVITY, METASTATIC TO LUNG
ROOM73	472F	8/ 3/65		14.4					MELANOMA
ROOM75	472H	8/ 3/65		15.5					CHOLANGIOHEPATITIS (COMMON BILE DUCT OBSTRUCTION)
ROOM76	472I	8/ 3/65		15.2					THYMOMA, PLEURAL CAVITY/CARDIAC TAMPOONADE
ROOF82	527A	2/23/66		17.1					ACUTE PERITONITIS
ROOF83	527B	2/23/66		11.5					PYOMETRA AND CONGESTIVE HEART FAILURE
ROOM86	527E	2/23/66		18.0					SEVERE CHRONIC CHOLECYSTITIS
ROOM87	527F	2/23/66		17.4					CHRONIC RENAL DISEASE (NEPHROSCLEROSIS)
ROOM89	529B	3/ 1/66		12.0					ORAL MELANOMA (NEAR FRENULUM)
ROOM90	529C	3/ 1/66		16.1					PNEUMONIA
ROOM91	529D	3/ 1/66		16.9					DISSEMINATED LYMPHOSARCOMA
ROOF94	548B	6/ 7/66		13.5					ACUTE RENAL FAILURE-IATROGENIC
ROOF95	548C	6/ 7/66		15.4					METASTATIC MAMMARY CARCINOMA
ROOM98	548F	6/ 7/66		15.8					DISSEMINATED LYMPHOSARCOMA
ROOX02	555B	6/26/66		1.9					ACCIDENTAL DEATH (STRANGULATION ON NECK CHAIN)
ROOX03	555C	6/26/66		14.0					MALIGNANT MAMMARY CARCINOMA
ROOX08	575C	10/17/66		.2					ENTERITIS
ROOY12	576A	11/ 7/66		13.7					CONGESTIVE HEART FAILURE
ROOY13	576B	11/ 7/66		15.1					SUPPURATIVE HEPATITIS (HEPATIC ABSCESSATION)
ROOY14	576C	11/ 7/66		17.8					LYMPHOSARCOMA
ROOX18	583D	12/ 1/66		14.9					METASTATIC MAMMARY CARCINOMA
ROOY19	583E	12/ 1/66		.3					ACCIDENTAL DEATH (ANESTHETIC DEATH)
ROOY20	583F	12/ 1/66		8.1					IDIOPATHIC EPILEPSY
ROOY21	583G	12/ 1/66		15.5					POSSIBLE ACUTE CONGESTIVE HEART FAILURE, Ruptured CHORDAE TENDINAE
ROOX22	595A	1/ 3/67		8.3					CHRONIC ACTIVE INTERSTITIAL PNEUMONIA
ROOX24	595C	1/ 3/67		13.0					CONGESTIVE HEART FAILURE
ROOY25	595D	1/ 3/67		12.6					CONGESTIVE HEART FAILURE, Ruptured CHORDAE TENDINAE
ROOX26	611A	5/11/67		12.9					INTERVERTEBRAL DISC DISEASE
ROOX27	611B	5/11/67		12.3					ADRENAL CARCINOMA
ROOX28	611C	5/11/67		13.2					PITUITARY CARCINOMA
ROOY30	611E	5/11/67		10.6					MALIGNANT LYMPHOMA
ROOX32	621B	6/ 7/67		14.3					PITUITARY CARCINOMA
ROOX33	621C	6/ 7/67		14.9					METASTATIC MAMMARY CARCINOMA
ROOY34	621D	6/ 7/67		10.3					ADRENOCORTICAL ATROPHY
ROOX36	625A	7/ 4/67		10.6					BCG SACRIFICE
ROOX37	625B	7/ 4/67		12.6					DIABETES MELLITUS
ROOY39	625D	7/ 4/67		13.3					MALIGNANT ORAL MELANOMA
ROOY41	625F	7/ 4/67		16.5					CHRONIC HEART DISEASE/LIVER DISEASE/KIDNEY DISEASE
ROOX42	629A	7/15/67		17.3					PROGRESSIVE POSTERIOR PARALYSIS
									CHRONIC RENAL DISEASE

BEAGLE NUMBER	LITTER NUMBER	BIRTH DATE	AGE AT TERM.	AGE AT DEATH	PEAK BODY BURDEN (UCI)	EXPOSURE (UCI/KG)	EXPOSURE DAYS	TOTAL DOSE (RADs)	COMMENTS
R00X43	629B	7/15/67		12.6					HEPATIC ABSCESS RUPTURE/ABDOMINAL HEMORRHAGE
R00X44	629C	7/15/67		14.2					ACUTE CONGESTIVE HEART FAILURE
R00Y45	629D	7/15/67		16.2					CHRONIC RENAL DISEASE

FIRST RUN

R05F03	293C	11/19/63		14.2	.08	.009	4767	91	METASTATIC MAMMARY CARCINOMA
R05F04	293D	11/19/63		12.6	.07	.008	4180	90	METASTATIC SALIVARY GLAND ADENOCARCINOMA
R05M05	293E	11/19/63		14.1	.09	.008	4727	113	HEPATOCELLULAR ADENOMA
R05M06	293F	11/19/63		14.7	.09	.007	4927	126	METASTATIC TESTICULAR SEMINOMA
R05F07	300A	12/10/63		13.5	.07	.007	4510	88	NEPHROSCLEROSIS, ACUTE PNEUMONIA AND CARDIOMEGALY
R05F08	300B	12/10/63		18.5	.06	.009	6319	103	MAMMARY ADENOCARCINOMA
R05M09	300C	12/10/63		16.6	.09	.009	5613	122	CUSHINGS DISEASE (PITUITARY ADENOMA)
R05M10	300D	12/10/63		15.0	.08	.009	5026	109	CEREBRAL HEMORRHAGE
R05F24	392A	7/12/64		5.4	.06	.006	1544	26	METASTATIC PANCREATIC ADENOCARCINOMA
R05F25	392B	7/12/64		9.5	.06	.007	3043	55	CHRONIC INTERSTITIAL PNEUMONIA
R05M27	392D	7/12/64		15.2	.07	.010	5101	75	INTRAVASCULAR THROMBOSIS/MYOCARDIAL AND RENAL INFARCTION
R05F29	412B	8/27/64		13.0	.09	.009	4324	91	MALIGNANT LYMPHOMA
R05F30	412C	8/27/64		14.1	.06	.007	4711	86	METASTATIC MAMMARY CARCINOMA
R05M31	412D	8/27/64		13.7	.07	.008	4574	74	TRANSITIONAL CELL CARCINOMA IN PROSTATIC URETHRA
R05M32	412E	8/27/64	14.1	14.3	.08	.007	4801	98	MALIGNANT LYMPHOMA
R05F34	417B	9/ 7/64		16.0	.05	.006	5392	72	CHRONIC RENAL FAILURE/NEPHROSCLEROSIS
R05F35	417C	9/ 7/64		15.7	.09	.010	5299	118	PANCREATIC ATROPHY/FIBROSIS
R05M37	417E	9/ 7/64		15.9	.08	.008	5378	96	MESENTERIC INFARCTION
R05M38	417F	9/ 7/64		15.0	.07	.006	5040	108	UNDETERMINED NEUROLOGIC DISEASE - CONVULSIONS
R05M39	417G	9/ 7/64		15.7	.09	.008	5301	102	PYELONEPHRITIS
R05F40	427A	10/ 7/64		9.2	.07	.006	2933	53	SQUAMOUS CELL CARCINOMA OF THE GINGIVA
R05F41	427B	10/ 7/64		15.9	.07	.006	5390	94	MAMMARY CARCINOMA
R05M43	427D	10/ 7/64		15.5	.07	.006	5232	83	BRONCHIECTASIS/CHRONIC SUPPURATIVE PNEUMONIA

21

SECOND RUN

R05F44	483A	8/31/65		11.2	.09	.011	3663	69	METASTATIC MAMMARY CARCINOMA
R05F45	483B	8/31/65		14.6	.07	.009	4881	87	ACUTE NECROTIZING PNEUMONIA-ASPIRATION
R05F47	483D	8/31/65	11.5	13.4	.08	.007	4465	88	TERMINATED-BCG EXPERIMENT BCG SACRIFICE
R05F48	483E	8/31/65		13.4	.07	.008	4468	64	METASTATIC MAMMARY CARCINOMA
R05M49	483F	8/31/65		16.1	.09	.008	5446	102	GINGIVAL FIBROSARCOMA
R05F51	494B	9/16/65		12.0	.09	.009	3953	102	METASTATIC MALIGNANT MELANOMA OF THE EYE
R05M52	494C	9/16/65		9.3	.11	.011	2965	98	NASAL CHONDROSARCOMA
R05M53	494D	9/16/65		13.2	.12	.012	4381	107	STRANGULATION OF LARGE BOWEL
R05M54	494E	9/16/65		13.6	.09	.009	4528	135	PROSTATIC ABSCESS
R05F56	547B	6/ 1/66		9.5	.08	.008	3036	56	MALIGNANT LYMPHOMA
R05F57	547C	6/ 1/66		13.6	.06	.007	4514	74	HISTIOCYTIC LYMPHOSARCOMA, DISSEMINATED
R05M58	547D	6/ 1/66		14.4	.08	.009	4832	97	ADRENAL CORTICAL NECROSIS-ADDISONIAN CRISIS
R05M59	547E	6/ 1/66		16.2	.09	.010	5499	120	INTERVETEBRAL DISC HERNIATION/PARAPLEGIA
R05F61	568B	9/14/66		17.6	.06	.006	5979	64	CHRONIC SPINAL DISEASE
R05M63	568D	9/14/66		15.9	.08	.009	5371	87	CHRONIC PYELONEPHRITIS
R05M64	568E	9/14/66		15.9	.08	.008	5368	80	METASTATIC MALIGNANT MELANOMA, ORAL
R05F68	588D	12/11/66		12.5	.06	.008	4129	63	NECROTIZING PNEUMONIA WITH SECONDARY PULMONARY THROMBOSIS
R05M70	588F	12/11/66		12.0	.06	.008	3957	78	CONGESTIVE HEART FAILURE
R05F71	623A	6/16/67		13.1	.10	.012	4352	99	METASTATIC MAMMARY CARCINOMA
R05F72	623B	6/16/67		17.0	.07	.010	5763	77	CHRONIC PYELONEPHRITIS
R05F73	623C	6/16/67		14.8	.07	.010	4962	86	CHRONIC RENAL DISEASE/PYELONEPHRITIS
R05F74	623D	6/16/67		17.2	.08	.010	5865	102	CHRONIC RENAL FAILURE
R05M76	623F	6/16/67		16.0	.08	.010	5401	111	INTERVETEBRAL DISC DISEASE

BEAGLE NUMBER	LITTER NUMBER	BIRTH DATE	AGE AT TERM.	AGE AT DEATH	PEAK BODY (UCI)	BURDEN (UCI/KG)	EXPOSURE DAYS	TOTAL DOSE (RADs)	COMMENTS
FIRST RUN									
R10F01	298A	12/ 7/63		14.8	.25	.024	4972	331	CONGESTIVE HEART FAILURE, PULMONARY EDEMA
R10M02	298B	12/ 7/63		12.7	.26	.024	4201	302	PITUITARY TUMOR WITH SECONDARY CUSHING'S DISEASE AND DISSEMINATED INTRAVASCULAR COAGULOPATHY
R10M04	298D	12/ 7/63		17.0	.30	.025	5764	364	MALIGNANT LYMPHOMA
R10M05	298E	12/ 7/63		14.3	.25	.020	4806	243	CHONDROSARCOMA OF VERTEBRA
R10F07	355B	5/13/64		15.7	.15	.027	5283	276	EOSINOPHILIC TRACHEITIS/BRONCHITIS-PARASITIC
R10M09	355D	5/13/64	14.6	16.4	.19	.023	5537	293	LYMPHOMA
R10F14	395A	7/14/64		12.7	14.5	.14	4871	219	TERMINATED-BCG EXPERIMENT BCG SACRIFICE
R10F15	395B	7/14/64		14.4	.12	.020	4825	219	ACUTE NECROTIZING ENTERITIS (PARVOVIRUS)
R10F17	395D	7/14/64		13.8	.10	.017	4618	153	CUSHING'S DISEASE
R10F18	395E	7/14/64		13.4	.12	.015	4458	141	DUODENAL ULCERS AND CHRONIC PERITONITIS
R10M20	395G	7/14/64		12.8	.16	.020	4248	190	CARDIAC AND PULMONARY THROMBOSIS
R10M21	395H	7/14/64		11.6	.21	.022	3817	208	MALIGNANT LYMPHOMA
R10F22	402A	7/26/64		14.8	.15	.019	4967	224	DEMELINATING ENCEPHALOPATHY
R10F23	402B	7/26/64		17.5	.17	.021	5974	289	DIFFUSE ARTERIOSCLEROSIS, CHRONIC RENAL DISEASE
R10F24	402C	7/26/64		12.9	.18	.021	4294	218	CONGESTIVE HEART FAILURE
R10M26	402E	7/26/64		12.9	.20	.023	4260	221	METASTATIC HEMANGIOSARCOMA OF THE L ILEUM
R10M27	402F	7/26/64		15.5	.19	.018	5238	299	MALIGNANT MELANOMA-LIP
R10M33	415D	9/ 2/64		18.2	.14	.016	6228	174	HEPATIC NECROSIS AND ABSCESSATION/PERITONITIS
SECOND RUN									
R10F38	478B	8/29/65		12.3	.14	.016	4068	181	METASTATIC BILE DUCT CARCINOMA
R10M39	478C	8/29/65		8.2	.15	.016	2563	157	PRIMARY BRAIN TUMOR
R10F41	534B	4/ 6/66		12.7	.24	.024	4214	217	HEPATOCELLULAR ADENOMA
R10M43	534D	4/ 6/66		13.6	.29	.025	4535	306	SALIVARY GLAND SARCOMA
R10M44	534E	4/ 6/66		14.4	.32	.026	4830	311	BRONCHOGENIC CARCINOMA
R10F46	570B	9/17/66		16.0	.22	.024	5399	280	PITUITARY TUMORS
R10F47	570C	9/17/66	10.6	12.3	.22	.021	4046	267	TERMINATED-BCG EXPERIMENT SEPTICEMIA SECONDARY TO TRANSITIONAL CELL CARCINOMA OF URINARY BLADDER AND URETHRA
R10M49	570E	9/17/66		12.3	.33	.031	4041	369	TRANSITIONAL CELL CARCINOMA-BLADDER/URETHRA
R10F53	574A	10/15/66		15.7	.23	.033	5300	364	CEREBRAL INFARCTION/NON-SUPPURATIVE ENCEPHALITIS
R10F54	574B	10/15/66		13.6	.31	.034	4538	429	ACUTE BRONCHOPNEUMONIA-BACTERIAL
R10M55	574C	10/15/66		10.2	.44	.038	3280	404	METASTATIC TRANSITIONAL CELL CARCINOMA OF URINARY BLADDER
R10M56	574D	10/15/66		17.8	.46	.049	6062	730	SUBDURAL HEMATOMA OF THE BRAINSTEM
R10F58	608B	4/28/67		13.7	.15	.022	4553	259	CONGESTIVE HEART FAILURE
R10M59	608C	4/28/67		13.9	.20	.027	4657	291	OSTEOSARCOMA THORACIC VERTEBRA
R10M60	608D	4/28/67		12.4	.28	.027	4106	267	CONGESTIVE HEART FAILURE
R10F61	615A	5/19/67		8.5	.19	.032	2686	251	METASTATIC MAMMARY CARCINOMA
R10F62	615B	5/19/67		16.1	.22	.032	5451	383	CHRONIC RENAL DISEASE
R10F63	615C	5/19/67		17.9	.24	.033	6087	433	OSTEOSARCOMA OF THE LEFT FEMUR
R10M65	615E	5/19/67		14.3	.26	.033	4783	375	FIBROSARCOMA, RIB AND SPINE
R10M66	615F	5/19/67		13.7	.24	.026	4578	382	CHRONIC PROSTATITIS
FIRST RUN									
R20F01	A 295A	11/30/63		15.5	.93	.101	5220	1526	INTERVERTEBRAL DISC DISEASE
R20F02	295B	11/30/63		13.9	.97	.112	4651	1427	ASTROCYTOMA (GRADE IV) AND NEUROFIBROSARCOMA
R20M03	295C	11/30/63		11.0	1.03	.102	3580	1103	OSTEOSARCOMA OF THE R ILLUM
R20M04	295D	11/30/63		14.8	.87	.094	4962	1290	CONGESTIVE HEART FAILURE
R20F05	297A	12/ 2/63		12.4	.79	.091	4076	928	HEPATOCELLULAR ADENOMA
R20F06	297B	12/ 2/63		12.8	1.18	.136	4250	1522	OSTEOSARCOMA OF THE 5TH LUMBAR VERTEBRA
R20F07	A 297C	12/ 2/63		11.3	1.34	.127	3676	1264	OSTEOSARCOMA R FRONT LEG
R20M09	297E	12/ 2/63		10.3	2.21	.164	3332	1706	MALIGNANT MELANOMA OF GINGIVA
R20F12	A 303B	12/11/63	9.6	9.7	1.46	.130	3092	1124	METASTATIC OSTEOSARCOMA
R20F18	377A	6/19/64	11.4	12.1	.79	.125	4000	1434	OSTEOSARCOMA OF THE L ILEUM

BEAGLE NUMBER	LITTER NUMBER	BIRTH DATE	AGE AT TERM.	AGE AT DEATH	PEAK BODY (UCI)	BURDEN (UCI/KG)	EXPOSURE DAYS	TOTAL DOSE (RADs)	COMMENTS
R20F20	377C	6/19/64		12.9	1.22	.125	4274	1491	SQUAMOUS CELL CARCINOMA OF THE GINGIVA
R20F21 A	377D	6/19/64		12.2	1.00	.117	4015	1366	MALIGNANT MELANOMA OF THE BUCCAL CAVITY
R20M22	377E	6/19/64		12.7	1.52	.147	4218	2089	OSTEOSARCOMA OF THE R FEMUR AND R HUMERUS
R20M23 A	377F	6/19/64		12.4	1.11	.112	4076	1409	HEPATOCELLULAR ADENOMA
R20F24 A	407A	8/ 8/64		10.7	1.24	.146	3487	1162	METASTATIC OSTEOSARCOMA
R20M26	407C	8/ 8/64		10.9	1.05	.141	3561	1032	OSTEOSARCOMA OF THE 10TH THORACIC VERTEBRA
R20M27 A	407D	8/ 8/64		10.0	.99	.119	3210	991	METASTATIC OSTEOSARCOMA (L FEMUR)
R20M28	407E	8/ 8/64		5.8	1.28	.141	1690	769	MALIGNANT LYMPHOMA
R20M32 A	438D	11/25/64		11.4	1.14	.109	3714	1271	OSTEOSARCOMA L HUMERUS AND PULMONIC STENOSIS

SECOND RUN

R20F34	488B	9/ 8/65		8.8	1.06	.142	2785	1132	OSTEOSARCOMA OF THE 4TH R RIB
R20F35	488C	9/ 8/65		9.4	.98	.095	3003	879	METASTATIC PANCREATIC ADENOCARCINOMA
R20F36	488D	9/ 8/65		10.0	1.10	.106	3232	1061	MALIGNANT LYMPHOMA
R20M37	488E	9/ 8/65		14.0	1.06	.100	4691	1456	CONGESTIVE HEART FAILURE
R20F40 A	493B	9/14/65		7.9	1.10	.122	2451	985	METASTATIC OSTEOSARCOMA
R20F41	493C	9/14/65		8.4	1.50	.162	2634	1290	OSTEOSARCOMA OF THE L & R HUMERI
R20M44 A	493F	9/14/65		15.0	.91	.138	5060	1844	TRANSITIONAL CELL CARCINOMA (URINARY OBSTRUCTION)
R20M45	493G	9/14/65		15.0	1.02	.127	5056	1957	MALIGNANT MELANOMA-ORIGIN UNDETERMINED
R20F48	501C	10/ 3/65		11.5	.66	.116	3756	1001	OSTEOSARCOMA OF THE SACRUM
R20F51	501F	10/ 3/65		14.4	.82	.131	4832	1601	CHRONIC SUPPURATIVE DERMATITIS
R20F52 A	501G	10/ 3/65		16.6	.79	.123	5639	1625	MAMMARY ADENOCARCINOMA WITH PULMONARY METASTASIS
R20F53	587A	12/10/66		10.9	1.11	.139	3558	1242	OSTEOSARCOMA OF THE 4TH CERVICAL VERTEBRA
R20M54 A	587B	12/10/66		12.1	1.62	.151	3984	1928	METASTATIC OSTEOSARCOMA-RIGHT RADIUS
R20M55	587C	12/10/66		7.5	2.21	.188	2286	1667	METASTATIC FIBROSARCOMA OF THE 8TH THORACIC VERTEBRA
R20F58	606A	4/13/67		11.3	1.28	.188	3710	1549	OSTEOSARCOMA-RIB
R20F60	606C	4/13/67		12.2	1.26	.181	4008	1554	OSTEOSARCOMA-MANDIBLE
R20F61	606D	4/13/67	8.6	8.6	1.66	.185	2714	1381	OSTEOSARCOMA OF THE L ILLUM
R20M63 A	606F	4/13/67		11.4	2.17	.205	3731	1905	OSTEOSARCOMA-TIBIA
R20M66	613B	5/15/67		11.9	1.19	.120	3916	932	PYELONEPHRITIS/PROSTATITIS
R20M68	613D	5/15/67		11.6	1.37	.138	3806	1285	POLIOMYELITIS/PROSTATITIS
R20M69 A	613E	5/15/67		6.0	1.89	.162	1753	1085	METASTATIC OSTEOSARCOMA
R20M70	613F	5/15/67		12.6	1.32	.107	4168	1474	RENAL CARCINOMA

23

FIRST RUN

R30F01	287A	10/28/63		8.7	2.81	.331	2733	2871	RADIATION OSTEODYSTROPHY L ULNA & L RADIUS
R30M02	287B	10/28/63		6.9	4.65	.340	2086	2487	SCLEROSING OSTEOSARCOMA OF VERTEBRA C-2
R30F04 A	302B	12/11/63		7.5	4.19	.455	2302	3163	OSTEOSARCOMA WITH HEPATIC METASTASIS
R30M05	302C	12/11/63		7.2	4.63	.429	2198	3212	OSTEOSARCOMA OF THE 4TH CERVICAL VERTEBRA
R30M06 A	302D	12/11/63		7.3	3.93	.339	2218	2765	METASTATIC OSTEOSARCOMA
R30F09	342B	4/13/64		10.1	1.96	.373	3236	2640	PATHOLOGIC FRACTURE OF THE L MANDIBLE
R30M10 A	342C	4/13/64		9.0	3.21	.382	2844	3041	INTERVERTEBRAL DISC HERNIATION (C 5-6)
R30F13	365A	6/ 3/64		7.3	2.25	.321	2219	1933	RADIATION OSTEODYSTROPHY L TEMPORAL BONE
R30F14 A	365B	6/ 3/64		10.1	2.04	.317	3260	2756	METASTATIC OSTEOSARCOMA
R30F15	365C	6/ 3/64		8.8	41.75	6.844	2773	2209	OSTEOSARCOMA OF THE 2ND CERVICAL VERTEBRA
R30M16 A	365D	6/ 3/64		6.8	4.30	.505	2059	3115	METASTATIC OSTEOSARCOMA
R30M17	365E	6/ 3/64		7.0	3.35	.385	2111	2576	OSTEOSARCOMA OF THE R ISCHIUM
R30F19	396B	7/14/64		12.9	2.28	.296	4278	2544	OSTEOSARCOMA OF THE L MANDIBLE
R30M23 A	396F	7/14/64		10.0	4.11	.540	3215	4144	OSTEOSARCOMA OF THE 4TH CERVICAL VERTEBRA
R30F25	413B	8/30/64		5.5	4.09	.397	1571	2374	OSTEOSARCOMA OF THE PELVIS
R30F26 A	413C	8/30/64	8.2	9.2	2.79	.344	2923	2857	OSTEO R RADIUS (LOW GRADE) OSTEO 6TH CERVICAL VERTEBRA

SECOND RUN

R30F29	477B	8/24/65		8.7	2.92	.439	2749	3303	OSTEOSARCOMA OF THE 3RD CERVICAL VERTEBRA
R30M30	477C	8/24/65		6.7	4.72	.480	2030	3371	SQUAM CELL CARCINOMA OF THE GINGIVA & OSTEOSARCOMA L FEMUR
R30M31 A	477D	8/24/65		8.3	4.33	.491	2583	3863	METASTATIC OSTEOSARCOMA
R30M32	477E	8/24/65		7.7	5.22	.531	2364	4145	OSTEOSARCOMA OF THE R ISCHIUM
R30M33	477F	8/24/65		2.3	5.97	.529	413	864	CULLED
R30F34 A	489A	9/10/65		9.0	3.09	.401	2862	3177	METASTATIC OSTEOSARCOMA OF THE L FRONTAL BONE

BEAGLE NUMBER	LITTER NUMBER	BIRTH DATE	AGE AT TERM.	AGE AT DEATH	PEAK BODY (UCI)	BURDEN (UCI/KG)	EXPOSURE DAYS	TOTAL DOSE (RADs)	COMMENTS
R30F35 A 489B		9/10/65		8.4	3.96	.487	2644	3169	SQUAMOUS CELL CARCINOMA OF THE GINGIVA
R30F36 489C		9/10/65		5.9	3.22	.438	1733	1894	PATHOLOGIC FRACTURE OF THE L MANDIBLE
R30M37 489D		9/10/65		9.5	4.08	.356	3020	3952	OSTEOSARCOMA OF THE R 10TH RIB (RECURRING)
R30M39 A 489F		9/10/65		6.8	5.61	.472	2056	3849	OSTEOSARCOMA OF THE L ISCHIUM
R30F42 A 499C		9/27/65		6.9	5.35	.586	2082	4121	OSTEOSARCOMA OF THE R MANDIBLE AND R HUMERUS
R30M43 499D		9/27/65		6.1	5.81	.538	1780	3887	OSTEOSARCOMA OF THE R SCAPULA
R30M44 499E		9/27/65		6.6	6.64	.621	1991	4280	OSTEOSARCOMA OF THE R ISCHIUM
R30M45 499F		9/27/65		3.1	7.32	.672	704	1819	EPILEPSY
R30F50 572A	10/ 3/66			6.9	3.85	.501	2068	2870	OSTEOSARCOMA OF THE R ISCHIUM
R30F51 572B	10/ 3/66			7.7	3.00	.359	2388	2859	OSTEOSARCOMA OF THE R ISCHIUM
R30F57 616C	5/21/67		8.9	8.9	2.39	.438	2818	3107	OSTEOSARCOMA R TIBIA OSTEOSARCOMA R HUMERUS
R30F58 A 616D	5/21/67		9.8	10.2	2.85	.387	3305	3340	OSTEOSARCOMA OF THE R RADIUS (TO FREDERICK CANCER RESEARCH CENTER)
R30F59 616E	5/21/67			7.0	3.69	.508	2114	2952	OSTEOSARCOMA OF THE 2ND CERVICAL VERTEBRA
R30M60 A 616F	5/21/67		5.5	5.6	5.28	.567	1626	3055	OSTEOSARCOMA OF THE L SCAPULA METASTATIC OSTEOSARCOMA
R30M61 616G	5/21/67			7.7	4.89	.504	2381	3715	OSTEOSARCOMA OF THE L ISCHIUM
R30M64 A 624C	6/25/67			7.3	3.93	.475	2235	3080	OSTEOSARCOMA OF THE 4TH CERVICAL VERTEBRA
R30M65 624D	6/25/67			7.9	3.90	.488	2458	3225	OSTEOSARCOMA OF THE R MANDIBLE
R30M66 A 624E	6/25/67			8.7	3.74	.496	2734	3613	OSTEOSARCOMA OF THE L ILLUM

FIRST RUN

R40F01 289A	11/ 5/63		5.2	12.29	1.408	1479	6218	OSTEOSARCOMA OF THE L FEMUR
R40F02 289B	11/ 5/63		5.0	11.32	1.057	1405	5827	OSTEOSARCOMA OF THE L MANDIBLE
R40F03 289C	11/ 5/63		5.5	11.53	1.138	1575	6452	OSTEOSARCOMA OF THE L RADIUS
R40M04 289D	11/ 5/63		5.4	18.58	1.407	1527	8656	OSTEOSARCOMA OF THE R HUMERUS
R40F05 290A	11/ 9/63		4.7	10.24	1.032	1286	4960	OSTEOSARCOMA OF THE L ILLUM
R40F07 290C	11/ 9/63		6.0	9.45	.974	1774	5684	OSTEOSARCOMA OF THE L HUMERUS
R40M09 A 290E	11/ 9/63		6.0	12.13	1.071	1745	6290	MALIGNANT LYMPHOMA
R40F13 312D	12/23/63		4.9	9.17	1.375	1347	6505	OSTEOSARCOMA OF THE 5TH LUMBAR VERTEBRA
R40F14 312E	12/23/63		4.8	14.58	1.503	1315	7498	OSTEOSARCOMA OF THE PELVIS
R40M15 312F	12/23/63		5.1	15.83	1.674	1438	9216	OSTEOSARCOMA OF THE L FEMUR
R40F20 A 337B	3/29/64		6.2	10.72	1.392	1829	7836	METASTATIC OSTEOSARCOMA
R40M21 337C	3/29/64		5.2	14.22	1.235	1456	7596	OSTEOSARCOMA OF THE L MANDIBLE
R40M22 337D	3/29/64		4.8	14.79	1.134	1319	6305	OSTEOSARCOMA OF THE R HUMERUS
R40M23 337E	3/29/64		5.0	16.74	1.240	1401	7359	OSTEOSARCOMA OF THE 5TH CERVICAL VERTEBRA
R40F24 408A	8/ 9/64		5.8	9.30	.987	1667	6439	FIBROSARCOMA OF L MANDIBLE, OSTEOSARCOMA OF R TIBIA & L URNA
R40F28 A 408E	8/ 9/64		6.1	9.62	1.028	1782	7065	OSTEOSARCOMA OF THE L TIBIA
R40M30 A 408G	8/ 9/64		5.0	12.92	1.097	1383	6007	OSTEOSARCOMA OF THE L HUMERUS
R40M33 433C	10/19/64		4.8	11.59	1.244	1317	6613	OSTEOSARCOMA OF THE R ISCHIUM
R40M34 433D	10/19/64		5.8	9.47	1.065	1688	6585	OSTEOSARCOMA OF THE PELVIS
R40M35 433E	10/19/64	7.2	7.2	9.44	.877	2208	9528	OSTEOSARCOMA OF THE FRONTAL BONE

24

SECOND RUN

R40F39 485D	9/ 1/65		5.1	12.86	1.165	1439	6109	OSTEOSARCOMA OF THE 2ND CERVICAL VERTEBRA
R40F40 A 485E	9/ 1/65		6.1	8.02	1.064	1798	5934	METASTATIC OSTEOSARCOMA
R40F41 486A	9/ 1/65		6.8	6.64	.844	2038	5154	OSTEOSARCOMA OF THE R ILLUM
R40F48 A 531A	3/ 9/66		6.1	9.73	1.131	1798	6842	OSTEOSARCOMA OF THE 4TH CERVICAL VERTEBRA
R40F49 531B	3/ 9/66		5.0	15.43	1.337	1373	7599	OSTEOSARCOMA OF THE 2ND CERVICAL VERTEBRA
R40M50 531C	3/ 9/66		5.6	14.11	1.603	1600	9654	OSTEOSARCOMA OF THE 1ST CERVICAL VERTEBRA
R40M51 A 531D	3/ 9/66		5.0	14.49	1.402	1378	7099	OSTEOSARCOMA OF THE L HUMERUS
R40M52 A 531E	3/ 9/66		5.7	15.38	1.386	1649	8483	OSTEOSARCOMA OF THE L MANDIBLE
R40F53 563A	7/18/66		5.4	16.05	1.679	1547	9340	FUNGAL TURBINITIS
R40F54 563B	7/18/66		4.8	12.46	1.593	1305	6579	OSTEOSARCOMA OF THE R ACETABULUM
R40F56 A 563D	7/18/66		4.2	17.38	1.997	1092	7619	PATHOLOGIC FRACTURE OF THE R FEMUR
R40M57 563E	7/18/66		4.7	18.33	1.870	1288	9645	OSTEOSARCOMA OF THE L ISCHIUM
R40M58 563F	7/18/66		5.0	19.49	1.778	1381	9002	OSTEOSARCOMA OF THE R HUMERUS
R40F59 578A	11/15/66		5.0	18.92	2.255	1393	12481	OSTEOSARCOMA OF THE R FEMUR
R40M62 578D	11/15/66		4.8	25.29	2.389	1315	13804	OSTEOSARCOMA OF THE 5TH CERVICAL VERTEBRA
R40M63 578E	11/15/66		4.5	26.24	2.673	1198	12460	OSTEOSARCOMA OF 3RD LUMBAR VERTEBRA, PATH FRACTURE L HUMERUS
R40M64 578F	11/15/66		3.9	23.59	2.891	974	10054	OSTEOSARCOMA OF THE L ISCHIUM

BEAGLE NUMBER	LITTER NUMBER	BIRTH DATE	AGE AT TERM.	AGE AT DEATH	PEAK BODY (UCI)	BURDEN (UCI/KG)	EXPOSURE DAYS	TOTAL DOSE (RADs)	COMMENTS
R40M65	578G	11/15/66		4.0	30.35	2.877	1028	12092	OSTEOSARCOMAS OF THE R & L TIBIA
R40F67	630B	7/20/67		5.5	12.71	1.478	1578	7900	OSTEOSARCOMAS OF THE L ISCHIUM & L SCAPULA
R40F68	630C	7/20/67		5.8	9.65	1.283	1670	5401	OSTEOSARCOMA L FEMUR & RADIATION OSTEODYSTROPHY L ULNA
R40F70 A	630E	7/20/67		5.3	11.06	1.400	1483	7462	METASTATIC OSTEOSARCOMA

FIRST RUN

R50F01	283A	10/21/63		5.4	27.09	3.626	1519	19630	PATHOLOGIC FRACTURES OF THE R HUMERUS & R FEMUR
R50F02	283B	10/21/63		4.8	26.06	3.261	1315	15660	OSTEOSARCOMA OF THE R HUMERUS
R50M03	283C	10/21/63		4.1	28.26	3.360	1072	12920	OSTEOSARCOMA OF THE PELVIS
R50M04	283D	10/21/63		3.9	25.08	3.228	981	11382	OSTEOSARCOMA OF THE NASAL BONE
R50M05	283E	10/21/63		5.2	33.03	3.806	1459	20994	OSTEOSARCOMA OF THE L HUMERUS
R50F06	359A	5/23/64		4.9	25.20	3.406	1340	17800	OSTEOSARCOMA OF THE R FEMUR
R50F07 A	359B	5/23/64		4.6	28.49	3.634	1236	14070	OSTEOSARCOMA OF THE R TIBIA
R50F08 A	359C	5/23/64		4.6	28.37	3.202	1236	15410	OSTEOSARCOMA OF THE L RADIUS
R50M09	359D	5/23/64		5.0	24.66	3.102	1387	15550	MALIGNANT MELANOMA OF THE EYE
R50M11	372B	6/12/64		4.5	45.47	4.023	1203	20490	OSTEOMYELITIS OF FACIAL BONES
R50M12	372C	6/12/64		4.4	40.23	4.289	1182	18830	OSTEOSARCOMA OF LUMBAR VERTEBRA #4
R50M14	372E	6/12/64		3.3	42.84	4.096	779	13260	SACRIFICED DUE TO SEIZURES
R50F20	421D	9/20/64		5.6	27.33	3.293	1606	18190	OSTEOSARCOMA OF THE R RADIUS & R ULNA
R50M22	421F	9/20/64		4.2	43.75	4.074	1103	17482	OSTEOSARCOMA OF THE L TIBIA
R50M25	422C	9/20/64		4.2	40.51	3.717	1101	17840	OSTEOSARCOMA OF THE L FEMUR
R50M26 A	422D	9/20/64		4.7	40.34	4.854	1270	22434	OSTEOSARCOMA OF THE R RADIUS
R50M28	422F	9/20/64		5.3	39.52	4.421	1485	24780	RADIATION OSTEODYSTROPHY, L TIBIA
R50F30	436B	11/23/64		4.5	28.28	3.403	1193	14260	OSTEOSARCOMA OF THE 10TH TO 13TH L RIBS
R50M34	436F	11/23/64		4.0	39.39	3.695	1038	16424	POSTERIOR PARALYSIS
R50M35	436G	11/23/64		5.2	38.00	3.357	1449	19844	OSTEOSARCOMA OF THE L RADIUS & L ULNA

SECOND RUN

R50F36	473A	8/ 7/65		2.8	40.55	4.347	579	10014	PATHOLOGIC FRACTURES OF THE L & R MANDIBLES
R50M37	473B	8/ 7/65		2.3	40.10	4.321	423	7388	APLASTIC ANEMIA
R50M38	473C	8/ 7/65		4.4	40.75	3.715	1159	17940	OSTEOSARCOMA OF THE 4TH CERVICAL VERTEBRA
R50F44	564C	8/ 3/66		4.6	25.58	2.914	1251	14290	OSTEOSARCOMA OF THE 1ST TO 3RD LUMBAR VERTEBRA
R50F45	564D	8/ 3/66		3.3	34.55	4.065	754	11014	OSTEOSARCOMA OF THE R MANDIBLE
R50M48 A	564G	8/ 3/66		3.8	42.05	4.295	942	14302	OSTEOSARCOMA OF THE R FEMUR
R50M49 A	564H	8/ 3/66		4.9	42.00	4.361	1352	22664	METASTATIC OSTEOSARCOMA
R50F50	604A	3/28/67		2.7	38.84	5.564	561	10130	PATHOLOGIC FRACTURES OF THE L TIBIA & L MANDIBLE
R50F52	604C	3/28/67		1.9	51.72	6.386	267	5176	RADIATION NEPHRITIS
R50F53	604D	3/28/67		3.0	33.05	4.287	674	10850	PATHOLOGIC FRACTURES OF THE L TIBIA & R RADIUS
R50M56	604G	3/28/67		3.0	43.45	5.094	673	13420	PATHOLOGIC FRACTURE OF THE R HUMERUS
R50F64 A	619C	6/ 2/67	4.6	4.8	35.56	5.015	1336	21181	OSTEOSARCOMA OF THE R MAXILLA
R50F66	619E	6/ 2/67		4.8	40.94	5.229	1313	23540	OSTEOSARCOMA OF THE L MAXILLA
R50M67	619F	6/ 2/67		3.4	74.73	7.179	801	19650	PATHOLOGIC FRACTURES OF THE L FEMUR & L HUMERUS
R50F69	633B	7/25/67		3.6	31.84	3.940	898	12540	UNDETERMINED (BONE MARROW INFARCTION)
R50F70 A	633C	7/25/67		4.9	35.44	4.603	1340	20440	UNDETERMINED (PRIOR OSTEOSARCOMA AMPUTATION)
R50F71	633D	7/25/67		5.0	31.76	3.710	1378	17900	OSTEOSARCOMA OF THE L HUMERUS
R50M72	633E	7/25/67		4.4	36.13	4.250	1174	17840	OSTEOSARCOMA OF THE 3RD LUMBAR VERTEBRA
R50F73 A	635A	8/29/67		4.5	27.91	4.216	1218	19280	OSTEOSARCOMA OF THE L TIBIA
R50M75	635C	8/29/67		3.1	38.90	4.130	713	12011	ACCIDENTAL DEATH (ANESTHETIC DEATH AT LETTERMAN DURING F18 SCAN)
R50M77 A	635E	8/29/67		4.5	39.01	4.622	1216	18910	OSTEOSARCOMA OF THE L 9TH RIB & RADIATION NEPHRITIS

4.6

R5XF01	630D	7/20/67		2.4	60.39	6.695	756	22080	PATHOLOGIC FRACTURES OF THE R TIBIA & L HUMERUS
R5XM02	629E	7/15/67		2.3	94.16	7.674	714	25844	OSTEOSARCOMA OF THE L TIBIA
R5XM03	629F	7/15/67		2.3	78.80	7.061	698	22902	OSTEOSARCOMA OF THE R MANDIBLE
R5XM04	639D	9/14/67		2.9	38.30	3.884	1000	16790	OSTEOSARCOMA OF THE L FEMUR
R5XM05	639E	9/14/67		2.7	46.09	4.134	908	15770	OSTEOSARCOMA OF THE R FEMUR
R5XM06	639F	9/14/67		2.7	42.91	4.821	918	17834	PATHOLOGIC FRACTURES OF THE R FEMUR, R TIBIA, & L HUMERUS

BEAGLE NUMBER	LITTER NUMBER	BIRTH DATE	AGE AT TERM.	AGE AT DEATH	PEAK BODY (UCI)	BURDEN (UCI/KG)	EXPOSURE DAYS	TOTAL DOSE (RADS)	COMMENTS
FIRST RUN									
S20F01	291A	11/12/63		14.1	10.01	.938	4614	781	BILATERAL NEPHROSCLEROSIS
S20F06	311B	12/22/63	13.3	13.7	6.86	.756	4447	521	TERMINATED-BCG EXPERIMENT MAMMARY CARCINOMA
SECOND RUN									
S20F37	484A	9/ 1/65		13.4	9.67	1.193	4339	733	METASTATIC MAMMARY CARCINOMA
S20M39	484C	9/ 1/65		14.0	16.77	1.298	4581	1326	CONGESTIVE HEART FAILURE
S20F41	508A	11/ 6/65		2.1	9.30	1.467	216	106	EPILEPSY
S20F42	508B	11/ 6/65		15.6	13.66	1.674	5156	1176	LYMPHOSARCOMA
S20F43	508C	11/ 6/65		6.4	9.21	1.050	1813	423	UNDETERMINED (POSSIBLE EPILEPSY)
S20M45	508E	11/ 6/65		13.9	17.12	1.542	4553	1320	CHRONIC ENTERITIS
S20M46	508F	11/ 6/65		7.4	13.86	1.195	2172	692	UNDETERMINED (POSSIBLE EPILEPSY)
S20F48	532B	3/18/66		12.2	12.00	1.188	3928	824	CONGESTIVE HEART FAILURE
S20M49	532C	3/18/66		16.8	16.58	1.353	5604	1193	CHRONIC INTERVERTEBRAL DISC DISEASE
S20M59	584I	12/ 2/66		15.4	8.76	.938	5067	803	UNDETERMINED
S20F62	603C	3/25/67		14.8	7.09	.787	4861	395	METASTATIC TRANSITIONAL CELL CARCINOMA
FIRST RUN									
S40F02	292B	11/19/63		10.7	89.95	8.879	3368	6058	OSTEOSARCOMA OF THE L PUBIS
S40M09	294E	11/23/63		16.5	78.46	7.949	5471	6020	SENILE CEREBRAL ATROPHY
S40F11	328B	3/ 7/64		14.2	76.37	9.246	4643	7782	ACUTE HEART FAILURE, CARDIAC INSUFFICIENCY
S40F12	328C	3/ 7/64		12.5	69.98	7.854	4021	5802	FIBROSARCOMA OF THE SOFT PALATE
S40F23	331D	3/12/64		14.6	72.26	7.155	4780	5015	PATHOLOGIC FRACTURE OF JAW
S40M27	348B	4/25/64		14.6	87.51	11.990	4791	8531	HEMANGIOSARCOMA-BONE
S40M30	348E	4/25/64		15.5	83.93	9.782	5134	8236	INTERVERTEBRAL DISC DISEASE
S40F34	416C	9/ 7/64	12.5	13.3	63.63	6.813	4327	5633	TERMINATED-BCG EXPERIMENT HEPATOCELLULAR CARCINOMA
SECOND RUN									
S40F36	487A	9/ 5/65		10.6	69.60	7.751	3344	5282	DIABETES MELLITIS
S40F37	487B	9/ 5/65		12.5	58.58	8.251	4033	3498	METASTATIC MAMMARY CARCINOMA
S40M39	487D	9/ 5/65		2.7	96.14	8.389	456	1419	HEAT PROSTRATION
S40M40	487E	9/ 5/65		5.5	100.70	9.202	1486	3747	CHRONIC PULMONARY DISEASE
S40M41	487F	9/ 5/65	12.1	12.1	93.38	9.031	3883	6482	TERMINATED-FREDERICK CANCER CENTER OSTEOSARCOMA
S40F42	498A	9/27/65		14.2	78.81	10.710	4637	7410	SQUAMOUS CELL CARCINOMA-GINGIVA
S40F43	498B	9/27/65		9.8	100.60	12.670	3034	6462	METASTATIC HEPATIC HEMANGIOSARCOMA
S40F44	498C	9/27/65		2.2	103.50	12.940	250	1151	CONVULSIONS (EPILEPSY OR CHLORDANE TOXICITY)
S40F45	498D	9/27/65		10.4	79.82	9.617	3251	6204	IDEOPATHIC NEUROLOGIC DISEASE, ASPIRATION PNEUMONIA
S40F46	498E	9/27/65		17.4	70.24	9.076	5812	6580	INVASIVE NASAL CARCINOMA
S40F51	544E	5/21/66		13.6	82.79	8.697	4413	7992	FIBROSARCOMA-ZYGOMATIC ARCH
S40M57	597D	2/ 3/67		12.1	102.30	9.316	3897	7549	MALIGNANT LYMPHOMA
S40M59	597F	2/ 3/67		13.3	89.10	8.327	4328	6478	AORTIC THROMBOSIS-RENAL INFARCTION
S40M65	626F	7/ 4/67		13.8	116.80	10.361	4517	8690	OSTEOSARCOMA, VERTEBRA
S40F66 A	639A	9/14/67		13.0	120.92	12.263	4225	8458	METASTATIC HEMANGIOSARCOMA-BONE
S40F67	639B	9/14/67		10.4	114.40	10.570	3252	7294	HEPATIC ABSCESSSES, HEMATOMAS

PROBLEM-ORIENTED MEDICAL RECORD SYSTEM

R. G. White
L. S. Rosenblatt

The Systematized Nomenclature of Medicine (SNOMED) system through which records have been kept on the beagle colony at UCD has always presented a number of difficulties. Important among them are its need for well-qualified medical records personnel, its inefficiency (tedious entry, superfluous records), its frequent misinterpretation of diagnoses and dates, and its lack of a hierarchical pattern of organization. An alternate method, called the Problem-Oriented Medical Record (POMR) system was developed at LEHR in 1982 and has seen enough use to establish its advantages over the other system. POMR is constructed around four fields, namely, the complaint, the procedure, the diagnosis and the resultant status of the dog. An example, which reduces 12 pages of hand-written narrative to a single, one-page table and integrates related data (symptom, procedures, results), is presented.

In 1976 we began the coding of our beagle clinical records using SNOMED (Systematized Nomenclature of Medicine). At present over 200,000 records have been entered into our computer data base. The number exceeds, to our knowledge, the total number of SNOMED records at all the other DOE beagle programs combined.

A retrospective look at the UCD SNOMED coding system has revealed a number of problems:

1. A consistent problem has been our inability to find and hire fully qualified medical record personnel. Most of the coders received on-the-job training and few had the background to sift knowledgeably through voluminous clinical records and extract that information which was truly relevant to a clinician.
2. Many of the records that were coded provided no useful information. For example, if hematological examination (CBC) was ordered, SNOMED would indicate on one record that the blood had been drawn, but the information that a CBC was performed would appear on another. Obviously, a CBC could not be done without drawing blood. Similarly, orders for urine collection for urinalysis and for radiological analysis were also coded separately. The SNOMED file on one long-lived dog consisting of 1,006 records contains 254 records (25%) that fall into this "useless" category.
3. Diagnoses were missing or misinterpreted.
4. Integration of a past clinical narrative as it pertained to a clinical problem was inadequate in that the SNOMED record would appear to indicate that a clinical problem began on the date the problem was identified even though the clinical record revealed that the problem was of long standing.
5. Certain exams (e.g., quarterly exams) were not being coded even though they often provided valuable information.

6. In regard to clinical diagnoses, no hierarchy was designed into the SNOMED system. If, for example, an animal was presented to the clinician for an observed problem and a physical exam revealed 10 clinical symptoms which, collectively, could result in a diagnosis, each symptom and the ultimate diagnosis were all coded as "clinician's diagnosis." Consequently, any attempt to obtain summation of clinical problems on an individual record resulted in a list of symptoms, body weights, possible diagnosis, probable diagnosis and the diagnosis.
7. SNOMED coding of clinical records was a tedious, time-consuming process. We estimated that the coding of a moderately long clinical record required 19-23 hours.

Because of the shortcomings of SNOMED, as given above, we began work in 1982 on an integrated system to make the clinical records more useful. This system was designated the POMR, the Problem-Oriented Medical Records system. POMR was constructed around four fields.

1. The Complaint - why was the dog seen by the clinician, i.e., what was the problem?
2. The Procedure - what procedures were carried out to effect a diagnosis of the problem?
3. The Clinician's Diagnosis.
4. The resultant status of the dog, i.e., was the problem resolved?

An example of the POMR is shown in Table 1 for dog S20F01 and is condensed from 12 pages of long, hand-written narrative. Diagnostic tests, e.g. BUN (blood-urea-nitrogen), are listed, but the results are not reported since these values can be found in other data bases (hematology, clinical chemistry).

The POMR record for this dog begins with its I.D. The example is for a single dog so the I.D. column has been omitted in Table 1. Events are sequentially coded as 1.00, 1.01, 1.02, . . . and the date of the complaint is shown as "E-date."

POMR then lists a "complaint" such as "vaginal mass," "weakness in hind quarters," etc. The source of the complaint is coded (S#), and may be a caretaker, radiologist, etc. In the record shown, source "A" is an observer (caretaker or clinician). The observer's name is recorded as well, but is not shown here. Source "C" is Clinical Pathology--special diagnostic, and source "H" is Physical Exam--special diagnostic. The date of each diagnostic procedure is given.

Diagnostic procedures are coded and are spelled out: P# (procedure) = "A" is physical exam, "B" is Radiology, "C" is Clinical Pathology (with name of test), "D" is Surgery (excision/biopsy), "E" is Surgery (exploratory/corrective), "G" is Necropsy.

The Diagnostic section contains the date, the type of diagnosis (D# = "A" is definitive, "B" is presumptive) and the actual diagnosis. The Status section contains the date, St# is the status type; "A" indicates that the problem was resolved with the dates given and "B" indicates that the problem was unresolved.

Table 1. PROBLEM ORIENTED MEDICAL RECORD FOR BEAGLE NUMBER S20F01.

Event	E-Date	C	Complaint	S#	Age	P-Date	P#	Comments	D-date	D	D#	Diagnosis	St-date	St#	Disp
1.00	8/11/71	C	Vaginal mass	A	7.75	8/11/71	A	Fibrous mass protruding from vagina	8/11/71	D	A	Vaginal polyp	9/2/71	A	A
1.01						8/11/71	D	Surgery/biopsy							
1.02						8/11/71	C	Urinalysis/culture							
1.03						8/26/71	C	Urine culture							
2.00	3/29/73	C	Weakness in hindquarters	A	9.38	3/29/73	A	Stilted gait, tense abdomen	7/23/73	D	B	Spondylosis L4-5		B	C
2.01						3/30/73	B	Radiology (abdomen)							
2.02						3/30/73	C	Urinalysis							
2.03						4/4/73	C	BUN, SGPT, TP							
2.04						5/4/73	A	Stilted gait, tense abdomen							
2.05						5/4/73	B	Radiology (spinal survey)							
2.06						5/9/73	C	Radiology (abdomen)							
2.07						5/10/73	C	Radiology (skeletal)							
2.08						6/7/73	A	Stilted gait							
2.09						6/18/73	A	Stilted gait							
2.10						7/23/73	A	Stilted gait							
3.00	1/28/75	C	Vaginal cyst	H	11.21	1/28/75	A	Labial cyst	1/28/75	D	A	Infection/labial cyst	2/10/75	A	C
3.01						1/28/75	E	Surgery/corr.-cyst drained							
4.00	9/11/75	C	Avulsion of toenail	A	11.83	9/11/75	A	Avulsion of toenail #2 L. forefoot	9/11/75	D	A	Avulsion of toenail #2 L. forefoot	9/23/75	A	C
5.00	8/24/76	C	Mammary Nodule L4	H	12.78	8/24/76	A	Nodule L4	9/01/76	D	A	benign mixed mammary tumor	9/9/75	A	C
5.01						9/1/76	D	Surgery/biopsy							
6.01	6/16/77	C	Abrasion of R. ischial callous	A	13.59	6/16/77	A	Abrasion of R. ischial callous	6/16/77	D	A	Abrasion of R. ischial callous	6/23/77	A	C
7.00	7/11/77	C	High BUN	C	13.66	7/11/77	C	BUN, CBC	7/27/77	D	A	Chronic glomerulonephropathy		B	C
7.01						7/14/77	C	BUN, Creatinine							
7.02						7/20/77	C	Urinalysis							
7.03						7/27/77	C	Radiology (IVP)							
7.04						8/31/77	C	CBC							
7.05						12/22/77	C	SMA/BUN/creatinine/SAP/SGPT/TP							
7.06						12/22/77	C	Necropsy							
8.00	7/12/77	C	Laceration of tail	A	13.66	7/12/77	A	Laceration of tail	7/12/77	D	A	Laceration of tail	7/19/77	A	C
8.01						7/12/77	E	Surgery/Corrective							

The Disposition code refers to the movement of the dog during or after the clinical problem, e.g., retained in hospital, discharged to its original pen, died-necropsied, etc.

It may be seen that there were 8 clinical problems in the life of S20F01, beginning when she was 7.8 years of age. The many earlier examinations of this dog revealed nothing of interest to the clinician, and only routine procedures (e.g., blood sampling and vaccinations) were performed. Three of the problems can be considered minor and were quickly resolved--avulsion of toenail, abrasion of right ischial callus and laceration of the tail. Three were somewhat more complex; a vaginal polyp that was removed, a vaginal cyst that was drained and a mammary nodule that proved to be a benign mixed mammary tumor. No recurrence of a mammary tumor was observed. The problem given as "weakness in hindquarters," and tentatively diagnosed as spondylosis of the 4th and 5th lumbar vertebrae, was never resolved and the dog retained a slightly stilted gait throughout life. The terminal problem, the cause of death, was glomerulonephropathy, initially diagnosed because of a high BUN. Thus, the information in the 12 pages of clinical records can now be quickly scanned and the record is much more amenable to statistical analysis.

SNOMED coding of Event and Diagnosis will be performed to facilitate retrieval and analyses of these parameters. In contrast to the original SNOMED, in which coding requires 19-23 hours, POMR coding takes 5-7 hours plus 1-2 hours for SNOMED coding of the Event and Diagnosis fields.

EMPTYING TIME FOR THE SMALL INTESTINE IN BEAGLE DOGS

T. Miyabayashi
J. P. Morgan
M. A. O. Atilola
L. Muhumuza

Fifteen contrast radiographic studies were performed on the upper gastrointestinal tracts of five standard adult Beagle dogs that were in normal condition and were free of internal parasites. Three studies, spaced at six-day intervals were made on each dog. Sequential radiographs were made at 30-minute intervals following administration of barium sulfate suspension until the entire contrast medium column was in the colon and cecum. The mean gastric emptying time (with standard deviation and range) was 76 ± 16.7 (30-120) minutes, small intestinal transit time was 73 ± 16.4 (30-120) minutes, and small intestinal emptying time was 214 ± 25.1 (180-300) minutes. This study offers the possibility that small-intestinal emptying time may be used to evaluate patients with suspected partial obstruction of the small intestine, partial obstruction, pseudo-obstruction, ischemia, or lymphangiectasia.

INTRODUCTION

Contrast radiographic studies of the upper gastrointestinal tract have been used in animals mainly to detect morphologic alterations, such as mechanical obstructions, paralytic ileus, constriction, ulceration, or abnormal mucosal patterns (Morgan and Silverman 1984). There is some information available from such studies on the functional parameters, gastric emptying times and small-intestinal transit times, but there is little information on small-intestinal emptying times following administration of a predetermined amount of barium sulfate suspension (Miyabayashi et al., 1986).

This study seeks to fill that gap. Its specific purposes were: (1) to measure small-intestinal emptying times in clinically normal Beagle dogs, (2) to study a possible relationship between gastric emptying time and small-intestinal emptying time, and (3) to examine the significance of small-intestinal emptying time in canine intestinal disease. An additional concern, which served as the initial stimulus for this work, was that the 15 dogs used in the study were being fed heavy doses of strontium-90 daily, for life, but had no higher rates of gastrointestinal tumor formation than the control animals. Information on time of passage was needed in order to calculate the total gastrointestinal dose being sustained by these animals.

MATERIALS AND METHODS

Five Beagle dogs were used (Table 1). The dogs were born and raised in a controlled experimental animal facility at the Laboratory for Energy-Related Health Research, University of California, Davis. The dogs were generally sound and free of internal parasites and of ongoing gastrointestinal problems. The ages of the dogs ranged from 2-8 years. Weights fell in the range of 12.4-13.7 kg. Three studies, spaced at six-day intervals, were made on each dog, with food but not water being withheld for 24 hours prior to each run. In each study a dose of 10 ml/kg bw of 60% wt/vol barium sulfate suspension was administered through a stomach tube. Data were not used in the analysis from dogs which were found, in survey radiographs, to have ingestra in the stomach or small bowel. The study was continued in cases where dogs had feces in any part of the colon.

No enemas were given. Sequential, ventrodorsal radiographs were made immediately after administration of the barium sulfate and at 30-minute intervals thereafter until the entire contrast medium column was in the colon and cecum. Representative radiographs, illustrating the three stages, are shown in Figure 1. Terms used in the study were defined as follows:

Gastric emptying time: Application time until the contrast medium has been passed into the small intestine, allowing minimal residual rugal coating.

Small-intestine transit time: Application time until the head of the contrast medium first lies within the cecum or ascending colon.

Small-intestine emptying time: Application time until passage of the contrast medium into the cecum and colon is completed, allowing minimal residual mucosal coating of the small intestine.

Table 1. A SUMMARY OF SMALL-INTESTINAL EMPTYING STUDY.

ID number	76K02W	76L01B	79G57Y	79J66U	82I19R
Sex	F	M	F	F	F
Age (yrs)	8	8	5	5	2
Weight (kg)	13.7	12.6	12.4	13.7	13.5
Amount of feces*					
1st	+	+++	++	+	++
2nd	-	++	+++	+	-
3rd	+	+	-	+	-
Gastric emptying time (min)					
1st	90	60	90	30	90
2nd	90	120	60	60	90
3rd	60	90	60	60	(120)
Mean	80	90	70	50	90
Mean and SD = 76.0±16.7 min (N=5)					
Transit time(min)					
1st	90	90	90	60	90
2nd	60	120	60	90	60
3rd	30	90	60	30	(30)
Mean	60	100	70	60	75
Mean and SD = 73.0±16.4 min (N=5)					
Small intestinal emptying time (min)					
1st	300	210	210	180	210
2nd	210	270	180	210	210
3rd	210	240	180	180	(180)
Mean	240	240	190	190	210
Mean and SD = 214±25.1 min (N=5)					

* + = feces in the descending colon; ++ = in the transverse colon;
+++ = in the ascending colon.

Data not included due to the presence of gravel in the stomach.

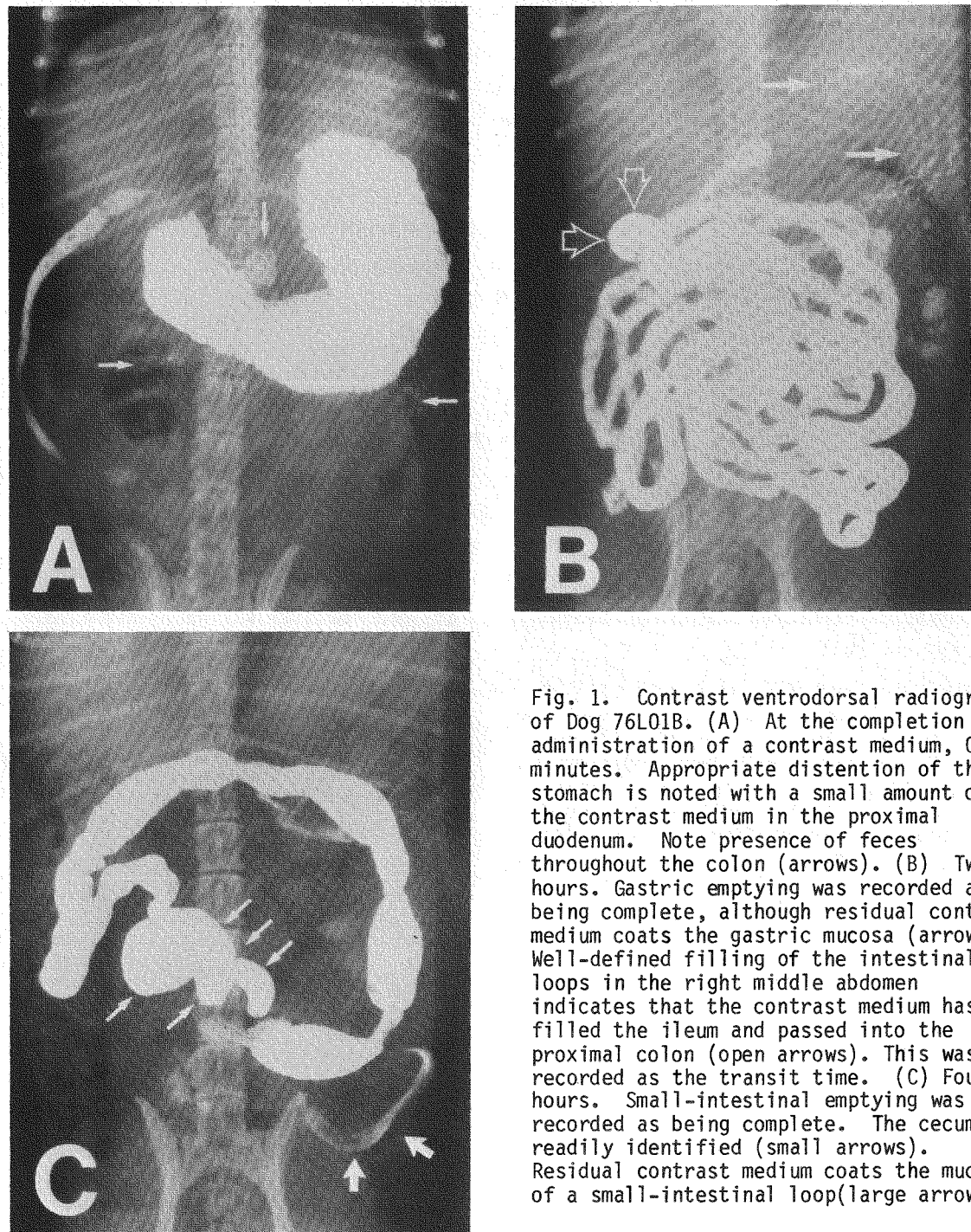


Fig. 1. Contrast ventrodorsal radiographs of Dog 76L01B. (A) At the completion of administration of a contrast medium, 0 minutes. Appropriate distention of the stomach is noted with a small amount of the contrast medium in the proximal duodenum. Note presence of feces throughout the colon (arrows). (B) Two hours. Gastric emptying was recorded as being complete, although residual contrast medium coats the gastric mucosa (arrows). Well-defined filling of the intestinal loops in the right middle abdomen indicates that the contrast medium has filled the ileum and passed into the proximal colon (open arrows). This was recorded as the transit time. (C) Four hours. Small-intestinal emptying was recorded as being complete. The cecum is readily identified (small arrows). Residual contrast medium coats the mucosa of a small-intestinal loop (large arrows).

RESULTS

The results of the examinations are summarized in Table 1. All upper gastrointestinal examinations were conducted without difficulty. The mean gastric emptying time (with standard deviation and range) was 76 ± 16.7 (30-120) minutes. Small intestinal transit time was 73 ± 16.4 (30-120) minutes, and small intestinal emptying time was 214 ± 25.1 (180-300) minutes. The mean and standard deviation were calculated from the five-dog means (three samples/dog), and hence are roughly analogous to the standard error of the mean. One dog (79J66U) was consistently excited during the examination. However, that did not appear to affect the small-intestinal emptying time. The amount of feces in the colon did not appear to influence the results of the study.

Despite the apparent consistency in the emptying and transit times, no significant correlation between the three means could be demonstrated. The correlation coefficient (*r*) for gastric vs. small-intestine emptying time was 0.702 and the small-intestinal emptying time, and between the gastric emptying time and the transit time was found, with *r*-values of 0.702 (*P* > 0.10) and for gastric emptying time vs small intestine transit time was 0.646 (*P* > 0.10).

DISCUSSION

Though *r*-values are weak, the consistency of the means suggests that both small-intestinal emptying time and transit time correlate positively with gastric emptying time. Discrepancies between gastric emptying time and expected small-intestinal transit and emptying times may suggest intestinal mobility problems, or at least intestinal passage resistance. Partial obstructive lesions, such as incomplete stenosis or partial constriction by neoplasia and fibrosis of the small intestine can probably cause this situation. Lymphangiectasia and early stages of ischemia are other conditions in which delayed small-intestinal emptying time might be used as clues for early diagnosis. The emptying time may be preferable to transit time for this, since the amplitude of its variation in relation to gastrointestinal pathology is likely to be greater.

The gastric emptying time, transit time, and small intestinal emptying time were rather consistent within each individual dog. This finding reflects normal functions of the gastrointestinal tract and suggests that one recording of small intestinal emptying time or transit time in a normal dog can be used in building a data base, provided that short time intervals between radiographic studies are used. Again small intestinal emptying time is probably the preferred indicator.

The presence or amount of feces did not appear to influence either transit or emptying time of the small intestine. Although the gastrocolic reflex exists, there is no known neurological pathway or reflex in which the colon acts as a primary stimulating site. This means that there will be cases in which performing an upper gastrointestinal study without an enema will be justified. Values for emptying and transit times might in fact be adversely affected by a high cleansing enema. However, feces can occasionally interfere with the interpretation of radiographs.

Radiographic safety may become a problem when many sequential films are made, as occurs when the radiographic technique is extended from an ordinary upper gastrointestinal study where only transit time is determined. This can be solved in part by limiting the additional films to 1-hour intervals using only ventrodorsal positioning until intestinal emptying is thought eminent. At that time, the interval may be shortened. A ventrodorsal radiograph with paddle compression on the right upper abdominal quadrant will produce excellent views of the ileoceccocolic area when the study is near completion. Although the use of chemical restraint eliminates the need for animal holders, and thus reduces x-ray exposures to the holders, commonly used drugs alter gastrointestinal motility.

A recent study suggested the use of dog food mixed with barium sulfate suspension as a contrast agent to evaluate gastric emptying time. This approach was based on gastric physiology and was intended to differentiate the functional pathology of the proximal and distal portion of the stomach more specifically (Miyabayashi and Morgan 1984). This approach may be applied in evaluating the motility of the small intestine, with emphasis on small-intestinal emptying time. Other modalities, such as nuclear medicine and fluoroscopy, may measure gastrointestinal motility more accurately (Koblik and Hornof 1985).

The procedure used in this work provides an additional, specific radiographic dimension for studies of gastrointestinal problems. The gastrointestinal functional values, such as gastric emptying time and small-intestinal emptying time, would be useful in cases where outflow resistance or passage problems are evident. The procedure should be useful, too, in evaluating morphologic changes of the gastrointestinal tract.

CONCLUSIONS

Small-intestinal emptying time may be measured clinically in suspected cases of partial obstruction of that part of the GI tract and early stages of stenosis. The study may also be helpful in diagnosing intestinal pseudo-obstruction, ischemia, or lymphangiectasia, all of which cause intestinal motility problems. However, clinical trials need to be performed to verify the use of small intestinal emptying time for this purpose.

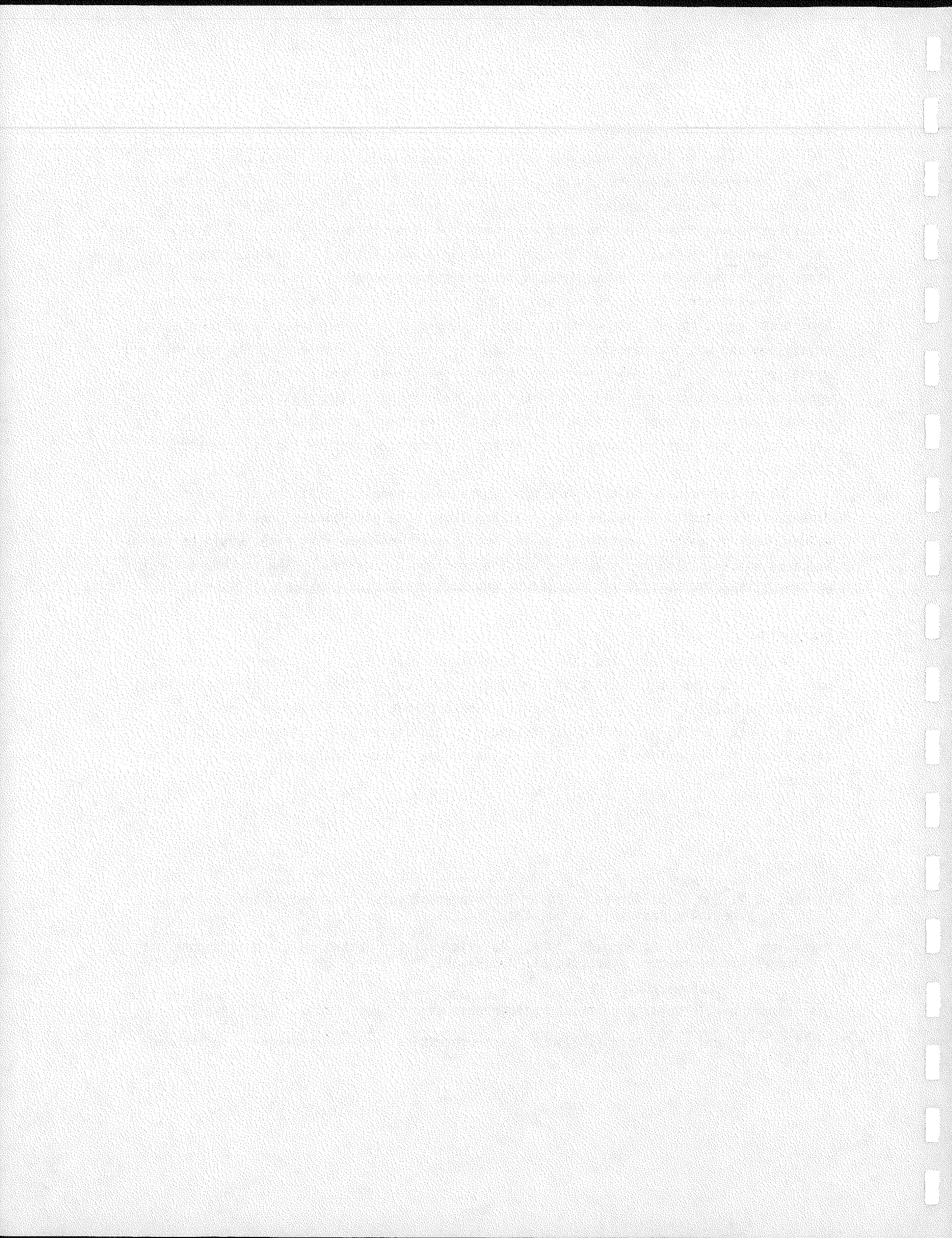
REFERENCES

Morgan, J. P. and S. Silverman. 1984. Techniques of Veterinary Radiography. 4th ed. Davis: Veterinary Radiology Associates.

Miyabayashi, T. and J. P. Morgan. 1984. Gastric emptying in the normal dog: a contrast radiographic technique. *Vet. Radiol.* 25:187-191.

_____, ___, M. A. O. Atilola, and L. Muhumuza. 1986. Small intestinal emptying time in normal beagle dogs: A contrast radiographic study. *Vet. Radiol.* 27:164-168.

Koblik, P. D. and W. J. Hornof. 1985. Gastrointestinal nuclear medicine. *Vet. Radiol.* 26:138-142.



SKELETAL BIOLOGY STUDIES

ASSESSMENT OF CORTICAL AND TRABECULAR BONE DISTRIBUTION IN THE BEAGLE SKELETON BY NEUTRON ACTIVATION ANALYSIS

N. J. Parks
W. S. S. Jee
R. B. Dell
G. E. Miller

The distribution of bone calcium between morphologically identifiable cortical and trabecular bone obtained by dissection and quantitated by neutron activation analysis (NAA) is described. The skeleton of a female beagle dog was dissected into approximately 400 pieces and assayed for ^{49}Ca produced in the University of California, Irvine TRIGA reactor. Weights of calcium in the complete, alcohol-fixed sections and in the cortical sections after removal of the trabecular bone are reported. Vertebrae were divided into three parts (body, spine, and transverse processes). Long bones were divided into 10-12 parts so that epiphysis, metaphysis, and diaphysis could each be characterized. The median percent cortical calcium values for cervical, thoracic, and lumbar vertebrae were 82, 56, and 66%, respectively, but values within the groups and among individual vertebral sections varied by a factor of two. For long bones, the median percent cortical calcium varied from between 90 to 100% in the midshaft to below 50% in the proximal and distal sections. The final calculated cortical-tissue-to-calcium mass ratio (TCR) varied from about 4.5 for midshafts of the long bones to about 9 for thoracic vertebral bodies and indicated that the mineral fraction of cortical bone is not constant throughout the skeleton. The ratio of cortical to trabecular calcium in the skeleton was 79.6:20.4.

INTRODUCTION

Knowledge of the distribution of the two major classes of bone, the high-density cortical type, seen close to the exterior of many bones, and the spongy trabecular bone, which is common in the interior, is important in the understanding of the tumors caused by bone-seeking radionuclides of strontium, radium and the actinides. Miller et al. (1985) have found a strong positive correlation between the number of tumors in beagle dogs caused by the bone-surface-seeking actinide, plutonium, and turnover rates of calcium. That turnover rate differs in the two classes of bone, and is presumably one of the factors lying behind the observation that radium induced tumors are more common in cortical bone of the appendicular skeleton of beagles than in trabecular bone (Parks, 1980, 1985). Not enough is known about the specifics of the distribution of the bone types, however, to clear up the confusing picture that we have when we try to link the actinide toxicity data in beagles to, say, a more general picture of radium toxicity in beagles and then transfer those conclusions on to humans. A detailed skeletal map of canine cortical and trabecular bone is clearly needed to make it possible for us to clarify these relationships and make the beagle work more readily applicable to humans.

The first step in developing such a map came from lifespan kinetic analyses at the whole-bone or bone-group level (Parks, 1980, 1985), which provided estimates of effective cortical and trabecular mass throughout the skeleton. Related studies made it possible to express calcium distribution in terms of the kinetically inferred effective mass of the bone, using a mathematical model which was described in the last annual report (and in

Hood, 1985). The linear relationship between the occurrence in the two types of bone of radium-induced tumors mentioned above was identified through these studies. Rates are lower in trabecular bone and higher in cortical bone of the appendicular skeleton. No such relationship was found in the axial skeleton, where a different pattern exists. The tumorigenic potential of the cervical vertebrae approximates that of the long bones of the appendicular skeleton but is two orders of magnitude lower in the thoracic and lumbar vertebrae.

One possible source of this disparity is that the kinetic model used assumptions from other work which suggested that the lumbar and thoracic vertebrae could be taken to be 100% trabecular bone in the calculation of mineral dynamics. The trabecular ash fraction of the full canine vertebral column is reported, however, to be 15%. A second source could be that bone turnover rates, which are directly related to the size of cell populations at risk, is different in the two classes of bone. Checking each of these possibilities will depend upon a more detailed picture of the distribution of cortical vs. trabecular bone.

The initial action in this part of the bone biology project was to find a method for distinguishing the two classes of bone that would provide the desired level of sensitivity within the limitations of the available resources. The early work of Gong et al. (1964) provided guidance. They dissected one complete male beagle skeleton and, in addition, examined the ash fraction of cortical bone from femoral shafts and of trabecular bone from lumbar vertebral bodies. However, the effort required to ash and weigh the projected 800 to 1000 samples, then to separate cortical and trabecular components by physical means, made their method impractical.

An attractive alternative which met our objectives was to take advantage of the thermal neutron nuclear reaction which transforms ^{48}Ca (0.187% abundant in naturally occurring bone calcium) to radioactive ^{49}Ca ($t_{1/2} = 8.72$ min). The amount of ^{49}Ca radioactivity induced by neutron activation is directly proportional to the mass of calcium present. In addition, ash weight can be closely approximated by employing the mean calcium to bone ash-weight ratio of about 0.38, thus permitting comparisons, where possible, to earlier work based on ashing techniques. The approach has been shown to be adequately sensitive in successful in vivo assessment of human whole body calcium as well as in human skeletal mineral assays.

MATERIALS AND METHODS

The procedure in preparation of bone specimens was as follows: The fresh frozen skeleton of a 9.74 kg, 5.4-year-old female beagle that had served as a control in an experiment at the University of Utah's Radiobiology Laboratory was defleshed and disarticulated; bones from the right limbs and ribs and the entire axial skeleton, including skull with mandible, plus sternebrae, were selected for use; each bone was weighed (including cortical and trabecular bone, marrow and cartilage at this point) and its length measured; bones were sectioned so that pieces would fit into special 14 by 50 mm reactor vials; bone pieces were fixed in ethanol there, then removed, drained, weighed again and returned to alcohol.

The bone sections were irradiated in a reactor at the University of California, Irvine, and measured for cortical plus trabecular calcium, using a lithium-drifted germanium detector. The ^{49}Ca decay peak at 3084 keV was used. Calcium content was initially estimated with a calibration function derived from measurement of standard calcium carbonate samples. The area under the 3084 keV peak corresponded to ca. 42,000 counts/min per gram Ca for these experiments.

After decay of short term radionuclides, trabecular bone was drilled away, using carbide dental drills (some bones being split for access). The remaining cortical pieces were weighed and returned to the reactor for quantification of cortical calcium alone. The final tissue-to-calcium ratio (TCR) provided for direct assessment of the variability in the mineral fraction of bone throughout the skeleton.

RESULTS

Tables 1 and 2 give the physical measurements of the larger bones of the appendicular and axial skeleton as taken for this survey. Tables 3 and 4 present detailed data on two representative types of bone, the cervical vertebrae and a long bone--the right femur. Total weight in these tables includes marrow. The cortical weight is what remains after trabecular bone and marrow have been removed. The two calcium values (Ca1 and Ca2) relate to those weights, total and cortical, respectively. Figures 1 and 2 show the manner in which two representative bones from the tables were sectioned.

Table 1. TOTAL WEIGHTS, DIMENSIONS, AND IDENTIFICATION CODES FOR BONES AND SKELETAL COMPONENTS.

Bone	Whole-bone weight (gm)	Length if listed (cm)	Code
Right humerus	24.290	11.00	R (right) H (humerus) 1-11 (beginning proximal) a-b
Right ulna	9.281	12.50	R (right) U (ulna) 1-12 (beginning proximal)
Right radius	8.515	9.75	R (right) R (radius) 1-12 (beginning proximal)
Right scapula	14.588	10.60	R (right) S (Scapula) 1-11 (beginning proximal) a-c
Right femur	26.204	11.50	R (right) F (femur) 1-12 (beginning proximal) a-b
Right tibia	20.636	12.00	R (right) T (tibia) 1-11 (beginning proximal) a-b
Right fibula	2.043	11.00	R (right) FB (fibula) 1-11 (beginning proximal)
Sternum	16.391		ST (sternum) 1-7, x (beginning proximal), x = xyphoid
Right calvarium	9.268	8.50	R (right) C (calvarium) 1-9 (front to back)
Right mandible	25.530	12.00	R (right) M (mandible) 1-12 (beginning front to back) a-b
Right pelvis	10.062	7.00	R (right) P (pelvis) IL (ilium) PB (pubic) IS (ischium) 1-12 (beginning proximal) a-b

Table 2. TOTAL WEIGHT AND IDENTIFICATION CODES FOR SKELETAL COMPONENTS:
VERTEBRAE AND SKULL

Bone	Weight (gm)	Code
Cervical Vertebrae		
CV1	7.550	CV (cervical vertebra)
CV2	8.407	1-7 (# of vertebra)
CV3	4.605	AS (arch + spine)
CV4	5.669	B (body)
CV5		TP (transverse process)
CV6	6.050	a-b (more than one vial)
CV7	6.110	
Thoracic vertebrae		
TV1	4.857	TV (thoracic vertebrae)
TV2	3.991	1-13 (# of vertebra)
TV3	3.681	A (arch)
TV4	3.584	B (body)
TV5	3.515	S (spine)
TV6	3.513	
TV7	3.385	
TV8	3.433	
TV9	3.482	
TV10	3.500	
TV11	4.307	
TV12	5.254	
TV13	5.656	
Lumbar vertebrae		
LV1	6.546	LV (lumbar vertebra)
LV2	6.967	1-7 (# of vertebra)
LV3	7.725	A (arch)
LV4	7.720	B (body)
LV5	7.981	S (spine)
LV6	7.919	TP (transverse process)
LV7	6.910	
Sacrum	9.864	SB (sacrum body) SP (sacrum spine) 1-2 (# of vials)
Tail-caudal vertebrae	12.467	TC (tail-caudal) 1 (4 vert) 2 (2 vert) 3 (2 vert) 4 (2 vert) 5 (3 vert) 6 (4 vert) a-b (more than one vial)
Right Skull	52.585	R (right) AT (anterior turbinate) PT (posterior turbinate) N (nasal) FS (frontal sinus) IN (incisive) MX (maxilla) AZA (anterior zygomatic arch) PZA (posterior zygomatic arch) FLP (frontal lacrimal palatine) TP (temporal) a-b (more than one vial)

Table 3. WEIGHTS (gm), CALCIUM CONTENT (gm), 95% CONFIDENCE INTERVAL, AND MEDIAN PERCENT CORTICAL CALCIUM FOR CERVICAL VERTEBRAE SECTIONS.

Section Code	Total Wt(g)	Cortical Wt(g)	Total Ca1(g)	Cortical Ca2(g)	% Cortical Ca		
					Lower 95% Limit	Median	Upper 95% Limit
CV1Ba	2.545	2.577	0.480	0.436	79.5	90.7	98.6
CV1Bb	2.555	2.394	0.408	0.391	87.0	95.7	99.8
CV1TP	1.756	1.703	0.331	0.303	83.4	91.6	98.7
CV2Ba	2.198	1.459	0.330	0.239	65.1	72.5	79.9
CV2Bb	2.181	1.535	0.288	0.274	87.7	95.1	99.7
CV2TP	3.731	3.151	0.587	0.442	62.9	75.4	87.9
CV3AS	1.919	1.329	0.254	0.238	86.5	93.8	99.4
CV3B	2.208	0.899	0.310	0.125	33.7	40.3	47.0
CV3TP	0.268	0.166	0.039	0.028	49.7	71.4	92.3
CV4AS	1.962	1.415	0.321	0.257	72.5	80.1	87.8
CV4B	2.278	0.988	0.303	0.172	49.8	56.5	63.3
CV4TP	1.145	0.703	0.175	0.117	58.9	67.2	75.6
CV5AS	2.086	1.642	0.362	0.304	75.5	83.9	92.4
CV5B	2.459	1.676	0.306	0.243	72.0	79.4	86.8
CV5TP	0.862	0.651	0.143	0.116	71.5	80.8	90.2
CV6AS	2.647	2.412	0.417	0.404	89.0	96.9	99.9
CV6B	2.277	1.522	0.323	0.258	72.2	79.9	87.5
CV6TP	0.828	0.750	0.144	0.135	85.6	94.2	99.6
CV7AS	2.370	0.982	0.221	0.196	81.1	88.5	95.8
CV7B	2.443	2.942	0.489	0.424	75.4	86.7	97.2
CV7TP	1.008	0.852	0.164	0.161	93.2	98.4	99.9

Table 4. WEIGHTS (gm), CALCIUM CONTENT (gm), 95% CONFIDENCE INTERVAL, AND MEDIAN PERCENTAGE CORTICAL CALCIUM FOR RIGHT FEMUR SECTIONS.

Section Code	Total Wt(g)	Cortical Wt(g)	Total Ca1(g)	Cortical Ca2(g)	% Cortical Ca		
					Lower 95% Limit	Median	Upper 95% Limit
RF1	2.636	0.266	0.356	0.030	1.6	8.4	17.7
RF2A	0.917	0.523	0.128	0.118	81.6	92.2	99.4
RF2B	1.137	0.630	0.144	0.116	70.2	80.6	90.9
RF3A	0.966	0.766	0.157	0.154	91.3	97.8	99.9
RF3B	1.138	0.084	0.200	0.164	73.4	82.1	90.8
RF4	1.397	1.015	0.266	0.242	82.2	91.1	98.7
RF5	1.262	1.172	0.260	0.252	92.1	98.8	99.9
RF6	1.210	1.054	0.250	0.226	81.8	90.5	98.3
RF7	1.295	1.050	0.243	0.237	91.0	97.6	99.9
RF8	1.563	1.000	0.264	0.222	75.6	84.2	92.7
RF9	1.571	1.000	0.246	0.208	75.8	84.3	92.8
RF10A	1.247	0.534	0.137	0.116	74.1	84.8	95.2
RF10B	0.955	0.405	0.106	0.094	76.1	88.9	98.8
RF11A	2.442	0.702	0.275	0.108	31.6	39.3	47.0
RF11B	2.565	0.158	0.246	0.121	41.3	49.2	57.1
RF12A	0.917	0.669	0.187	0.127	59.0	67.8	76.7
RF12B	0.731	0.186	0.069	0.016	7.1	23.8	40.9

Fig. 1. Diagram of cervical vertebra showing sectioning for neutron activation analysis.

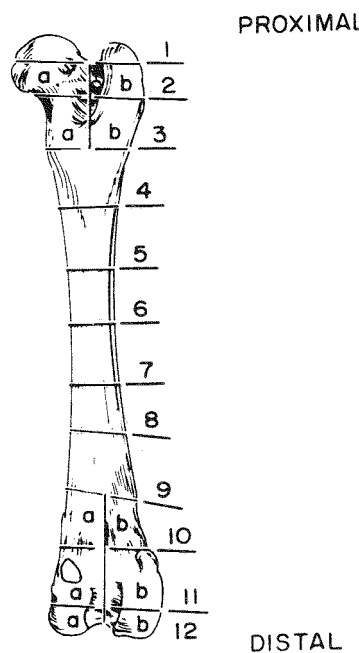
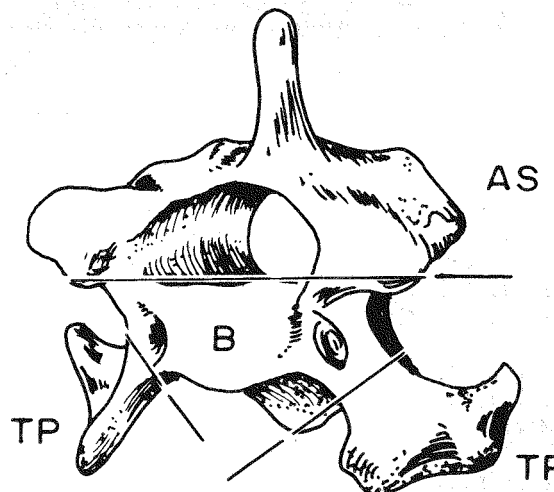


Fig. 2. Right femur as sectioned for neutron activation analysis.

Table 5 presents a summary of total Ca in each bone group and a comparison of our summation of section values from NAA to the whole bone or bone group values obtained by Gong et al. (1964) and Spiers and Beddoe (1983) by ashing techniques. Table 6 provides a comparison of cortical tissue weight to calcium weight (TCR) for all the sections of the cervical, thoracic, and lumbar vertebrae. The TCR is directly proportional to the hydrated, non-mineralized organic component of bone (Robinson, 1975) and inversely proportional to the fractional calcium weight or the fractional ash weight (about 1/0.38 TCR). The values range from about 4.6 to 10 and represent approximately the same range as found throughout the skeleton for sections that are exclusively cortical bone and do not contain any cartilage.

Table 5. SUMMARY PERCENTAGE CORTICAL BONE MEASUREMENTS BY NEUTRON ACTIVATION ANALYSIS OF CALCIUM.

	Ca (gm)	% Cortical Ca				Spiers & Beddoe (1983)
		Low 95%	Median	High 95%	Gong et al. (1964)	
Cervical Vertebra	6.40	70.8	82.3	93.7		
Thoracic Vertebra	6.22	35.6	55.8	76.0		
Lumbar Vertebra	6.22	45.5	62.4	79.3		
Tail-Caudal Vertebra	1.24	78.8	86.2	93.6		
Sacrum	0.84	51.5	61.3	71.2		
All Vertebrae	20.92	51.3	67.4	83.5	84.3	
Rt. Calvarium	1.70	91.8	97.0	99.8		
Rt. Maxilla	3.09	82.0	89.9	97.5		
Skull	3.11	66.7	82.3	96.6		
Whole Cranium	7.85	78.6	89.0	98.6	81.4	
Rt. Mandible	4.35	79.6	90.8	99.1	93.1	
Rt. Femur	3.53	60.6	72.9	84.9	68.5	81.5
Rt. Radius	1.48	73.1	83.1	93.0	90.0	90.4
Rt. Ulna	1.52	78.7	92.0	99.5	85.1	89.1
Rt. Humerus	3.42	53.4	67.2	81.0	75.9	78.1
Rt. Tibia	3.29	74.1	82.8	91.5	77.0	86.5
Rt. Fibula	0.13	42.7	78.9	98.7	90.0	92.8
Rt. Forepaw	2.09	49.6	81.0	98.8		
Rt. Hindpaw	2.95	53.1	82.4	98.9		
Rt. Feet	5.04	51.4	81.8	98.8	93.0	
Rt. Ribs + cartilage	4.66	53.5	81.7	98.7	49.1	
Rt. Ribs no cartilage	4.46	74.4	91.4	99.5		
Rt. Scapula	2.89	60.3	81.0	97.6		
Rt. Pelvis	2.87	60.3	73.0	85.6	78.6	
Sternum	0.75	13.5	43.0	73.0		

Table 6. COMPARISON OF CORTICAL WEIGHT (WET WEIGHT 2) TO CALCIUM (Ca2) VALUES FOR VERTEBRAE.

Section Code	Arch	Body	Spine	Transverse process	Arch- Spine	Section Code	Arch	Body	Spine	Transverse process	Arch- Spine
CV1		5.45		5.61		LV1	5.94	8.23	6.18	6.59	
CV2		5.27		6.97		LV2	5.73	6.82	5.94	5.58	
CV3		7.11		5.55	5.59	LV3	5.07	7.87	5.17	6.43	
CV4		5.71		5.94	5.45	LV4	5.00	7.11	5.97	5.32	
CV5		6.85		5.57	5.35	LV5	5.24	7.01	5.63	5.33	
CV6		5.85		5.56	6.00	LV6	5.27	6.88	5.73	5.50	
CV7		6.89		5.31	5.00	LV7	5.37	7.59	4.61	5.68	
TV1	5.83	7.17	5.73			Mean CVs		6.16		5.78	
TV2	5.71	9.35	5.69								
TV3	5.48	7.54	5.70								
TV4	6.02	10.02	5.09			Mean TVs		5.73		5.38	
TV5	6.21	9.70	5.24								
TV6	5.68	9.41	4.93								
TV7	5.48	9.40	5.93			Mean LVs		5.38		5.60	
TV8	5.89	9.21	5.08								
TV9	5.59	9.06	5.38								
TV10	5.64	7.10	5.12			Mean of Col.		5.36		5.60	
TV11	6.07	8.13	5.29								
TV12	5.76	7.19	5.87								
TV13	5.08	6.47	4.85								

DISCUSSION

The overall quality of the data is confirmed by the comparisons given in Table 5. Specifically, values for percent of cortical bone are remarkably consistent with those of Gong et al. (1964) and Spiers and Beddoe (1983), who report values obtained by microdissection and ashing techniques. Our median values are weighted by dividing calculated amounts by the total grams of calcium (Ca1 in the Tables 3 and 4).

By using a mean Ca-to-ash ratio of 0.38 (Robinson, 1975) to convert our calcium values obtained by NAA to the equivalent mass of bone ash, we can compare our femoral midshaft predicted value for tissue-to-ash weight ratio with that of Gong et al., who reported 1.70 (sd, 0.02). Using TCR values (ratio of total weight to cortical tissue weight) for femur sections 5, 6, 7, and 8 (Table 4, Figure 3) and applying Ca:ash of 0.38, we obtain a midshaft value of 1.73 (sd, 0.04). This provides additional evidence that the calcium measurements are, in general, tracking the same phenomena as were the ashing methods of those earlier investigators.

The sum of Ca1 values for all sections (multiplying right side sections by 2) was 102.77 g. This value is sufficiently close to 100 that the Ca/bone column can be read, in an approximate way, as percent distribution of Ca in this skeleton, after multiplying by two where appropriate. These values are consistent with both earlier reports on Ca mass distribution and with the ⁹⁰Sr distribution in whole bones of uniformly labelled beagle skeletons reported by Parks (1985).

A similar summation of wet weight 1 values ("Total Wt." in Tables 3 and 4) to that of the Ca1 values gave a value of 718.35 g. Comparison to the precut weights where available showed that about 6% of the total bone-plus-marrow mass was lost. This leads to an estimate of total Ca of approximately 109.3 g and a total skeleton weight of 764 g. The summed cortical calcium (multiplying by 2 as appropriate) was 79.4% of the total calcium summation, leaving 20.6% accounted for by trabecular bone.

There are discrepancies between this and other studies. For example, our data show median values for ribs of between 78 and 86 percent cortical bone, vs. 49% in the work by Gong et al. (1964). Also, we show 67% cortical bone in all vertebrae vs. 84% in earlier work. Though our median values in the latter case are based on 90 measurements, the possibility exists that our experimental animal was aberrant. All the other evidence indicates, however, that our female specimen was a typical representative of the breed in terms of skeletal mineralization parameters (Goldman, 1970; Garsd et al., 1981). An especially important observation in this study is that vertebrae in the various groups are so different that a combined value is likely to obscure critical information. The same is true of individual vertebrae in the cervical group.

The vertebral data provide a good basis for initial discussion because of past uncertainty and their importance in understanding radionuclide-induced tumor distributions. The calculations in Table 6 show that the mineral density is about the same in the bodies of the cervical vertebrae as it is in the processes. The thoracic vertebrae differ considerably from the cervicals. In the former group, cortical percentages cluster around 70% in the arches and spines but are between 30 and 40% in the

bodies of the bones. It is apparent that the mineral density of the thoracic bodies is appreciably less than the cervical bodies or even the thoracic arches and spines, and that the amount of hydrated, non-mineralized organic material is higher. The lumbar vertebrae form a relatively homogeneous group and represent an intermediate case with respect to mineral density.

In typical long bones such as the femur (Table 4), the epiphyseal-metaphyseal regions contain from 8 to 50% cortical Ca, with a regular progression of values toward the 90 to 100% range in the mid-shaft region. The greatest degree of mineralization and smallest TCR values (typically about 4.5) are found in the long-bone midshaft region. The proximal and distal ends commonly have TCR values in the 6.5 to 7.5 range, with a few reading as high as 11 or 12.

USE OF THE DATA

Estimates of the trabecular bone mass removed from each section can be obtained by the straightforward procedure of multiplying the TCR value (cortical wet wt. 2 divided by Ca2) by the intact-section calcium value (Ca1) to estimate the mass of total bone in the intact section. The difference between the total bone value and cortical wet wt. 2 is the trabecular mass estimate. These estimates are subject to the variability of the wet weight measurements, which are likely to be random. A possible bias toward the lower limit may exist because the mineralization of trabeculae may be less than the cortical bone from which the estimates were generated (Gong et al., 1964). Arguing against such a notion is the fact that we have observed that the mineralization of cortical bone surrounding typical highly trabeculated areas such as long bone epiphyses and vertebral bodies was less than that of diaphyseal cortical bone. Consequently, estimates of trabecular mass in a highly trabeculated section may be relatively bias free.

Estimates of trabecular bone mass in sections revealed by a high TCR value to contain cartilage can be made but require the assumption of an TCR value appropriate for bone. Estimates of marrow mass can be made for entire bones by subtracting the cortical and trabecular bone mass from the intact section weight (wet wt. 1). However, it must be realized that the propagation of uncertainty at this point tends to make only the summation of marrow mass over an entire bone meaningful. This follows from the expectation that measurement errors tend to cancel out when summing over several sections.

It is clear that the data reported here will provide for improved dosimetry of bone-seeking radionuclides. First of all, the local dose can be defined throughout the skeleton at a detailed level comparable to our ability to identify the origin of tumors (Pool et al., 1973; Pool and Williams, 1975.) In their discussion of intra-cortical bone lesions induced by radium in beagles and humans, Pool et al. (1983) noted that about half the bone tumors in the dogs they examined were in the midshaft of the long bones, which are the sections for which we obtained the smallest TCR values. Given that bone tumors are not distributed in an "average" way, it is clear that responses to skeletal insults that are site specific are better defined when related to site-specific mass and composition parameters for cortical and trabecular bone.

Pool et al. (1983) also noted that successful maintenance of a vascular bed by dogs led to a higher fraction of shaft tumors than observed in humans. The vascular bed is an intimate part of the fluid-dynamics system of bone which is in turn an intimate part of the chemical-dynamics system which defines the deposition of calcium phosphates from supersaturated solutions and subsequent maintenance of bone mineral. The vascular bed is the support system for the cell populations responsible for bone remodelling dynamics; consequently, the ongoing task is to complement this description of skeletal statics with an experimental and theoretical description of cortical bone remodelling dynamics (Hood, 1985) to match the trabecular dynamics research already done.

Another example of clarification now available is the opportunity to revise the radiochemically derived predictions of effective surface to mass relationships (Parks, 1980) that were based on an assumed 100% trabecular character for thoracic and lumbar vertebrae. Now the arguments can include not only the current estimates of 44.2 and 37.6% trabecular for thoracic and lumbar vertebrae, respectively, that we report here, but also the issue of variable TCR for cortical bone, and presumably trabecular bone, throughout the skeleton can be addressed.

We believe the data presented here will provide for improved use of the dog in research using *in vivo* bone mass measurement as an experimental probe. Our present study with a young adult female dog provides for cross-calibration of this important animal model with humans where data exists and provides guidance where they do not exist. It is now apparent that extension of the total skeletal distribution measurements to include an age range of dogs is feasible and would be beneficial.

RELATIONSHIP TO OTHER WORK

The early results from this work were compared to the tumor-site distributions found in the alkaline-earth, ^{226}Ra , studies at University of California, Davis, and in the ^{226}Ra and actinide (^{239}Pu and ^{241}Am) work at the University of Utah. It is clear that these relationships are complex functions of several variables, but it now appears that about 50% of the tumor-site predilection can be explained by the association of tumor-appearance frequency at a given site with the fraction of cortical or trabecular bone present.

We expect the data for the total skeleton reported here to provide guidance for relating the results of bone-seeking radionuclide studies to detailed fluid space measurements and ion-transport studies in specific parts of both canine and human skeletons. These results also admit the possibility of improved theory and modeling for maladies induced by other bone-seeking metals such as aluminum-caused osteomalacia and lead toxicity. The method is practical and the logical extension is to an age range comparison of beagle and human material so that the vast amount of beagle research can be used more effectively in diagnosis and therapy for human skeletal disease.

REFERENCES

Garsd, A., M. Goldman and L. S. Rosenblatt. 1981. The prediction of skeletal mass in growing and adult beagles. *Growth* 45:29-41.

Goldman, M. 1970. Skeletal Mineralization. In The Beagle as an Experimental Dog, E.C. Andersen (ed.), pp. 216-225. Ames, Iowa State University Press.

Goldman, M. and L. K. Bustad (eds.) 1972. Biomedical Implications of Radiostrontium Exposure, U.S. Atomic Energy Commission, Washington, D.C., 404 pp.

Gong, J. K., J. S. Arnold and S. H. Cohn. 1964. Composition of trabecular and cortical bone. *Anat. Rec.* 149:325-332.

Hood, S. J. 1985. A partial differential equation model of the bone remodelling process: Cell population dynamics in canine cortical bone. (Ph.D. Thesis, University of California, Davis; Laboratory for Energy-related Health Research and Department of Mechanical Engineering, 120 pp.).

Miller, S. C., W. S. S. Jee, J. M. Smith and W. R. Wronski. 1985. Tissue characteristics of high and low incidence Pu-induced osteogenic sarcoma sites in lifespan beagle studies. In Lifespan Radiation Effects Studies in Animals: What Can They Tell Us?, R.D. Thompson and J.A. Mahaffey (eds.), pp. 286-298. U.S. Department of Energy Technical Information Center, Oak Ridge, Tennessee.

Parks, N. J., 1980. Lifespan dynamics of intra-skeletal radionuclide distribution in radium-injected beagles. *Health Phys.* 38:11-20.

Parks, N. J. 1985. Dynamics of lifespan strontium-90 distribution in beagles with uniformly labelled skeletons acquired by radionuclide ingestion from in utero to adulthood. In Metals in Bone, N.D. Priest (ed.), pp. 107-115. Lancaster, MTP Press.

Pool, R. R., J. R. Williams, M. Goldman and L. S. Rosenblatt. 1973. Comparison of bone-tumor sites in beagles continually fed ⁹⁰Sr or injected with ²²⁶Ra as a means of scaling risk to humans. In Radionuclide Carcinogenesis, C.L. Sanders, R.H. Busch, J.E. Ballou, and D.D. Mahlum (eds.), pp.475-486. CONF-720505, U.S. Atomic Energy Commission, Washington.

Pool, R. R. and R. J. R. Williams. 1975. Distribution of ²²⁶Ra-induced primary bone sarcomas in beagles. In Radiobiology Laboratory Annual Report, pp. 128-129. USERDA Rep. UCD 472-122. University of California, Davis.

Pool, R. R., J. P. Morgan, N. J. Parks, J. E. Farnham, and M. S. Littman. 1983. Comparative pathogenesis of radium-induced intracortical bone lesions in humans and beagles. *Health Phys.* 44 (Suppl. 1):155-177.

Robinson, R. A. 1975. Physicochemical Structure of Bone. *Clin. Orthop.* 112:263-315.

Spiers, F. W. and A. H. Beddoe. 1983. Sites of incidence of osteosarcoma in the long bones of man and the beagle. *Health Phys.* 44 (Supplement 1):49-64.

CELLULAR AND MOLECULAR STUDIES

ALLOTRANSPLANTATION OF CANINE MYELOID LEUKEMIA

T. G. Kawakami
G. R. Cain

Radiation-induced canine myeloid leukemic cells were successfully allografted in immunosuppressed newborn and adult dogs. Transplantability and metastases in the allogenic host indicated the transformed malignant property of the cells. Leukemias in serially passed animals were similar to that in the original host animal, and the affected cells could serve as a source for radiation-induced leukemic cells. Using single cell clones from established cell lines of leukemic dogs, allograftability of the leukemic cells was found to depend on a unique property of the leukemic cell in addition to immunosuppression of the allogenic host.

Radiation- and non-radiation-induced canine myeloid leukemias occur infrequently and are most commonly an acute disease leading to early death of the afflicted animal. The survival period after the onset of clinical disease is typically from a few months to half a year. Because the disease is both infrequent and acute, myeloid leukemic cells are not readily available for laboratory work. In order to overcome the problem of short supply of the cells which are responsible for radiation-induced myelomonocytic leukemia in dogs, Shifrine et al. (1971) developed a fetal transplantation technique. While fetal transplantation was successful, their technique was difficult, involving a high degree of surgical expertise and special facilities. This report describes an alternative method which not only provides a source of myeloid leukemic cells without special surgical requirements, but also makes it possible to differentiate hyperplastic from neoplastic myeloid cells.

Transplantation studies in canine fetuses at LEHR have indicated that successful transplantation is dependent upon immunocompetence of the fetuses. Early experimentation showed eight out of eight transplantations succeeding in 43-day-old fetuses. None of four transplantations in neonates succeeded (Shifrine and Bryant, 1976). They found the 43-day-old fetuses to be immuno-incompetent, whereas neonates were immuno-competent.

In this project we immunosuppressed neonates beagles by subjecting them to 100 cGy whole-body irradiation. Adult dogs were immunosuppressed by a combination of 800 cGy whole-body irradiation and the immunosuppressant drug, cyclosporin. Each of the latter animals was injected IP with $1-2 \times 10^8$ cells per kilogram of body weight. The results of the sequential allografting of radiation-induced myeloid leukemia are summarized in Tables 1 and 2. Table 1 summarizes the successful sequential transplantation of radiation-induced monocytic leukemia in newborn and in adult dogs. The leukemic cells were readily transplantable into either immunosuppressed newborn puppies or immunosuppressed adults. The latent period varied but the transplantation was highly successful.

These results support the conclusions (1) that induction of leukemia by radiation involves transformation of hematopoietic cells, and (2) that the leukemic cells have malignant properties.

Table 1. TRANSPLANTATION OF LEUKEMIC CELLS IN DOGS:
REPRESENTATIVE SEQUENCE.

Passage	Animal #	
0	82D10P	(monocytic leukemia) Neonate 100 cGy
1	84H53F	(45 days, monocytic leukemia) Neonate 100 cGy
2	84J61C	(23 days, monocytic leukemia) Adult 800 cGy Cyclosporin
3	75F01A	(27 days, monocytic leukemia) Adult 800 cGy Cyclosporin
4	73G01B	(16 days, monocytic leukemia)

Table 2. SUMMARY OF EXPERIENCE WITH LEUKEMIA-TRANSPLANTED DOGS.*

Initial X dog** w/Leukemia	Type of Leukemia	Number of Sequential Transplantations	Treatment Resulting in Leukemia	No. of Dogs	Days to Leukemia
79G63G	Myelomonocytic Leukemia	5	Neonate, 100 cGy	8	45
			I/U	4	54
			Adult, 800 cGy + Cyclosporin	1	34
			Neonate	1	45
82D10P	Monocytic Leukemia	4	Neonate, 100 cGy	3	38
			Adults, 800 cGy	3	19
82H18S	Megakaryocytic leukemia	1	Neonate, 100 cGy	1	23
			I/U	1	15

* Injected IP with 1×10^8 cells per Kg body weight into adults, and 10^8 cells per neonate and fetus.

** All 3 leukemia donors were exposed to 9.4 cGy/d in the cobalt field.

Although allotransplantation of canine myeloid leukemic cells from animals with myeloid leukemia was successful and immunosuppression played an important role, the transplanted leukemic cells, which involved transplantation of all mononuclear cells separated from the peripheral blood of a leukemic animal were not generally of a homogenous clonal cell population. Thus, the role of the canine leukemic cell in allotransplantation could not be determined. In murine species, there is evidence that the cell surface macromolecules of the TA3 mammary carcinoma cell line played an important role in allotransplantation.

Recently, we successfully established three canine myeloid leukemic cell lines: K9ML-1, radiation-induced monocytic leukemia; K9ML-2, spontaneous myelocytic leukemia; and K9ML-3, radiation-induced myelocytic leukemia. In an attempt to determine whether the cells from each cell line played a role in the allotransplantability of these cells in neonates, we injected the tertiary and subcloned leukemic cells from these cell lines. The results are summarized on Table 3.

Table 3. ALLOTTRANSPLANTATION OF CANINE MYELOID LEUKEMIC CELL LINES IN IRRADIATED NEONATES.

Cell Line	# Leukemia/# Injected	Latent Period
K9ML-1	0/4	>6 months
K9ML-2	2/2	14 days
K9ML-2-0*	3/3	14 days
K9ML-2-6*	0/1	> 5 months
K9ML-2-8*	1/1	14 days
K9ML-3	2/2	92 days

* Subcloned cultures established from single cell clones in soft agar.

These results indicate that 2 of the 3 established cells are allotransplantable in neonates and are malignant. Although K9ML-1 was established from allotransplantable monocytic leukemia, the K9ML-1 cell line appears to have lost the transplantable malignant properties. On the other hand, both K9ML-2 and K9ML-3 were readily transplantable in neonates. Using the same number of cells, we found K9ML-2 to be a highly aggressive leukemia which was capable of inducing the disease after only a short latent period. However, one of three subclones of K9ML-2 failed to develop leukemia, which suggests that the property essential for allotransplantation was lost in this subclone.

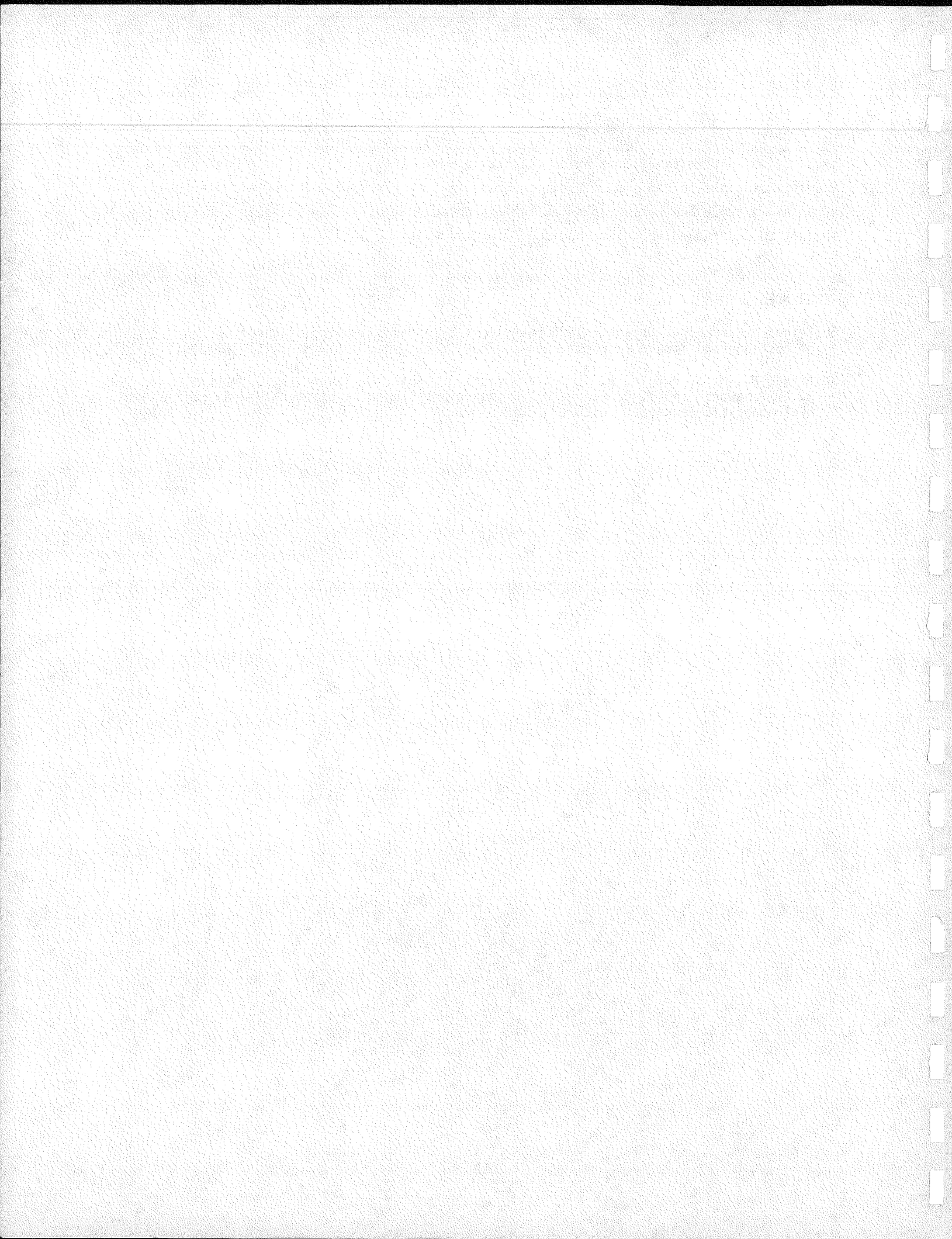
Since radiation is highly carcinogenic and transforms cells after 1 cGy in vitro, the continuous irradiation of canine hematopoietic cells should have the potential of transforming many cells. Yet the induction of myeloid leukemia in irradiated dogs requires exposures greater than 1000 cGy. This suggests that other factors in addition to

cell transformation are required for initiation of the clinical disease, myeloid leukemia. It is possible that the unique property of escaping immunosurveillance during the initial onset of leukemia and allotransplantation is similar. Characterization of the specific property which permits allotransplantation of a myeloid leukemic cell line may help in understanding the mechanisms of leukemogenesis. Further studies of the molecular changes of transplantable and nontransplantable myeloid leukemic cells may give the necessary insight to understanding the mechanism of leukemogenesis.

REFERENCES

Shifrine, M. and B. J. Bryant. 1976. Leukemia allotransplants: Influence of host age and immune responsiveness. *Proc. Soc. Expt. Biol. Med.* 151:307-309.

Shifrine, M., M. S. Bulgin, N. E. Dollarhide, H. G. Wolf, N. Taylor, F. D. Wilson, D. L. Dungworth and Y.-C. Zee. 1971. Transplantation of radiation-induced canine myelomonocytic leukemia. *Nature* 232:405-406.



NUCLEAR MEDICAL STUDIES

COORDINATION CHEMISTRY OF THE ^{212}Pb - ^{212}Bi
NUCLEAR TRANSFORMATION: ALPHA-EMITTING RADIOPHARMACEUTICALS

N. J. Parks
W. R. Harris¹
C. L. Keen²
S. R. Cooper³
S. Zidenberg-Cherr²
K. W. Musker⁴
P. K. Bharadwaj⁵
P. D. Schneider⁶

This project is seeking a way to overcome the problem of the short half-life of ^{212}Bi (1.01 h) in order that it might be used on an organic molecule as a radiopharmaceutical. A solution could be to attach its precursor, ^{212}Pb ($t_{1/2} = 10.6$ h) to the molecule, but the problem then becomes one of finding an organic ligand that can survive the $^{212}\text{Pb}/^{212}\text{Bi}$ transition. Trithiosuccinyl compounds and 1,1-dithio ligands are being examined as potentially most promising, since some of them bind strongly to both metals discriminately against possible competitors. A source of ^{212}Pb has been developed which also produces quantities of two bismuth radionuclides that have proven value as tracers in (1) determining binding properties of ligands and (2) following movements in the body of ligand-bound Pb and Bi. Those movements are being traced to specific tissues and organs using liposomes in a mouse melanoma model. New experiments are carrying the transport studies to the subcellular level in rats in an effort to determine binding properties with natural proteins and to anticipate possible unwanted radiation effects.

INTRODUCTION

Alpha-emitting bismuth-212 ($t_{1/2} = 60$ m) has potential as a radiopharmaceutical agent, but its *in vivo* use is limited because the time required to reach the target across the vascular barrier may be longer than is desirable within the constraints of this half-life. Our intent is to create an alpha-emitting moiety chemically that has an effective half-life of approximately 11 hours by developing coordination complexes of the ^{212}Pb (10.6 hr) parent of ^{212}Bi . This moiety would need to be designed to retain the daughter bismuth radionuclide after the nuclear transformation by beta decay. Although this decay has an energy that does not, on average, lead to recoil of the ^{212}Bi daughter out of the parent complex, the high positive charge on the daughter (associated with the emission of Auger electrons and electron shake-off) can be as high as 10 to 11 in the first few attoseconds (10-18) after decay. This leads to charge redistribution in a time frame of about 10^{-15} seconds, which is short compared to the typical bond vibration period of 10^{-12} seconds. This project is aimed at developing and testing the efficacy of electron-rich coordination complexes that can withstand the charge redistribution process and retain the ^{212}Bi daughter.

Other aspects of the project are: (1) Experiments to determine which organs and tissues these forms of bismuth are deposited in and (2) studies to determine precisely where the ^{212}Bi may end up within the cells. Organ location is significant in terms of putting the radiopharmaceutical adjacent to tumors as well as determining potential

¹ Dept. of Chemistry, University of Missouri, St. Louis, MO

² Department of Nutrition, University of California, Davis

³ Inorganic Chemistry Laboratory, The University of Oxford, UK

⁴ Department of Chemistry, University of California, Davis

⁵ Dept. of Chemistry, India Institute of Technology, Kampur, India

⁶ Dept. of Surgery, University of California Medical Center, Sacramento

radiotoxic effects on various organs and tissues if the ^{212}Bi is not effectively chelated and goes to non-target sites. Information on location inside cells is important in anticipating effects of both the recoil atoms and the alpha particle on key chemical constituents of the cell and its nucleus.

Bismuth radionuclides show promise, also, as tracers, particularly in studies of the binding properties of possible carriers and of the movement and localization of this element in the body. Both of these types of tracer studies are essential preliminaries to the development of radiotherapeutic applications. Two such isotopes are ^{205}Bi (15.31 d) and ^{206}Bi (6.24 d) (Parks et al., 1987).

The study has been organized to address five problems that grow out of these concerns:

- (1) Finding a way to prepare no-carrier-added (NCA) ^{212}Pb , which is the precursor to ^{212}Bi . An important aspect of this work is the development of sources of the bismuth radiotracers with half lives longer than 60 minutes.
- (2) Designing, synthesizing, and characterizing chelating agents which will retain both ^{212}Pb and ^{212}Bi under physiological conditions and permit attachment to an antibody or a specific ligand.
- (3) Evaluating intramolecular chemical effects of the nuclear transformation, which is to say, possible damage to the ligand from the transition of ^{212}Pb to ^{212}Bi . In this case, the work has had to start with the development of new experimental methods.
- (4) Finding where bismuth goes in the body and determining how it is bound to proteins there so that binding constants of synthetic chelating agents can be selected to match.
- (5) Screening new ligands for Pb-Bi administration, using bismuth binding constants gained from the other work.

Since it was initiated in 1985 this project has attracted some very capable people, working in a wide variety of fields, and we are already able to report considerable progress, primarily in radioengineering and organic chemistry.

RADIOCHEMICAL ENGINEERING

In collaboration with the Crocker Nuclear Laboratory at UCD we have been able not only to produce the needed ^{212}Pb from natural lead but to produce $^{205},^{206}\text{Bi}$ as well in sufficient quantities to use as tracers in continuing biological and chemical studies (Lagunas-Solar et. al., this report).

ORGANIC CHEMISTRY

The work in organic chemistry began with the synthesis of a crown thiaether. This group has a high affinity for lead and shows promise of surviving the nuclear transformation from lead to bismuth. Spectroscopic structural analysis revealed that lead atoms did not fit into the cavity as well as theoretically predicted, so we attempted then

to open the crown and allow the metal to be complexed. A next step was to close the molecular structure somewhat in an effort to gain the high stability needed for survival in physiological fluids. Trisuccinyl-substituted compounds were theoretically attractive on this ground but have proven to be difficult to synthesize. We are continuing to experiment with the synthesis of substituted succinyl compounds but have been exploring an alternative as well. This is to substitute 1,1-dithio groups in the coordination complexes of lead, which we have successfully done. These molecules have much the same hexacoordinate properties as the succinyl compounds, and they are known both to complex with heavy metals and to have more tractable synthetic routes. Little was known, however, about their structure and stability, so we have engaged a number of co-workers in investigations of these compounds. The result has been a spate of publications. Bharadwaj and Musker present results of their studies of a dithiocarboxyl complex with lead in this annual report.

Studies are progressing also on the chelating abilities of 1,1-dithio ligands. These ligands have been found to be very attractive on two accounts: 1) they can strongly bind both Pb and Bi in aqueous media in a wide pH range, and 2) they can bind Pb and Bi discriminately against essential transition metals. The Bharadwaj and Musker report, mentioned above, focuses in part on this subject.

CHEMICAL EFFECTS OF NUCLEAR TRANSFORMATION

First steps have been taken in the development of new methods for studying the effects on the coordination complex of the decay of ^{212}Pb to ^{212}Bi . Quantities of the metals are 10 orders of magnitude lower than those which are typically seen in macroscopic studies, so we have adapted methods from research on chemical effects of nuclear transformations (CENT) and "hot atom chemistry." One special problem has been that our NCA materials react with the stainless steel, glass, and titanium components of the available radio-high performance liquid chromatography (HPLC) equipment. The separation of inorganic ions and coordination complexes through electrophoresis can, in principle, provide a solution to the problem, but we have found the process too slow to meet our general needs. Radioscanners are being developed now to provide greater speed. Another option for eliminating these reactions is to construct the radio-HPLC system entirely from fluorocarbon polymer, which we are proceeding to do.

CELLULAR RADIobiOLOGY OF ALPHA PARTICLES

In vitro and in vivo melanoma models are being used to relate alpha energy deposition from intracellular Pb/Bi-212 to response distribution (Hill et al., 1986). Fluorescent-labelled liposomes are being used in cell culture systems to carry the $^{212}\text{Pb}/^{212}\text{Bi}$ into the cell. This radiobiology work provides the benchmark against which the efficacy of radiotherapeutic alpha emitter molecules will be tested. We can also commence in vivo studies of the chemical competition between bismuth-binding proteins (and other naturally occurring ligands) and synthetic ligands designed to retain both parent lead and daughter ^{212}Bi after the nuclear transformation.

REFERENCES

Hill, A., P. D. Schneider, K. C. Chelton, and N. J. Parks. 1986. Murine Model for intracellular therapeutic radiation of melanoma. *Surgical Forum* 37: 425-427 (Extended Abstract).

Parks, N. J., K. C. Chelton, A. C. Mishra, et al. 1987. In: *Laboratory for Energy-related Health Research. 1985 Annual Report.* UCD 472-131, pp 124-129.

CYCLOTRON PRODUCTION OF NO-CARRIER-ADDED ^{206}Bi (6.24 d) AND ^{205}Bi (15.31 d)
AS TRACERS FOR BIOLOGICAL STUDIES AND FOR THE DEVELOPMENT
OF ALPHA-EMITTING RADIOTHERAPEUTIC AGENTS

M. C. Lagunas-Solar
O. F. Carvacho
L. Nagahara
A. Mishra
N. J. Parks

The production and radiochemical purification of no-carrier-added (NCA) bismuth isotopes (i.e., 6.24 d. ^{206}Bi and 15.31 d ^{205}Bi) was studied. The Bi isotopes are intended for use as tracers in biodistribution studies and in the design and testing of alpha-emitting radiotherapeutic agents. The total cross sections and yields for production of ^{206}Bi and ^{205}Bi from the proton bombardment of natural Pb targets were measured using the stacked-foils technique. A radiochemical method for the separation and purification of NCA Bi radioactivities from a multi-gram Pb target was also tested, modified and improved to provide aqueous solutions of chemically and biologically useful amounts of NCA ^{206}Bi , ^{205}Bi for measuring tissue and subcellular-distribution, and for studies covering several chemical aspects of the development of Pb/Bi-radiotherapeutic agents.

INTRODUCTION

The isotopes of bismuth have been passed over as potential therapeutic agents because none have the appropriate decay properties (half-life, decay mode, etc.) for general use. As a consequence, little is known about the biological distribution and binding properties of bismuth. The development in recent years of radiotherapeutic modalities that place radionuclides close to a biological target (i.e., tumor) has increased the possibility that bismuth isotopes might be used for such treatment. The general concept is that after administration and localization of the radionuclide, decay will take place and cause highly localized quantities of energy to be deposited in the cells, creating an intensely ionized chemical environment which will result in lethal metabolic changes. ^{212}Bi (from the decay of ^{212}Pb) is an α -emitting isotope that could be put to such a use. The alpha particles from the decay of ^{212}Bi (1.01 h) and of its short-lived daughter, ^{212}Po (0.3 μ sec), will deposit 6 and 8.8 MeV, respectively, in a 60-100 μm range in living tissue (approximately 6 to 10 cell diameters). Two other isotopes, ^{205}Bi and ^{206}Bi , show promise as tracers for biological studies (Parks et al., 1985).

Unfavorable radiochemical, thermodynamic and biological effects are possible, however, from all of these isotopes. Specifically, the binding of the metals, Pb and Bi, must survive the nuclear transition from ^{212}Pb to ^{212}Bi , and the bismuth must then be radiolytically stable for the agent to remain effective. Bismuth-212 which is lost at this time could damage normal tissue.

If bismuth isotopes are to be used as therapeutic agents, it is important that we know more about its in vivo distribution. Studies of the movement and localization of bismuth in the body could, in fact, be aided by the use of the two short-lived isotopes, ^{205}Bi and ^{206}Bi .

Research has been under way for some years regarding the nature, behavior and availability of a number of isotopes of lead and bismuth which show promise as tracers for biological studies. This project supplements the work of Acerbi et al. (1976) and

Birattari et al. (1981) on the production and separation of $^{206,205}\text{Bi}$ from natural Pb targets in the 7 to 44 MeV energy range. Our work covers the 8.8 to 67.5 MeV region of proton-induced reactions on natural Pb, in which both excitation functions and thick-target yields were measured. It also describes a no-carrier-added (NCA) radiochemical separation of the Bi radioactivities which results in radiochemically and chemically pure $^{206,205}\text{Bi}$. These isotopes have proven to be appropriate for high efficiency (> 70%) protein antibody labelling.

METHODS

An external proton beam of the 1.93-m isochronous cyclotron at the University of California, Davis, Crocker Nuclear Laboratory was used in all of the irradiations. Metallic Pb of natural isotopic composition (i.e., 1.42% ^{204}Pb , 24.1% ^{206}Pb , 22.1% ^{207}Pb , and 52.3% ^{208}Pb) was used as target material. Thin (0.1 mm) Pb foils of >99.99% purity were used in the fabrication of both the stacked thin-foil targets, which were used for excitation-function and thin-target-yield measurements, and of thick targets, used for thick-target yields and radiochemistry studies.

Because the induced Bi radioactivities contained both short-lived (< 1 day) and long-lived (> 1 day) radionuclides, the radioassays were conducted using two different high resolution detectors: A high efficiency Ge(Li) coaxial detector for assaying ^{205}Bi (15.31 d) and ^{206}Bi (6.24 d), and a lower efficiency, high purity Ge detector for ^{203}Bi (11.8 h) and ^{204}Bi (11.2 h). The different radionuclide yields were measured by assaying the highest gamma ray energy for which good counting statistics (<10% errors) were obtained. This criterion was the determining factor in electing to use two different high resolution detectors with different characteristics and efficiencies. Table 1 gives the nuclear decay characteristics of the radionuclides of interest which were used in the radioassays, and for the evaluation and quantitation of the data.

The data from the radionuclide assays were analyzed using an existing program provided by the ND-66 multi-channel analyzer. This program includes a multi-point, linear-background subtraction capability which was utilized to obtain net integrated areas (i.e., count rate) for each of the regions of interest. Details on corrections, Pb-target energy calculations, radionuclide yields and calculation of uncertainties (which totalled $\pm 13.5\%$) for those yields are given in Lagunas-Solar et al. (1987).

The procedure for radiochemical separation of Bi from Pb was based upon a combination of precipitation and ion-exchange methods. Emphasis was placed upon finding a simple, efficient, reliable and reproducible operation. Personal safety was a consideration, too, in seeking to automate the process.

RESULTS AND DISCUSSION

The Q-values for some relevant proton-induced reactions leading to the production of Bi isotopes are given in Table 2. Because a 67.5-MeV proton beam was used in this work, all of the Bi isotopes listed in Table 2 were produced. Furthermore, as is indicated in Table 3, the decay of the induced Bi radioactivities lead to the formation of other Pb,

Table 1. GAMMA RAYS AND THEIR RELEVANT PROPERTIES USED IN DATA EVALUATION.*

Radionuclide	Half Life	Gamma-Ray Energy (keV)	Probability per Decay (%)
203Bi	11.76 h	126.46	1.18
		264.19	5.13
		820.23	29.00
		825.21	14.30
203Pb	52.02 h	279.18	81.00
		401.32	2.90
204Bi	11.22 h	374.74	74.45
		899.15	100.00
		983.98	59.00
205Bi	15.31 h	703.45	31.00
		987.66	16.08
206Bi	6.24 h	184.02	15.82
		398.00	10.74
		497.06	15.31
		516.18	40.75
		537.45	30.41
		803.1	98.90
		881.01	66.16
		895.12	15.66

* Data from: "Table of Isotopes," C.M. Lederer and V.S. Shirley (eds.), 7th Edition, John Wiley & Sons, Inc., New York (1978).

Table 2. Q-VALUES (MeV) FOR PROTON-INDUCED REACTIONS PRODUCING Bi ISOTOPES FROM NATURAL Pb TARGETS.*

Target:	204Pb (1.42%)	206Pb (24.1%)	207Pb (22.1%)	208Pb (52.3%)
Reaction	Product nuclides (- Q MeV)			
(p,n)	204Bi (5.59)	206Bi (5.06)	207Bi (3.70)	208Bi (4.17)
(p,2n)	203Bi (12.88)	205Bi (12.09)	206Bi (11.80)	207Bi (11.07)
(p,3n)	202Bi (21.15)	204Bi (20.41)	205Bi (18.83)	206Bi (19.17)
(p,4n)	201Bi (29.22)	203Bi (27.70)	204Bi (27.15)	205Bi (26.20)
(p,5n)	200Bi (38.23)	202Bi (36.33)	203Bi (34.44)	204Bi (34.52)
(p,6n)	199Bi (46.17)	201Bi (44.04)	202Bi (43.07)	203Bi (41.81)
(p,7n)	198Bi (55.54)	200Bi (53.06)	201Bi (50.78)	202Bi (50.44)
(p,8n)	197Bi (63.50)	199Bi (60.99)	200Bi (59.80)	201Bi (58.15)

* All atomic masses for these calculations were obtained from Nuclear Data Tables 9, 4-5 (1971).

Table 3. PRODUCT AND DAUGHTER NUCLIDES PRODUCED WITH HIGH-ENERGY PROTONS ON NATURAL Pb TARGETS.*

Product Nuclides (Half Life)	Daughter Nuclides (Half Life)
^{208}Bi (3.68×10^5 a)	\rightarrow ^{208}Pb (s)
^{207}Bi (38 a)	\rightarrow ^{207}Pb (s)
^{206}Bi (6.24 d)	\rightarrow ^{206}Pb (s)
^{205}Bi (15.3 d)	\rightarrow ^{205}Pb (1.4×10^7 a) \rightarrow ^{205}Tl (s)
^{204}Bi (11.2 h) (87%)	\rightarrow ^{203}Pb (s) (13%) \rightarrow ^{204m}Pb (66.9 m) \rightarrow ^{204}Pb (s)
^{203}Bi (11.8 h) (77%)	\rightarrow ^{203}Pb (52.02 h) \rightarrow ^{203}Tl (s) (23%) \rightarrow ^{203m}Pb (6.1 s) \rightarrow ^{203}Pb (52.02 h)
^{202}Bi (1.67 h)	\rightarrow ^{202}Pb (3×10^5 a) \rightarrow ^{202}Tl (12.2 d) \rightarrow ^{202}Hg (s)
^{201g}Bi (1.77 h)	\rightarrow ^{201}Pb (9.4 h) \rightarrow ^{201}Tl (73.5 h) \rightarrow ^{201}Hg (s) \rightarrow ^{201m}Pb (61 s) \rightarrow ^{201}Pb (9.4 h)
^{201m}Bi (59.1 m)	\rightarrow ^{201}Pb (9.4 h) \rightarrow ^{197}Tl (2.83 h) \rightarrow ^{197}Hg (64.1 h) \rightarrow ^{197}Au (s)
^{200}Bi (36.4 m)	\rightarrow ^{200}Pb (21.5 h) \rightarrow ^{200}Tl (26.1 h) \rightarrow ^{200}Hg (s)
^{199}Bi (27 M)	\rightarrow ^{199}Pb (90 m) \rightarrow ^{199}Tl (7.4 h) \rightarrow ^{199}Hg (s)
^{198}Bi (11.85 m)	\rightarrow ^{198}Pb (2.4 m) \rightarrow ^{198}Tl (5.3 h) \rightarrow ^{198}Hg (s)
^{198m}Bi (7.7 s)	\rightarrow ^{198}Bi (11.85 m)
^{197}Bi (8.0 m)	\rightarrow ^{197}Pb (unknown) \rightarrow ^{197}Tl (2.83 h) \rightarrow ^{197}Hg (64.1 h) \rightarrow ^{197}Au (s)

* Decay schemes from Lederer and Shirley Table of Isotopes, 7th ed., Wiley, N.Y. 1978.

Tl, and Hg radionuclides. These decay-produced radionuclides must be taken into account when defining the best parameters for the production of $^{206},^{205}\text{Bi}$ radioactivities. The production and/or presence of the majority of the decay-produced daughter radioactivities (Table 3) can be eliminated and/or minimized in three ways: (1) By limiting the incident energy of the proton beam, (2) by allowing a decay period prior to the final radiochemical separation/formulation of the $^{206},^{205}\text{Bi}$ solution, or (3) by the proper selection of the Pb target material. These options are discussed below.

Cross Sections and Thick-Target Yields

In the 8.8- to 67.5-MeV energy region covered in this work, the production of ^{206}Bi was measured as 2.75 ± 0.27 (13.5%) mCi/ μAh . The total cross section reaches a maximum of 533 ± 72 (13.5%) mbarn at 31.6 ± 0.6 (1.9%) MeV. On the other hand, in the same energy region the production of ^{205}Bi was measured as 1.72 ± 0.23 (13.5%) mCi/ μAh , and the excitation function (i.e. cross section as a function of energy) showed two maxima: at 38.0 ± 0.5 (1.3%) MeV, with a cross-section value of 846 ± 114 (13.5%) mbarn, and at 21.3 ± 0.6 (2.8%) MeV, with a value of 257 ± 35 (13.5%) mbarn.

Thick-Target Production

This work indicates that the production of the longer-lived $^{206},^{205}\text{Bi}$ radionuclide mixture that is needed for radiotracer applications can best be accomplished by limiting the proton beam to less than 42 MeV. In this manner, the majority of the reactions leading to the formation of the shorter-lived (< 1 d) Bi radionuclides can be greatly minimized. Because the production of $^{206},^{205}\text{Bi}$ falls rapidly at energies below 20 MeV, the Pb target thickness should provide a 22-MeV energy degradation. Therefore, a 20- to 42-MeV thick Pb target (2.18 g/cm^2 ; 0.19 cm thick) would be required. Under these conditions, the theoretical yield for ^{206}Bi is 1.69 ± 0.23 (13.5%) mCi/ μAh (or 60% of the theoretical yield in the 8.8- to 67.5-MeV energy region), while the yield of ^{205}Bi decreases to 56%, or 0.963 ± 0.13 (13.5%) mCi/ μAh . Several batches of $^{206},^{205}\text{Bi}$ have already been produced using this procedure. Agreement with these theoretical yields has been excellent. Commercial radionuclide production facilities with high intensity 42-MeV proton beams can utilize existing target techniques for the bombardment of metallic Pb with high beam currents (up to 150 μA). In this manner, yields of 254 ± 34 mCi/h of ^{206}Bi and 144 ± 19 mCi/h of ^{205}Bi can be achieved.

Because natural composition Pb targets were used, no distinction between the different reactions and contributions to the measured Bi yields was possible. The two cross-section maxima for the production of ^{205}Bi (Figure 1) clearly indicate the predominant contributions of the reactions which are also influenced by the relative abundance of the different Pb target nuclides (Table 2). Because of energetic considerations (i.e. Q values), it appears that the 21.3-MeV maximum for ^{205}Bi production corresponds to the $^{206}\text{Pb}(p,2n)$ ($Q = 12.09$ MeV) reaction. In the energy region up to 23-24 MeV, the reported total cross section (Figure 2) would correspond to the absolute cross section of the $^{206}\text{Pb}(p,2n)$ reaction. However, in order to obtain the correct values for the absolute cross section, a correction for the abundance of the ^{206}Pb target nuclides (24.1%; or a 4.15 factor) would have to be made. With this factor, the maximum cross section for the $^{206}\text{Pb}(p,2n)$ reaction at 23.1 MeV would equal $1,066 \pm 144$ (13.5%) mbarn. However, in the energy region covered in this work, no other analysis of this nature can be made for other cross section. Unfolding the absolute cross sections which contribute to the total cross sections would require the use of highly enriched Pb target materials.

Fig. 1. Thin-target and cumulative yields ($\mu\text{Ci}/\mu\text{Ah}$) for ^{206}Bi and ^{205}Bi as a function of proton energy (MeV). Experimental data points are shown for each of the measured yields from the single-foil targets. Solid lines are also shown to represent the best eye-fitted approximation for the yield/energy functions.

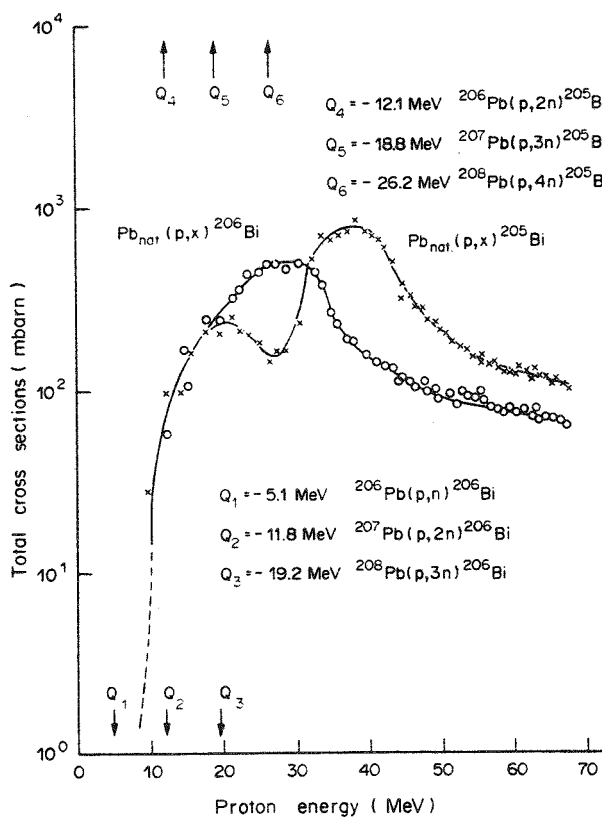
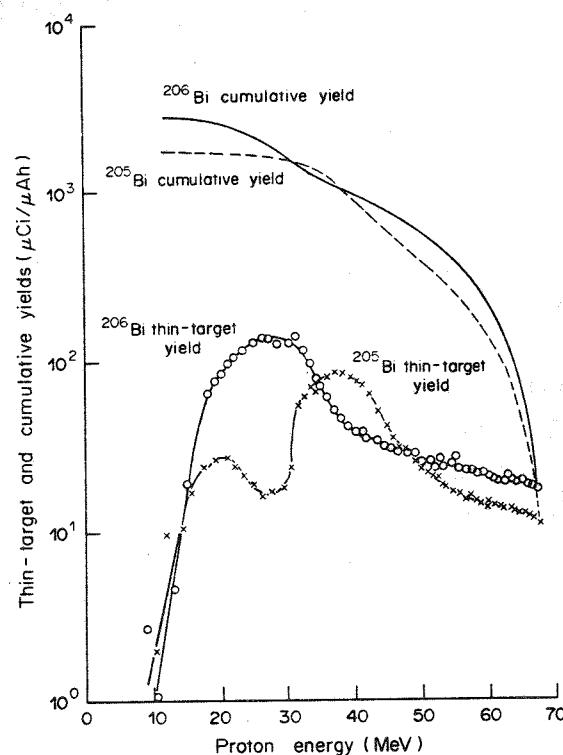


Fig. 2. Total cross sections (mbarn) for the production of ^{206}Bi and ^{205}Bi as a function of proton energy (MeV). The Q values for each of the contributing reaction channels are also shown.

Radiochemistry

A decay period of three days was all that was required to reduce the level of unwanted Bi and Pb radioactivities prior to radiochemical separation of 206 , 205 Bi from the natural lead target. The forms of bismuth were 11.22-h 204 Bi and 11.76-h 203 Bi. The 52.02-h daughter of 203 Bi, 203 Pb turned out to be useful as a tracer for evaluating the progress and efficiency of the Bi-Pb radiochemical separation, which was done by ion exchange. This separation is efficient enough and the production of 203 Bi at proton energies above 42 MeV is abundant enough that it has proved possible, as a consequence of this work, to develop a generator system for the production of NCA 203 Pb, which is potentially useful for diagnostic applications in nuclear medicine (Lagunas-Solar et al., 1987).

Radiochromatographic analysis of the Bi radioactivities produced in this work (Figure 3) indicates that only one cationic form of Bi^{3+} is present in the final solution--a form that was found to be stable even when adjusted to pH 4-6 as a step in using it to label proteins and antibodies.

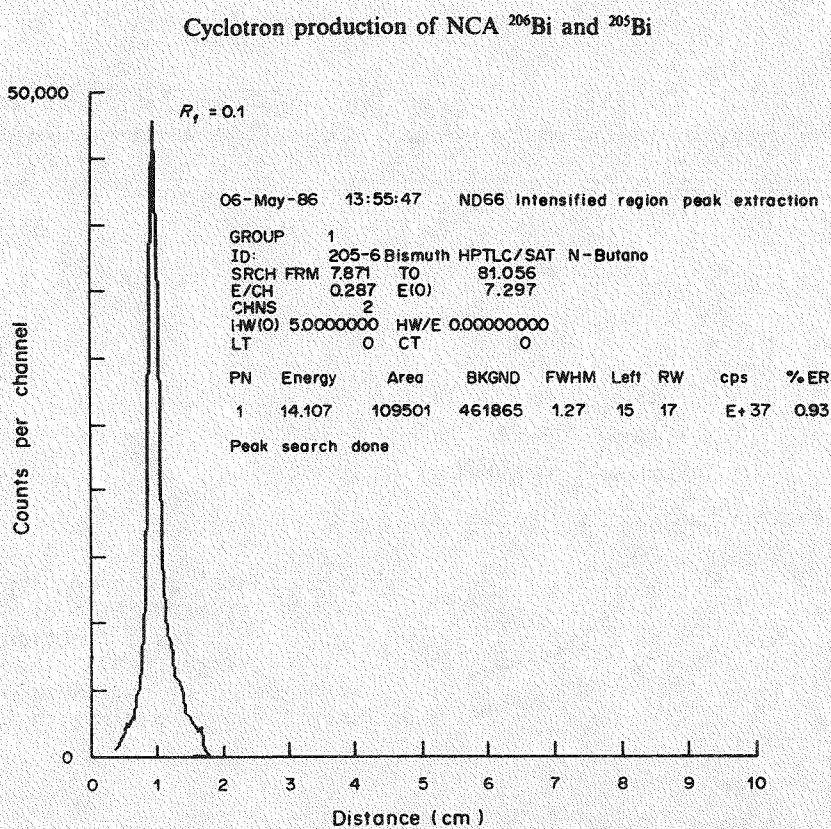


Fig. 3. Radiochromatographic analysis (HPTLC) of a NCA 206 , 105 Bi solution (in 1 N HNO_3). This analysis corresponds to the Bi^{3+} cationic form ($R_f=0.1$), and is stable for many weeks.

The radiochemical procedure described in this work also provides an excellent separation of Bi from Pb, Tl, and Hg. Once the Pb target (i.e. carrier) material was removed by double precipitation (a step that does not contribute to the removal of Tl and Hg), the Tl and Hg radionuclidic contaminants were easily removed because they have no detectable retention in the ion-exchange column. A sample of a typical radionuclidic assay of a $^{206,205}\text{Bi}$ radionuclide mixture is shown in Figure 4. All of the detected gamma-rays shown in the spectrum were identified with the decay of either ^{206}Bi or ^{205}Bi . No other radionuclidic impurities were detected.

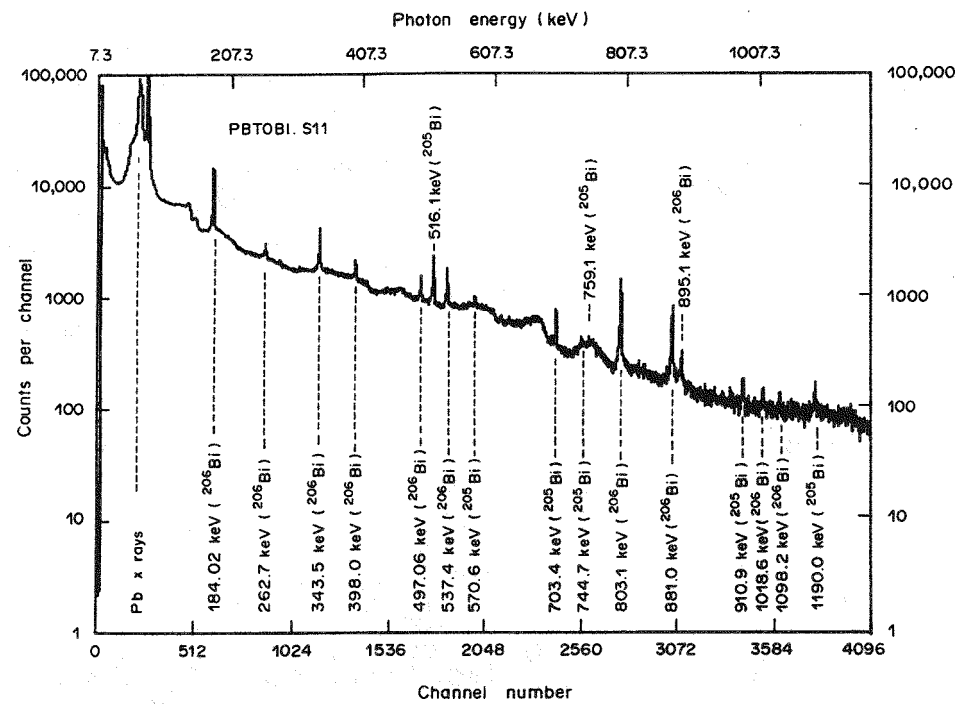


Fig. 4. High-resolution (Ge detector) gamma-ray spectrum of a $^{206,205}\text{Bi}$ solution in 1 N HNO_3 . All of the gamma rays detected were identified with the decay of either ^{206}Bi or ^{205}Bi . No Pb, Tl, or other radioactivities were detected.

Use of radiogenic Pb targets

This work has helped clarify options that are available to increase the purity of $^{206,205}\text{Bi}$, which are needed as a mixture of high specific activity radionuclides. The option of using expensive, highly purified Pb target material cannot be justified on the basis of current levels of Bi tracers, which is for non-human applications. It develops, too, that production of ^{206}Bi can be maximized only by eliminating or minimizing production of ^{205}Bi . This is due to the higher energy required for the production of ^{205}Bi , which must be stripped of one more neutron.

A less expensive alternative to using enriched Pb targets would be to use radiogenic ^{206}Pb as a target for the production of high purity ^{206}Bi via the $^{206}\text{Pb}(\text{p},\text{n})$ ($Q=$ -5.06 MeV) reaction. Similar techniques could be based on radiogenic ^{207}Pb , using a 19 MeV proton beam, and ^{208}Pb , using a <26.20 MeV. Other reactions are involved (Lagunas-Solar, et al., 1987). These radiogenic Pb target materials can be obtained from the Oak Ridge National Laboratory's Isotope Distribution Program.

CONCLUSIONS

This work has shown that a high-energy proton irradiation of natural Pb targets produces acceptable amounts of $^{206},^{205}\text{Bi}$ for radiotracer studies and that a simple and reliable radiochemistry process results in Bi radiotracers of high-specific activities which are able to satisfy the needs for protein/antibody labeling. With a proper target and radiochemistry setup, the amounts of $^{206},^{205}\text{Bi}$ to be produced are sufficient to satisfy the present and near-future estimated needs. Other possible routes for the production of ^{206}Bi have also been identified based upon the use of either enriched Pb or radiogenic Pb targets.

REFERENCES

Acerbi, E., C. Birattari, M. Castiglioni and F. Resmini. 1981.
J. Radioanal. Chem. 34: 191.

Birattari, C., M. Bonardi and M.C. Gilardi. 1981.
Radiochem. Radioanal. Letters 49(1): 25-36.

Lagunas-Solar, M.C., O.F. Carvacho, and D. Manthei. 1987.
Int. J. Appl. Radiat. Isot. (to be submitted).

Lagunas-Solar, M.C., O.F. Carvacho, L. Nagahara, A. Mishra and N.J. Parks. 1987.
Cyclotron production of no-carrier-added ^{206}Bi (6.24 d) and ^{205}Bi (15.31 d) as
tracers for biological studies and for the development of alpha-emitting
radiotherapeutic agents. Appl. Radiat. Isot. (Int. J. Appl. Instrumentation, Part A)
38:129-137.

Parks, N.J., W.R. Harris, C.L. Keen, S.R. Cooper, S. Zindenberg-Cherr, P.D. Schneider,
M.C. Lagunas-Solar, K. Musker, K.C. Chelton, and A. Mishra. 1985. Coordination
chemistry of the $^{212}\text{Pb}-^{212}\text{Bi}$ nuclear transformation: Alpha emitting
radiopharmaceuticals. In Laboratory for Energy-Related Health Research 1984 Annual
Report, UCD 472-130. pp. 124-127.

A 1,1-DITHIOCARBOXYLATE LIGAND WITH AN
EASILY DERIVITIZABLE GROUP. SYNTHESIS AND STRUCTURE OF
TRIS[2-(ETHYLAMINO)CYCLOPENT-1-ENE-1-DITHIOCARBOXYLATO]BISMUTH(III).

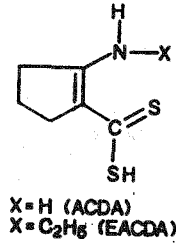
P. K. Bharadwaj¹
W. K. Musker

As one step in the development of radiopharmaceuticals that take advantage of the decay of ^{212}Pb to ^{212}Bi , a carrier molecule is being sought that will remain bound to the carrier after the transition. This paper provides the first report on the crystal structure of a member of one promising group, the 1,1-dithiocarboxylates. That complex with bismuth, tris[2-(ethylamino)-cyclopent-1-ene-1-dithiocarboxylato]bismuth-(III), has a trigonal antiprismatic coordination geometry, in which bismuth is coordinated asymmetrically so that there are three short and three long Bi-S bonds. Similarities to and differences from better-known dithiocarbamates are discussed.

INTRODUCTION

1,1-Dithio ligands (dithiocarbamates, dithiophosphates, dithioxanthates, dithiocarboxylates) have been the subject of intense investigation over the last two decades (Coucouvanis, 1979). Most studies are concerned with transition-metal complexes of 1,1-dithio ligands having only alkyl or aryl substituents. Only a few examples of complexes of 1,1-dithio ligand are known in which the ligand has free functional groups not involved in coordination.

1-Aminocyclopent-1-ene-1-dithiocarboxylic acid (ACDA) a compound having antifungal properties, forms complexes with transition metals (Ni(II), Pt(II), Pd(II), Mo(IV)) that were believed to be monomeric, neutral species with S,S rather than N,S bonding to the metal. However, no crystallographic information on any of these complexes was obtained because of their limited solubility in common organic solvents. However, it is easy to derivatize the amine group of the ligand by transamination reactions to give species having a variety of substituents at the nitrogen atom. These derivatives give complexes with improved solubility characteristics. As part of a research program to develop a radiopharmaceutical that can bind strongly to both Pb(II) and Bi(III) and, in addition, have latent functionality to bind to a suitable carrier, we have prepared the Bi(III) complex of 2-(ethylamino)cyclopent-1-ene-1-dithio-carboxylic acid (EACDA) and have been able to determine its crystal structure. This appears to be the first complex with a non-transition metal on which a crystal structure has been reported.



¹ Dept. of Chemistry, India Institute of Technology, Kampur, India

METHODS

ACDA was prepared in our laboratory for this study and converted to EADCA by transamination reaction with ethylamine. The EADCA was recrystallized from acetone, and complexes with Bi(III) were then formed in ethanolic solution. Single crystals of EADCA were grown by slow evaporation from solution in THF.

For the X-ray diffraction studies, a crystal of $\text{Bi}(\text{H}_2\text{EACDA})_3$ was mounted at the end of a glass fiber. All diffraction measurements were made at 130K with a Syntex P21 diffractometer. Details of data collection and refinement are given in Table 1.

Table 1. CRYSTAL AND REFINEMENT DATA

formula	$\text{BiS}_6\text{N}_3\text{C}_{24}\text{H}_{36}$
fw	767.909
<i>a</i> , Å	10.835 (4)
<i>b</i> , Å	14.854 (4)
<i>c</i> , Å	18.936 (5)
β , deg	105.98 (2)
<i>V</i> , Å ³	2930.0 (10)
space group	<i>P</i> 2 ₁ /c
<i>Z</i>	4
no. of reflcns used to determine cell const	15
<i>d</i> _{calcd} , g/cm ³	1.74
$\lambda(\text{Mo K}_\alpha)$, Å	0.71069
monochromator	graphite
linear abs coeff, cm ⁻¹	61.50
cryst dimens, mm	0.16 × 0.19 × 0.24
transmissn factor	0.22 < <i>T</i> < 0.48
range	
diffractometer	Syntex P2 ₁
data collcn method	ω -scan
2 θ range, deg	0 ≤ 2 θ ≤ 50
temp., K	130 (1)
ω -scan range, deg	1.0
wt scheme ^a	$w = 1/[(\sigma^2(F_0) + gF_0^2)]$
no. of std reflcns	2
% variation in std intens	<±0.1
octants collcd	+ <i>h</i> , + <i>k</i> , ± <i>l</i>
no. of unique data collcd	5163
no. of data used in refinement	4318
<i>R</i> (MERGE) ^b	0.000
data:param ratio	~14
final GOF	1.87
final <i>R</i> _f	0.0287
final <i>R</i> _{wF}	0.0306
syst absences	0 <i>k</i> 0, <i>k</i> = 2 <i>n</i> + 1; <i>h</i> 0 <i>l</i> , <i>l</i> = 2 <i>n</i> + 1
final largest shift/esd	0.046
highest peak in final diff map, e/Å ³	0.58

^a *g* was refined by fitting $(F_0 - F_c)^2$ to $[\sum(F) + (\text{abs}(g))F^2)/K]^2$ (where *K* is a scale factor) to put the weight on an approximately absolute scale. For the present structure *g* = 0.00021 and *K* = 1.00428.

^b *R*(MERGE) = $(\sum(N)\sum(w(F(\text{mesn}) - F)^2))/\sum((N - 1)\sum(wF^2)))^{1/2}$, where the inner summations are over the *N* equivalent reflections averaged to give *F*(mean) and the outer summations are over all unique observed reflections.

The structure (Figure 1) was solved by the heavy-atom method and refined on F by a full-matrix least-squares technique, using the SHELX81 program package (SHELXTL, Version 4, crystallographic program). The bismuth atom could be located from the Patterson map. The remaining non-hydrogen atoms were located from successive difference Fourier maps. Several H atoms could be located in the difference map at the isotropic convergence. However, coordinates of all H atoms were calculated by assuming an idealized geometry with C-H bond lengths of 0.96 Å and added to the atom list. H atom temperature factors were set as $U(H) = 1.2U_{eq}(C)$, where $U_{eq}(C)$ is the equivalent isotropic thermal parameter of the C atom to which the H atom is bonded. Hydrogen atom parameters were not refined. Anisotropic refinement of all non-hydrogen atoms led to convergence with $R_F = 0.0287$ and $R_{WF} = 0.0306$. Corrections of anomalous dispersion were applied to all atoms. Neutral atom scattering factors were those of Cramer and Waber. Final atomic parameters are listed in Table 2. Additional details are given in Bharadwaj and Musker (1987).

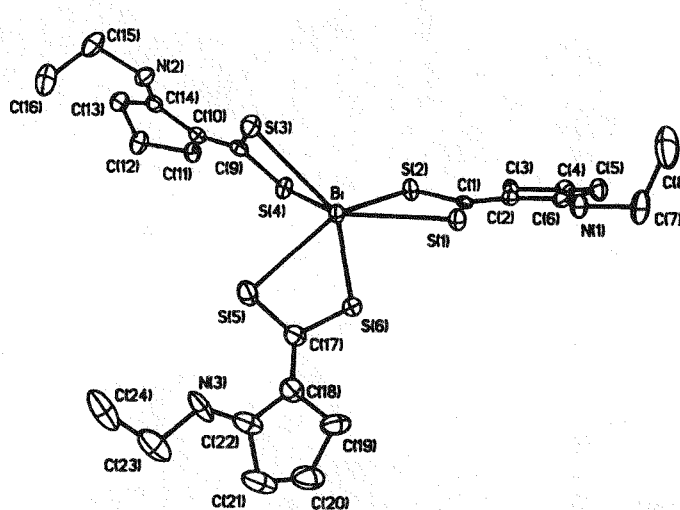
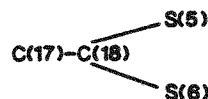


Fig. 1. ORTEP view of the title complex showing the atom-numbering scheme. Hydrogen atoms have been omitted for clarity.

RESULTS AND DISCUSSION

The $\text{Bi}(\text{H}_1\text{EACDA})_3$ complex can be prepared by treatment of either a solution of BiCl_3 or a suspension of BiOCl in ethanol with EACDA. The structure exhibits discrete neutral $\text{Bi}(\text{C}_8\text{H}_{12}\text{NS}_2)_3$ species with S_6 ligand donor sets. The N atom is not coordinated to the $\text{Bi}(\text{III})$ ion as it is at least 5.808 Å away. Each of the $\text{C}-\text{CS}_2$ units is planar to within ± 0.004 Å. The plane described by



(third ligand; Figure 1) makes an angle of 74.6° with the plane described by the same unit of the first ligand and an angle of 86.0° with the plane described by the second ligand. Thus, the coordination geometry around $\text{Bi}(\text{III})$ can be described as trigonal antiprismatic. Only one other structure of a $\text{Bi}(\text{III})$ 1,1-dithio complex, tris(diethyldithiocarbamato)-bismuth(III) ($\text{Bi}(\text{Et}_2\text{Dtc})_3$), has been reported, and a similar coordination geometry is present in that complex.

Table 2. FRACTIONAL ATOM COORDINATES ($\times 10^4$) AND THERMAL PARAMETERS ($\text{\AA}^2 \times 10^3$).

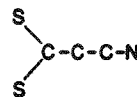
atom	x	y	z	U_{eq}^a
Bi	783 (1)	6471 (1)	5836 (1)	18 (1)
S(1)	1959 (1)	4980 (1)	5069 (1)	22 (1)
S(2)	3080 (1)	5839 (1)	6532 (1)	23 (1)
S(3)	-1211 (1)	6324 (1)	6689 (1)	24 (1)
S(4)	1237 (1)	7365 (1)	7078 (1)	23 (1)
S(5)	-579 (2)	8124 (1)	5168 (1)	34 (1)
S(6)	2099 (2)	7602 (1)	5270 (1)	29 (1)
N(1)	3960 (4)	3601 (3)	4941 (2)	25 (2)
N(2)	-2764 (4)	7089 (3)	7651 (3)	24 (2)
N(3)	-1227 (5)	9591 (4)	4038 (3)	42 (2)
C(1)	3225 (5)	5095 (4)	5829 (3)	16 (2)
C(2)	4406 (5)	4659 (4)	5964 (3)	18 (2)
C(3)	5536 (5)	4860 (4)	6620 (3)	24 (2)
C(5)	6061 (5)	3616 (4)	5892 (3)	28 (2)
C(6)	4729 (5)	3949 (4)	5548 (3)	22 (2)
C(7)	4349 (5)	2859 (4)	4534 (3)	37 (2)
C(8)	4160 (7)	1925 (5)	4833 (5)	67 (4)
C(9)	-288 (5)	7151 (4)	7206 (3)	18 (2)
C(10)	-626 (5)	7674 (4)	7734 (3)	18 (2)
C(11)	242 (5)	8375 (4)	8202 (3)	24 (2)
C(12)	-679 (5)	8949 (4)	8506 (3)	30 (2)
C(13)	-1813 (5)	8347 (4)	8500 (3)	26 (2)
C(14)	-1796 (5)	7653 (4)	7922 (3)	20 (2)
C(15)	-4002 (5)	7135 (4)	7836 (3)	31 (2)
C(16)	-4919 (6)	7803 (4)	7356 (4)	40 (3)
C(17)	763 (6)	8291 (4)	8469 (3)	28 (2)
C(18)	903 (7)	8898 (4)	4344 (3)	36 (2)
C(19)	2079 (7)	8984 (5)	4056 (4)	44 (3)
C(20)	1873 (7)	9886 (5)	3634 (4)	57 (3)
C(21)	419 (7)	10052 (5)	3411 (4)	54 (3)
C(22)	-59 (7)	9506 (4)	3955 (3)	38 (3)
C(23)	-2180 (7)	10221 (5)	3597 (4)	53 (3)
C(24)	-3374 (7)	10164 (5)	3866 (4)	62 (3)
C(4)	6636 (5)	4266 (4)	6520 (3)	25 (2)

^aEquivalent isotropic U defined as one-third of the trace of the orthogonalized U_{ij} tensor.

As also seen in the tris(diethyldithiocarbamate) complex, bismuth is coordinated asymmetrically by each dithio ligand in such a way that there are three short Bi-S bonds [Bi-S(2), 2.647 (1) Å; Bi-S(4), 2.626 (1) Å; Bi-S(6), 2.617 (2) Å] and three long Bi-S bonds [Bi-S(1), 3.108 (2) Å; Bi-S(3), 3.040 (5) Å; Bi-S(5), 2.963 (5) Å]. Thus, S(1), S(3), and S(5) and likewise S(2), S(4), and S(6) form triangular faces in the coordination polyhedron. The molecular symmetry around Bi(III) is closer to C3. The asymmetric binding of the dithio ligand may be attributed to the presence of a stereochemically active lone pair on the Bi(III) ion. If the lone pair lies along the 3-fold axis, the S(1), S(3), and S(5) atoms on the same side as the lone pair are pushed away from the Bi(III) ion, resulting in longer Bi-S bond lengths.

The S-C-S bond angles, which range from 116.3 (3) to 118.8 (3) $^{\circ}$, are also similar to those found in the diethyldithiocarbamate complex of Bi(III). In contrast, when 1,1-dithio ligands are bound to metal ions in a symmetrical fashion (both M-S bonds equal in length), the S-C-S angles are shorter (110 (1) to 113 (1) $^{\circ}$), signifying greater strain at the sp^2 C atom. S-Bi-S bond angles are within 61.6-63.7 $^{\circ}$, as found in other Bi(III) complexes. The C-C bond lengths between the C atom of the CS_2 group and the one bonded to it lie between 1.394 (7) and 1.381 (9) \AA , showing appreciable double bond character.

The

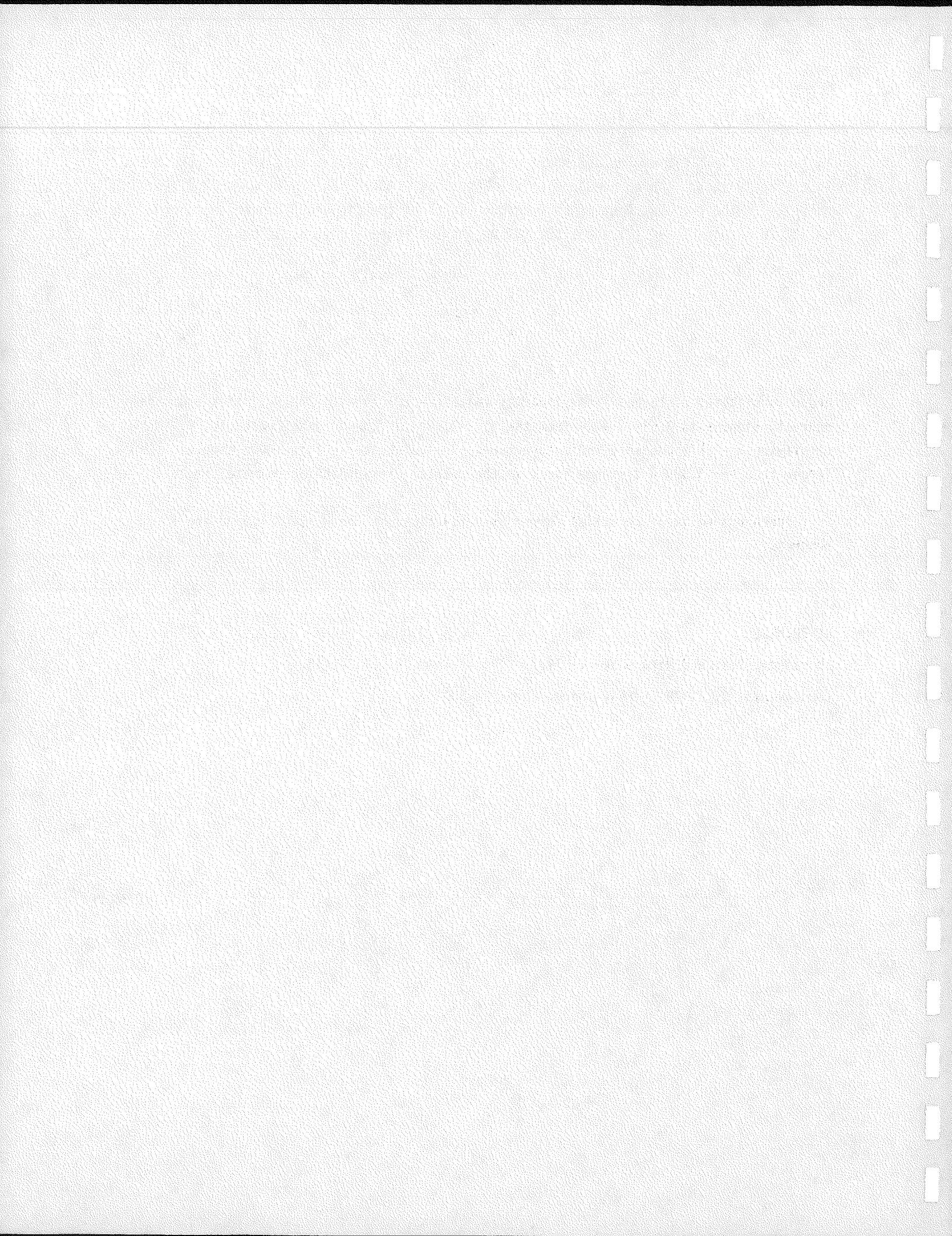


group is slightly distorted from planarity (within = $\pm 0.014 \text{ \AA}$). The S(1) atom from the nearest neighbor is 3.689 \AA away from the Bi(III) ion of the original molecule, signifying a weakly bonded dimeric structure. This distance in this EACDA complex is much longer than the 3.389 \AA distance found in the related diethyldithiocarbamate complex.

Further studies of complexes formed by derivatives of the H₁ACDA ligand are in progress.

REFERENCES

Bharadwaj, P.K. and W.K. Musker. 1987. Inorg. Chem. 26:1453-1455.
Coulouvanis, D. 1979. Prog. Inorg. Chem. 26:301-469.



RADIONUCLIDE METABOLISM STUDIES

METABOLIC EVALUATION IN NONHUMAN PRIMATES OF BONE AND LIVER RISKS FROM INTERNALLY DEPOSITED ACTINIDES

O. G. Raabe
M. Al-Bayati
F. Gielow

The movement of ultrafine particles (diameters in the deka-angstrom range) through the lungs, into the blood and on to deposition points in other organs or to excretion via urine and feces is under study in experimental groups of dogs (beagles) and cynomolgous monkeys (*Macaca fascicularis*) in an effort to obtain risk estimation data for scaling to humans. Initial lung burdens declined rapidly in the beagle, with 70.4% already being translocated to the liver and bones after only 30 days. The liver burden leveled at about 20% during the first year. Bone burdens fluctuated in the 34-42% range. Monkeys, on which we have just 6 months' data at this point, retained the particles longer in the lungs and built the skeletal burden more slowly. The liver burden declined from 28% to 19% between the 30 and 180-day points. A small proportion of the total ^{241}Pu was continually being removed in both species by excretion in urine and feces.

INTRODUCTION

This project provides needed information on the physiological behavior of biologically mobile ultrafine particles of plutonium-241 as it relates to long-term exposures at very low concentrations. Plutonium can enter the environment inadvertently or may be released accidentally in the nuclear industry as a consequence of nuclear power development, particularly plutonium recycling and breeder reactors. When carried as ultrafine particles, actinides such as ^{241}Pu may escape normal protective systems and will be relatively mobile in the environment. They can be expected to be released as oxides which, in the ultrafine size range, will tend to enter the blood shortly after inhalation and pass to other organs (principally liver and bone) more rapidly than would be demonstrated by the larger, compact particles usually used in inhalation toxicology studies. This project does not address lung toxicology, and lung retention is minimized by using ultrafine particles and small molecular clusters rather than respirable-sized oxide particles.

This study considers the dosimetrically important differences that may exist between the inter-organ and intra-organ distribution of the important actinides ^{241}Pu and its daughter, ^{241}Am , in beagles and the cynomolgous monkey, *Macaca fascicularis*, following identical exposures emphasizing a physiologically realistic regimen. The monkeys provide metabolic models of transport of ultrafine particles from lung to bone and liver which are needed to permit scaling from beagles to people in risk estimation. We report here on the initial year of a study that was originally scheduled to go five years (Table 1).

APPROACH

The animals used in the study included (1) 31 beagles, which were a part of the colony being maintained at the Laboratory for Energy-Related Health Research (LEHR) at the University of California, Davis, and (2) 31 specimens of the monkey, which were part of the colony reared at the California Primate Research Center, also associated with UCD.

Table 1. EXPOSURE REGIMEN.

Nuclide	Number of Dogs	Number of Primates	Sacrifice Post-Exposure
^{241}Pu	3	2	30 d
^{241}Pu	2	2	180 d
^{241}Pu	2	2	1 yr
^{241}Pu	2	2	3 yr
^{241}Pu	2	3	5 yr
Controls	1	1	
^{241}Am	2	2	30 d
^{241}Am	2	2	180 d
^{241}Am	2	2	1 yr
^{241}Am	2	2	3 yr
^{241}Am	2	2	5 yr
^{238}Pu	2	2	30 d
^{238}Pu	2	2	180 d
^{238}Pu	2	2	1 yr
^{238}Pu	2	2	3 yr
^{238}Pu	2	2	5 yr
Totals for complete project	31	31	

The experimental animals were exposed using a chemically-produced, aqueous, colloidal suspension of ultrafine particles of plutonium. Particles diameters were in the deka-angstrom range. The suspensions were prepared in a physiological saline solution and instilled into chosen lung lobes by intratracheal intubation, using catheters. This would not be an appropriate way to introduce the material into the lungs if we were intending to study lung exposure, but given that an essential condition of the experiment was that lung exposure must be minimized, this represents a useful way physiologically to move the material into the blood. We find that translocation of plutonium particles from lung to blood and thence to bone and liver (and whatever other organs might prove to be involved) is realistically and efficiently modeled by this route of exposure. We are calling it a "pseudochronic lung-blood pathway" and believe it to approximate the normal sequence of physical and biochemical processes that will occur in actual environmental exposures to ultrafine insoluble particles. It contrasts with the more widely used method in this type of experiment whereby a bolus of some chelated actinide (e.g., citrate of Pu) is injected intravenously, resulting in a pulsed labeling of bone.

Because this is essentially a new approach, a significant portion of the project, in its early stages, was concerned with methods to be used in separating ^{241}Pu from ^{241}Am in our laboratory in order to be certain that the material being instilled would be free of the latter radionuclide. It was an essential part of the study, as originally planned, for exposure levels in beagles and monkeys to be set so that ^{241}Am being produced by decay of ^{241}Pu in the various organs following translocation be detectable. The initial work in establishing exposure levels was done on rats.

The schedule of instillation dates for beagles and monkeys, is given in Table 2, followed by the combined schedule for the sacrificing of animals for analysis of radionuclide contents of the organs (Table 3). In the latter analyses, data were obtained on all major organs, with special attention being given to bone, liver, kidney, and gonads. Both sexes were studied. Radiochemical analysis was carried out by digestion, ashing, and both liquid scintillation and alpha spectroscopy to provide macro measurements of organ burdens and excreta.

Table 2. THE FOLLOWING DOGS AND PRIMATES WERE INSTILLED WITH Pu-241.

Dog I.D.	Instillation Date		Primate I.D.	Instillation Date	
77G18Y	6	April	1982	MCY21058	10 August 1983
79K71Y	6	April	1982	MCY21059	10 August 1983
78K43X	8	July	1982	MCY21060	10 August 1983
79G57X	8	July	1982	MCY21065	10 August 1983
77F12D	5	October	1982	MCY21067	10 August 1983
79G57Z	5	October	1982	MCY21062	18 November 1983
78K43C	16	November	1982	MCY21063	18 November 1983
79E51D	16	November	1982	MCY21064	18 November 1983
79E51A	5	April	1983	MCY21066	18 November 1983
79E51B	5	April	1983	MCY21068	18 November 1983
81C11U	5	April	1983	MCY21069	18 November 1983

Table 3. THE FOLLOWING DOGS AND PRIMATES WERE SACRIFICED AND TISSUE ANALYSIS FOR Pu-241 AND Am-241 HAVE BEEN COMPLETED.

Dog	Sacrifice Date		Primate	Sacrifice Date	
77F11Y Control	20	April	1982	MCY21061 Control	9 August 1983
77G18Y	6	May	1982	MCY21059	9 September 1983
79K71Y	7	May	1982	MCY21064	19 December 1983
78K43X	13	January	1983	MCY21065	15 February 1983
81C11U	5	May	1983	MCY21062	18 May 1984
78K43C	16	May	1983	MCY21060	10 August 1984
79G57X	6	July	1983	MCY21069	19 November 1984
79E51A	6	April	1984		

Not all of the analyses had been completed in time for this annual report, so we present data here for organ analyses as follows:

Dogs (n = 3), 1 month post-instillation, Table 4

Dogs (n = 2), 6 months post-instillation, Table 5

Dog (n = 1), 12 months post-instillation, Table 6

Primates (n = 2), 1 month post-instillation, Table 7

Primate (n = 1), 6 months post-instillation, Table 8

Table 4. Pu-241 DISTRIBUTION IN DOG AT 1 MONTH POST-INSTILLATION.*

Tissue Type	As % of Initial Lung Burden
Blood	1.01 ± 0.88
Trachea	0.11 ± 0.14
Lung	11.74 ± 13.22
Liver	33.99 ± 4.41
Kidney	0.48 ± 0.23
Spleen	0.50 ± 0.17
Testes	0.026 ± 0.006
GI Tract and Contents	0.60 ± 0.38
Muscle	1.23 ± 0.50
Skeleton	36.42 ± 9.24

* X ± S.D. is represented, n=3.

Table 5. Pu-241 DISTRIBUTION IN DOG AT 6 MONTH POST-INSTILLATION.*

Tissue Type	As % of Initial Lung Burden
Blood	0.09 ± 0.03
Trachea	0.13 ± 0.07
Lung	8.56 ± 2.40
Liver	19.91 ± 5.10
Kidney	0.34 ± 0.33
Spleen	0.26 ± 0.02
Testes	0.03
GI Tract and Contents	0.14 ± 0.01
Muscle	1.34 ± 1.16
Skeleton	42.06 ± 1.65

* X ± S.D. is represented, n=2; except testes n=1.

Table 6. PU-241 DISTRIBUTION IN DOG AT 12 MONTHS POST-INSTILLATION.*

Tissue Type	As % of Initial Lung Burden
Blood	0.08
Trachea	0.03
Lung	4.77
Liver	21.87
Kidney	0.58
Spleen	0.13
Testes	0.01
GI Tract and Contents	0.32
Muscle and Skin	0.45
Skeleton	34.12

* One male at five years of age.

Table 7. Pu-241 DISTRIBUTION IN PRIMATE AT 1 MO. POST-INSTILLATION.*

Tissue Type	As % of Initial Lung Burden
Blood	0.313 \pm 0.072
Trachea	0.079 \pm 0.032
Lung	52.819 \pm 10.132
Bronchial Lymph Nodes (one gram)	0.305 \pm 0.089
Liver	27.673 \pm 8.873
Kidney	0.183 \pm 0.096
Spleen	0.135 \pm 0.022
Muscle and Skin	16.255 \pm 1.124
GI Tract and Contents	0.530 \pm 0.299
Testes	0.045

* X \pm S.D. is represented, n=2; except testes n=1.

Table 8. Pu-241 DISTRIBUTION IN PRIMATE AT 6 MONTHS POST-INSTILLATION*

Tissue Type	As % of Initial Lung Burden
Blood	0.113
Trachea	0.032
Lung	15.543
Bronchial Lymph Nodes (one gram)	0.334
Liver	19.105
Kidney	0.05
Spleen	0.10
Muscle and Skin	0.725
Skeleton	29.815
GI Tract and Contents	0.566

* Female at five years of age

Data were also obtained on the content of radionuclides in the urine and feces of the living animals during the course of the study (Table 9).

Table 9. EXCRETION OF ^{241}Pu IN DOGS AND MONKEYS.*

Post- Instillation Period	n	% of Initial Lung Burden	
		Urinary Excretion	Fecal Excretion
<u>Beagles</u>			
Days 1-31	6	2.42 \pm 1.94	32.77 \pm 15.23*
Days 32-180	3	5.07 \pm 2.61	12.22 \pm 6.96
Days 181-365	2	1.14 \pm 0.63	2.45 \pm 3.23
<u>Monkeys</u>			
Days 1-30	3	1.56 \pm 0.21	19.53 \pm 6.74*
Days 31-180	1	3.52	28.87

* Percent of initial dosage.

RESULTS

Rapid transfer of ^{241}Pu to liver and bone is confirmed in the beagle (Table 4). After 30 days only 11.7% of the initial lung burden remained there, vs. 70.4% in the two major receiving tissues. About half (4.4% of the initial lung burden) of the remaining 8.9% was excreted (Table 9).

Changes in the ^{241}Pu burden of the respective organs of the dogs through the first year can only be reported as apparent trends because of the small sample size (3 at 30 days, 2 at 180 days and 1 at 1 year, Tables 5 and 6). Thus, the lung burden appears to decline gradually, according to these data, from 11.7 to 4.8%. The liver burden (stated as per cent of the initial lung burden) was at its highest level in the 30-day analysis but steadied in the 19 to 22% range in the 180-day and 1-year samples. The skeletal burden rose from around 36% to about 42% after 6 months but fell to near the 30-day level (34.1%) after a year. The loss through the urine (Table 9) was small (9.9%) during the year but was somewhat greater (14.6% or more) through the feces, though the latter value is obscured somewhat since some early quantities must be assumed to contain a portion of the initial dose that was not passed through the blood, etc.

Results for the monkeys (Tables 7 and 8) are more limited, with only two individuals being available for the 30-day sample and one for 180-day class. We lack data for the one year period at this time. The picture for monkeys is a little different from beagles, viz., 50% of the initial burden remained in the lungs after 30 days, with most of the remainder appearing in the liver (27.7%) and in the skeleton (16.3%). The lung burden had dropped to 15.5% in the single 180-day individual, with loading in the liver down to 19.1% and the skeletal burden being up to 29.8%. Data on excretion (Table 9) show about the same loss in the two species through the urine during the first six months-- 7.5% for the dog vs. 5.1% for the monkey. A much greater loss through the feces is apparent in the monkey (29% or more vs. 12+ in the dog).

REFERENCES

Raabe, O. G., M. A. Al-Bayati, F. Gielow, J. P. Schreider, and N. J. Parks. 1984. Studies of the distribution in beagles of Pu-241 after intratracheal instillation of ultrafine insoluble particles. *Health Physics* 47: 210 (Abstract).

Raabe, O. G., M. A. Al-Bayati, F. Gielow, J. P. Schreider, and N. J. Parks. 1984. "Studies of the distribution in beagles after intratracheal instillation as ultrafine insoluble particles." Presented at the Health Physics Society Annual Meeting, New Orleans, LA, June 1984.

Raabe, O. G., M. A. Al-Bayati, and F. Gielow. 1985. "Metabolism of Pu-241 in beagles and non-human primates after intratracheal instillation as ultrafine insoluble particles." Presented at the Health Physics Society Annual Meeting, Chicago, IL, May 1985.

PUBLICATIONS AND PRESENTATIONS

PUBLICATIONS LIST

Cain, G. R., R. P. Gale and R. Champlin. 1986. Fetal liver cell transplantation in dogs. *Journal of Cellular Biochemistry, Suppl. 10D*, p. 224. (Abstract).

Cain, G. R., B. F. Feldman, T. G. Kawakami and N. C. Jain. 1986. Platelet dysplasia associated with megakaryoblastic leukemia in a dog. *Journal of the American Veterinary Medical Association* 188(5): 529-530.

Champlin, R., G. R. Cain, K. A. Stitzel and R. P. Gale. 1985. Fetal liver cell transplantation in dogs: Results with DLA-compatible and incompatible grafts. In R. P. Gale and G. Lucarelli (eds.), Fetal Liver Transplantation. Excerpta Medica, Amsterdam, pp. 195-204.

Dyck, J. A., M. Shifrine, A. K. Klein, L. S. Rosenblatt and T. G. Kawakami. 1986. Spontaneous cell-mediated cytolysis by peripheral blood cells obtained from whole body chronically irradiated beagle dogs. *Radiation Research* 106: 31-40.

Goldman, M. 1986. Experimental carcinogenesis in the skeleton. In A. C. Upton (ed.), Radiation Carcinogenesis. Chapter 14. Elsevier Science Publishing Co., Inc. pp. 215-231.

Jee, W. S. S., N. J. Parks, S. C. Miller and R. B. Dell. 1986. Relationship of bone composition to the location of radium-induced bone cancer. *Strahlentherapie* (supple.) 80: 75-78.

Kawakami, T. G. and G. R. Cain. 1986. Growth-stimulating factor for canine myelopoiesis. *Journal of Cellular Biochemistry, Suppl. 10D*, p. 224. (Abstract).

Morgan, J. P. and L. Rosenblatt. 1986. Canine Hip Dysplasia: the pelvic inlet parameter in diagnosis. *California Veterinarian* 40(3): 15-18.

Morgan, J. P. and M. Stephens. 1985. Radiographic Diagnosis and Control of Canine Hip Dysplasia. Venture Press, Davis, CA.

Mishra, A. C., K. C. Chelton and N. J. Parks. 1986. Design and operation of a generator system for studies of reactions activated by nuclear transformation and synthesis of alpha-emitting radiopharmaceutical compounds. American Chemical Society, Nuclear Chemistry Division, 192nd National Meeting, Anaheim, CA, Sept. 7-12, 1986. (Abstract)

Miyabayashi, T., J. P. Morgan, M. A. O. Atilola and L. Muhamuza. 1986. Small intestinal emptying time in normal beagle dogs. *Veterinary Radiology* 27(6): 164-168.

Parks, N. J., W. S. S. Jee, R. B. Dell and G. E. Miller. 1986. Assessment of cortical and trabecular bone distribution in the beagle skeleton by neutron activation analysis. *The Anatomical Record* 215: 230-250.

Parks, N. J., A. C. Mishra and P. K. Bharadwaj. 1986. Reactions of nucleogenic lead and bismuth activated by the $^{216}\text{Po}(-\alpha)$ ^{212}Pb and $^{212}\text{Pb}(-\beta)$ ^{212}Bi nuclear transformations. American Chemical Society, Nuclear Chemistry Division, 192nd National Meeting, Anaheim, CA, Sept. 7-12, 1986. (Abstract).

Phalen, R. F., W. C. Hinds, W. John, P. J. Lioy, M. Lippman, M. A. McCawley, O. G. Raabe, S. C. Soderholm and B. O. Stuart. 1986. Rationale and recommendations for particle size-selective sampling in the workplace. *Applied Industrial Hygiene* 1(1):3-14.

Raabe, O. G. 1986. Reply to Wrenn, Lloyd, Mays and Taylor concerning the carcinogenicity of Ra and bone-seeking actinides. *Health Physics* 51(5):679-682.

Raabe, O. G. 1986. Risk estimation for lung injury and cancer from inhaled radionuclides utilizing three-dimensional response surfaces. In Proceedings of the Thirty-first Annual Meeting of the Health Physics Society, No. 50, Suppl. 1: S57. June 29-July 3, 1986. (Abstract)

Raabe, O. G., R. S. Howard and C. E. Cross. 1986. Aerosol considerations in asthma. In M. E. Gershwin (ed.), Bronchial Asthma, Principles of Diagnosis and Treatment, Chapter 22, Grune & Stratton, Inc., Orlando, Florida, pp. 495-514. 1986.

PRESENTATIONS

Cain, G. R., T. G. Kawakami, and K. A. Stitzel. Radiation-induced myeloid leukemia in dogs. Annual Meeting American College of Veterinary Pathologists. Denver, Colorado. December, 1985.

Cain, G. R., R. Champlin, and K. A. Stitzel. Fetal liver transplantation in dogs. Annual Meeting American College of Veterinary Pathologists. Denver, Colorado. December, 1985.

Cain, G. R. Congenital myelofibrosis in pigmy goats - a model of human agnogenic myeloid metaplasia? Annual Meeting American College of Veterinary Pathologists. Denver, Colorado. December 1985.

Cain, G. R., R. P. Gale, and R. Champlin. Fetal liver transplantation in dogs. UCLA Symposium on Bone Marrow Transplantation. Keystone, Colorado. April, 1986.

Cain, G. R., K. A. Stitzel, and R. Champlin. Successful transplantation of DLA-mismatched fetal liver hematopoietic cells (FLC) in dogs using total body irradiation (TBI) and cyclosporine. XI International Congress of the Transplantation Society. Helsinki, Finland. August, 1986.

Goldman, M. Dog Days in Davis (or, the toxicity of radiostrontium). Health Physics Society, Northern California Chapter. Davis, CA, October 17, 1985.

Goldman, M. Pre-Assessment of Chernobyl. U.S. Delegate to WHO Working Group. Bilthoven, Netherlands. June 25-28, 1986.

Goldman, M. The Chernobyl Accident. Northern California Chapter of the Health Physics Society. Davis, CA. July 17, 1986.

Goldman, M. Environmental and Health Impact of the Chernobyl Accident. Australian Nuclear Association. Sydney, Australia. July 30, 1986.

Goldman, M. Post-Accident Review of the Chernobyl Accident. U.S. Delegate to the IAEA Meeting. Vienna, Austria. August 24-29, 1986.

Goldman, M. The Chernobyl Accident. American Nuclear Society, Bethesda, Maryland. September 15, 1986.

Kawakami, T. G. and G. R. Cain. Growth stimulating factor for canine myelopoiesis. 1986 UCLA Symposia on Growth Factors, Tumor Promoters and Cancer Genes. Steamboat Springs, Colorado. April 6-13, 1986.

Kawakami, T. G., A. Aotaki-Keen, L. S. Rosenblatt and M. Goldman. Evaluation of Diethyleneglycoldinitrinate (DEGDN) and two DEGDN containing compounds. U.S. Army Medical Bioengineering Research and Development Laboratory, 1986 Extramural Review. Fort Detrick, Frederick, MD. September 15-19, 1986.

Mishra, A. C., K. C. Chelton and N. J. Parks. Design and operation of a generator system for studies of reactions activated by nuclear transformation and synthesis of alpha-emitting radiopharmaceutical compounds. American Chemical Society, Nuclear Chemistry Division, 192nd National Meeting, Anaheim, CA, Sept. 7-12, 1986.

Parks, N. J., A. C. Mishra and P. K. Bharadwaj. Reactions of nucleogenic lead and bismuth activated by the $^{216}\text{Po}(-\text{alpha})^{212}\text{Pb}$ and $^{212}\text{Pb}(-\text{beta})^{212}\text{Bi}$ nuclear transformations. American Chemical Society, Nuclear Chemistry Division, 192nd National Meeting, Anaheim, CA, Sept. 7-12, 1986.

Raabe, O. G. "Effects of Airborne Particulate Matter," California Air Resources Board Health Effects Conference, University of California, Irvine, March 20, 1986.

Raabe, O. G. "Inhalation Uptake of Selected Chemical Vapors at Trace Levels," California Air Resources Board Health Effects Conference, University of California, Irvine, March 20, 1986.

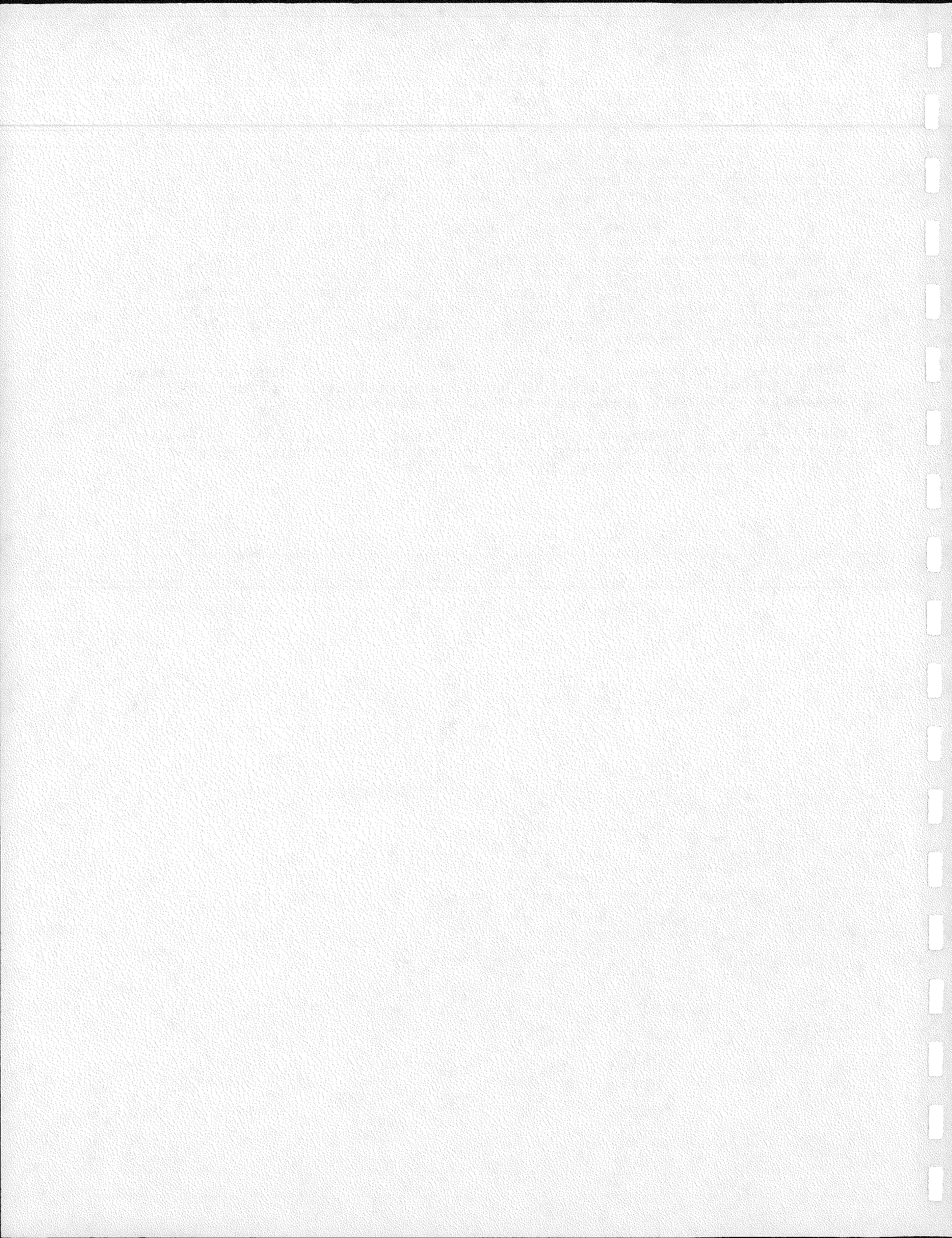
Raabe, O. G., "Risk Estimation for Lung Injury and Cancer from Inhaled Radionuclides Utilizing Three-dimensional Response Surfaces," Thirty-First Annual Meeting of the Health Physics Society, Pittsburgh Convention-Expo Center, Pittsburgh, PA, June 29-July 3, 1986.

Raabe, O. G. and S. V. Teague, "A Simple Vibrating Stream Monodisperse Aerosol Generator," The 1985 Annual Meeting of the American Association for Aerosol Research, Marriott Hotel, Albuquerque, New Mexico, November 18-22, 1985.

Raabe, O. G., M. A. Al-Bayati, S. V. Teague and A. Rasolt, "Regional Deposition and Pulmonary Distribution of Inhaled Monodisperse Aerosol Particles in Small Laboratory Animals," Second International Conference on Aerosols, Technical University of Berlin, West Germany, 21-25 September, 1986

Raabe, O. G., D. A. Braaten, R. L. Axelbaum, and S. V. Teague, "Calibration and Validation of the Drum Sampler," The 1985 Annual Meeting of the American Association for Aerosol Research, Marriott Hotel, Albuquerque, New Mexico, November 18-22, 1985.

Raabe, O. G., D. A. Braaten, R. L. Axelbaum, S. V. Teague, and T. A. Cahill, "Calibration Studies of the DRUM Impactor," Second International Conference on Aerosols, Technical University of Berlin, West Germany, 21-25 September, 1986



LABORATORY FOR ENERGY-RELATED HEALTH RESEARCH PERSONNEL

LABORATORY FOR ENERGY-RELATED HEALTH RESEARCH
PERSONNEL

Administrative Staff

James W. Overstreet	Director
Otto Raabe	Associate Director - Science
Cecilia Bauernhuber	Management Services Officer

Clerical

Charles Baty	Administrative Assistant	Donna Madding	Secty/Receptionist
Pamela Carroll	Sr Word Proc Specialist	¹ Ellen Moxley	Principal Clerk
Laura Creely	Principal Clerk	¹ Sue Schafer	Financial Assistant
Cathy Diaz	Administrative Assistant	Diane Schroeder	Financial Assistant
Debbie Hicks	Secretary		

Professional Staff

Gary Cain	Sr. Veterinarian	Roy Pool	Pathologist
M. Roger Culbertson	Pathologist	Leon Rosenblatt	Biostatistician
Marvin Goldman	Radiologist	John Schwind	Electronics Engin
Thomas Kawakami	Cancer Biologist	William Spangler	Pathologist
Joe Morgan	Radiologist	Russell White	Clin Veterinarian
Norris Parks	Radiochemist	Teresa Wolfe	Asst Veterinarian

Technical Staff

Mohammed Al Bayati	² SRA-Aerosol	1Kenneth McFarland	SRA-Aerosol
¹ Amy Aotaki-Keen	SRA-Biology	¹ Laurie McKinney	RA-Radiology
Martha Conard	SRA-Histology	Lynne Morrin	SRA-Clin Lab Science
Norman Cone	SRA-Toxicology	Susan Munn	SRA-Clin Lab Science
¹ Elfriede DeRock	SRA-Immunology	Maximita Nasr	SRA-Biochemistry
¹ Suzanne Fellows	Lab Help-Toxicology	¹ Michael Obasaju	RA-Immunology
Bradley Foster	SRA-Biochemistry	¹ Roy Roenbeck	SRA-Biochemistry
⁴ William Gee	SRA-Toxicology	¹ Judith Shimizu	³ CLT-Exptl Hematol
Fiorella Gielow	SRA-Radiochemistry	David Silberman	SRA-Chemistry
John Henderson	SRA-Toxicology	¹ Janelle Sonoda	Lab Asst-Toxicology
¹ Mary Herman	RA-Endocrinology	Sophie Soo	SRA-Bone Pathology
Debra Johnson	SRA-Biochemistry	Roger Sullivan	SRA-Pathology
Tom Kellner	RA-Toxicology	¹ Nancy Taylor	SRA-Immunology
A. Kimi Klein	SRA-Exptl Hematol	Steve Teague	SRA-Aerosol
Steven Maslowski	An Resources Mgr	Dale Uyeminami	SRA-Aerosol

¹Terminated

²Staff Research Associate

³Clinical Lab Technologist

⁴Retired

⁵Associated Western University Staff (summer only)

Data Processing

Victor Pietrzak Programmer/Analyst

Laboratory Services

Donald Ballard	Sr Lab Mechanician	Evelyn Profita	E H & S Officer
¹ Edmund Hinz	Pr Electronics Tech	¹ Ken Shiomoto	Pr Illustrator
Carl Foreman	E H & S Officer		

Animal Technicians

¹ Nancy Bacon	Animal Technician	¹ Chester Patterson	Asst Animal Tech
Scott Hammond	Asst Animal Tech	Carol Rasmussen	An Health Tech
¹ Robert Klein	Animal Technician	¹ Terri Roth	Asst Animal Tech
¹ Gary Kramer	Animal Technician	Kiyo Senda (50%)	Pr Animal Tech
¹ Kazuo Nishimoto	Animal Technician		

Postdoctoral Scientists

Parimal Bharadwaj
Takayoshi Miyabayashi
Sheri Zidenberg-Cherr

Graduate Students

¹Kitty Chelton
¹Kerstin Hansson
¹Sarah Hood
Awanish Mishra

5 AWU Staff

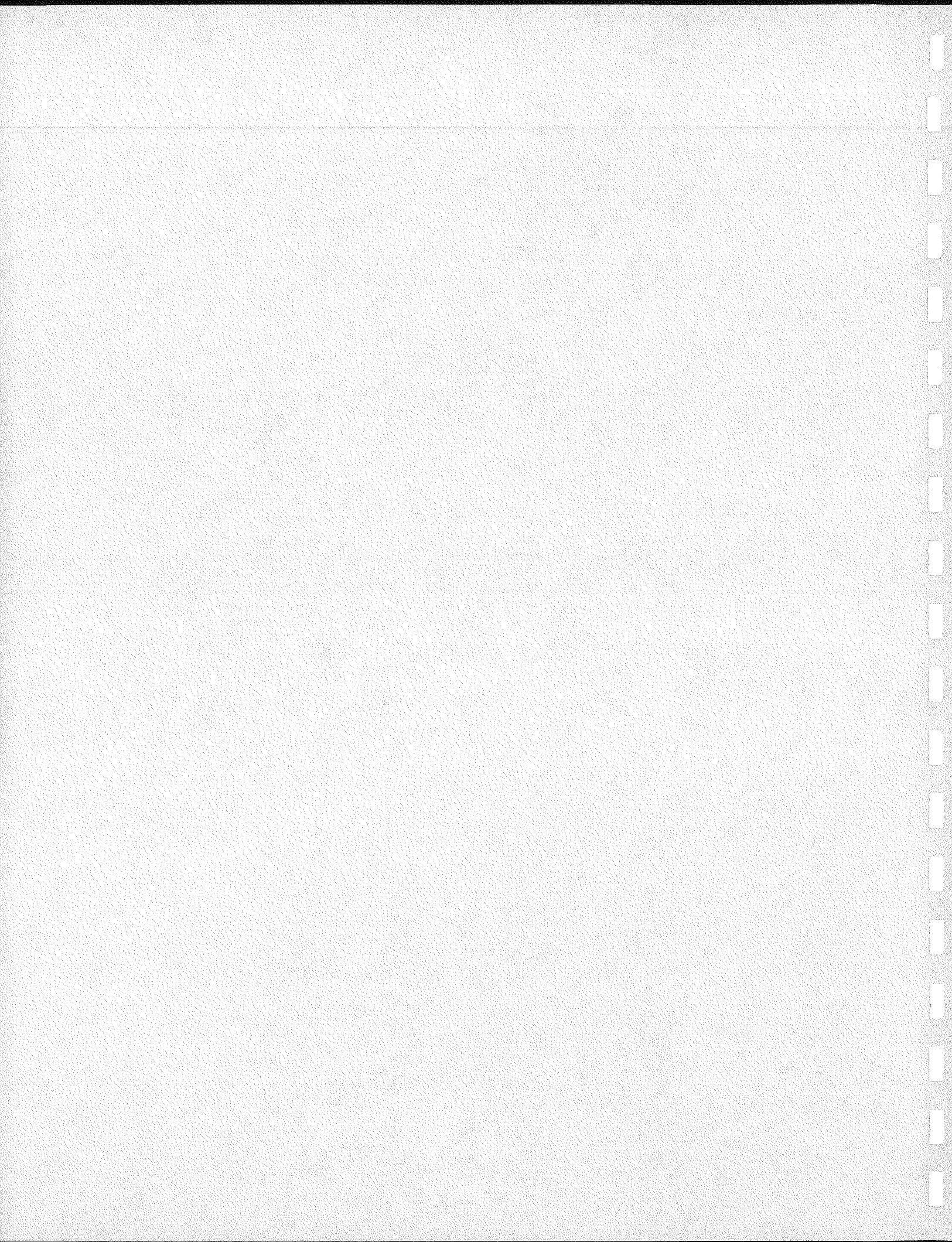
Brian Arbuckle
Damon Getman
Timothy Jamison
Margaret Inokuma
Jennifer Lowry
Lisa Miller

Visiting Scientists

¹Zhixian Zhu

Student Assistants

¹Shura Bugreeff
¹Frank Cruz
¹Jacquelyn Dieter
¹Christine Fletcher
Scott Folwarkow
¹Laurie Herman
¹Bruce Kerwin
¹Laurie McKinney
¹Nancy Miller



ADVISORY COMMITTEE AND COLLABORATORS

ADVISORY COMMITTEE AND COLLABORATORS

University of California Advisory Committee

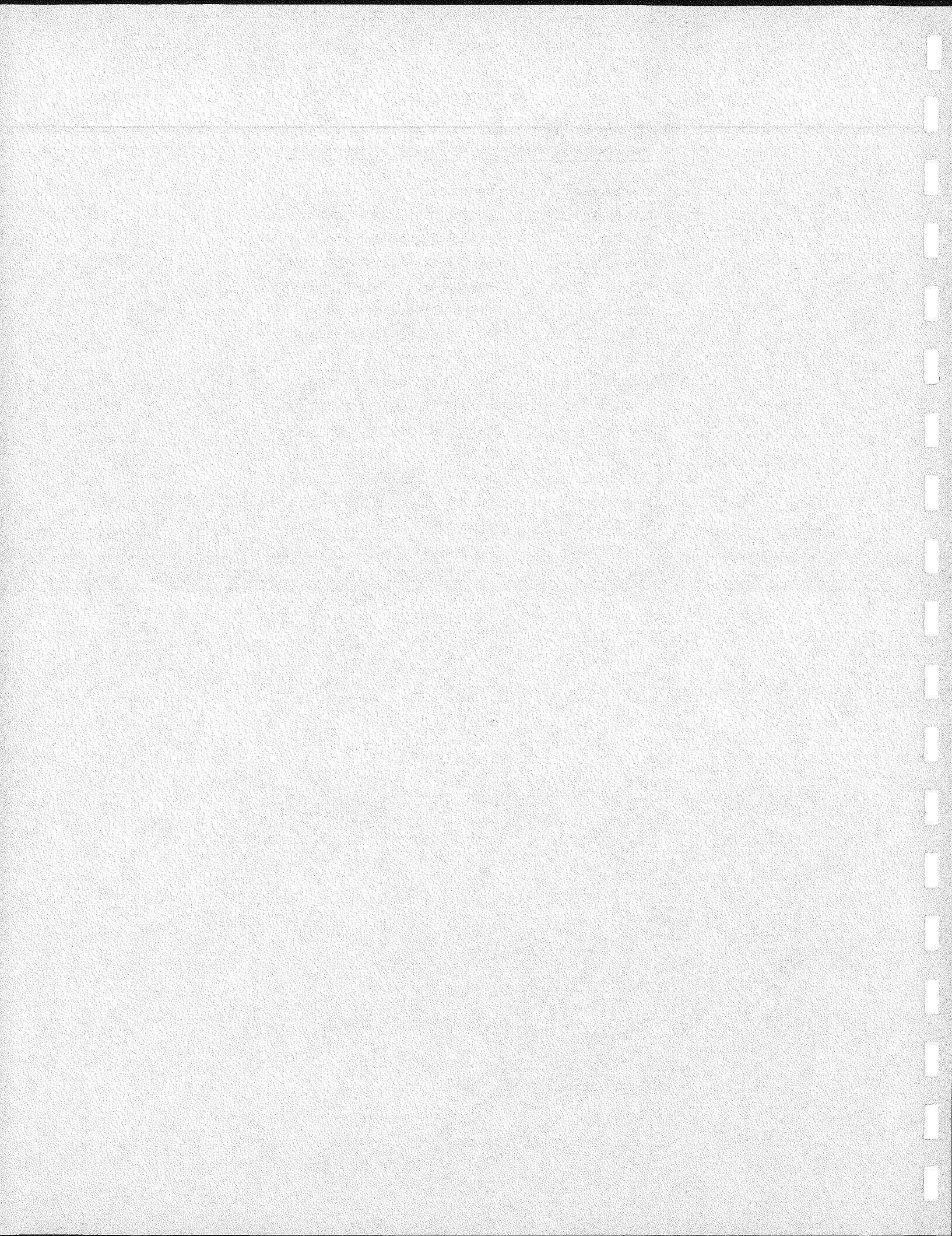
A G Hendrickx	Chairman	Anatomy
E L Barrett		Food Science & Technology
T A Cahill		Physics
R D Cardiff		Medical Pathology
G DeNardo		Radiology

Extramural Collaborators

P K Bharadwaj	Chemistry	India Institute of Technology, Kampur, India
L K Bustad	Physiology	Washington State University, Pullman, Washington
R A Champlain	Oncology/Hematology	UC Los Angeles, Los Angeles, California
S R Cooper	Chemistry	Inorganic Chemistry Laboratory, The University of Oxford, UK
T Feinstat	Gastroenterology	Laurel Hills Medical Center, Sacramento
T E Fritz	Radiation Effects	Argonne National Laboratory, Illinois
R P Gale	Oncology/Hematology	UC Los Angeles
W R Harris	Chemistry	University of Missouri, St. Louis
W S S Jee	Skeletal Studies	University of Utah, Salt Lake City, Utah
A T Keane	Center for Human Radiobiology	Argonne National Laboratory, Illinois
D W Later	Chemical Methods & Kinetics	Battelle Northwest Laboratories, Richland, Washington
H R Maxon	Thyroid Radiobiology	University of Cincinnati Medical Center
J F Remsen	Biochemistry	California Dept. of Food and Agriculture, Sacramento, California
R Schlenker	Skeletal Studies	Argonne National Laboratory, Illinois
T Seed	Division of Biological/Medical Research	Argonne National Laboratory, Illinois
J N Stannard	Radiobiology	UC San Diego, California
K A Stitzel	Human & Environmental Safety Division	The Proctor and Gamble Co., Cincinnati, Ohio
H M Vriesendorp	Immunogenetics	John Hopkins Hospital, Baltimore, MD

University of California, Davis, Collaborators

B Arbuckle	Chemistry
A R Buckpitt	Vet Pharmacology & Toxicology
R D Cardiff	Medical Pathology
A Hendrickx	Calif Primate Research Center
R S Holdstock	Environmental Health & Safety
D Hsieh	Environmental Toxicology
D Katz	Medical Reproductive Biology
C Keen	Nutrition
J Knaak	Calif Dept Food Agriculture
L Wiley	Medical Reproductive Biology
F J Meyers	Medical Hematology/Oncology
J P Morgan	VM Radiological Sciences
J E Moulton	Veterinary Pathology
K W Musker	Chemistry
R R Pool	Pathology
P Schneider	UCD Medical Center
B W Wilson	Avian Sciences



AUTHOR INDEX

AUTHOR INDEX

Al-Bayati, M A	76	Miller, G E	38
Atilola, M A O	31	Mishra, A	60
Bharadwaj, P K	56, 69	Miyabayashi, T	31
Cain, G R	50	Morgan, J P	31
Carvacho, O F	60	Muhumuza, L	31
Cooper, S R	56	Musker, K	56, 69
Culbertson, M R	2	Nagahara, L	60
Dell, R B	38	Parks, N J	2, 38, 56, 60
Gielow, F	76	Raabe	76
Harris, W R	56	Rosenblatt, L S	2, 27
Jee, W S S	38	Schneider, P D	56
Kawakami, T G	50	Spangler, W L	2
Keen, C L	56	White, R G	27
Lagunas-Solar, M	60	Zidenberg-Cherr, S	56

DISCLAIMER

This report was prepared as an account of work sponsored by an agency of the United States Government. Neither the United States Government nor any agency thereof, nor any of their employees, makes any warranty, express or implied, or assumes any legal liability or responsibility for the accuracy, completeness, or usefulness of any information, apparatus, product, or process disclosed, or represents that its use would not infringe privately owned rights. Reference herein to any specific commercial product, process, or service by trade name, trademark, manufacturer, or otherwise, does not necessarily constitute or imply its endorsement, recommendation, or favoring by the United States Government or any agency thereof. The views and opinions of authors expressed herein do not necessarily state or reflect those of the United States Government or any agency thereof.